MOBILE COMMUNICATIONS SERIES

CDMA Systems Engineering Handbook

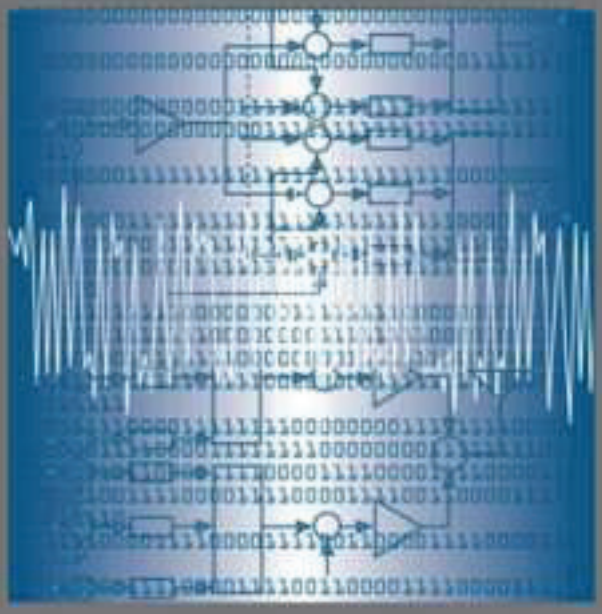

Jhong S. Lee
Leonard E. Miller

Artech House Publishers

CDMA Systems Engineering Handbook

Jhong Sam Lee
Leonard E. Miller

Artech House
Boston • London

Library of Congress Cataloging-in-Publication Data
Lee, Jhong S.
CDMA systems engineering handbook /Jhong S. Lee, Leonard E. Miller.
p. cm. — (Artech House mobile communications library)
Includes bibliographical references and index.
ISBN 0-89006-990-5 (alk. paper)
1. Code division multiple access. 2. Mobile communication systems.
I. Miller, Leonard E. II. Title. III. Series.
TK5103.45.L44 1998
621.382—dc21 98-33846
CIP

British Library Cataloguing in Publication Data
Lee, Jhong S.
CDMA systems engineering handbook.— (Artech House mobile communications library)
1. Code division multiple access—Handbooks, manuals, etc.
I. Title II. Miller, Leonard E.
621.3'84'56

ISBN 0-89006-990-5

Cover design by Lynda Fishbourne

International Standard Book Number: 0-89006-990-5
Library of Congress Catalog Card Number: 98-33846

10 9 8 7 6 5 4 3

To our wives, Helen Lee and Fran Miller

Table of Contents

Preface

The first North American digital cellular standard, based on time-division multiple-access (TDMA) technology, was adopted in 1989. Immediately thereafter, in 1990, Qualcomm, Inc. proposed a spread-spectrum digital cellular system based on code-division multiple-access (CDMA) technology, which in 1993 became the second North American digital cellular standard, known as the IS-95 system. This book is written for those who are interested in learning all about the technical basis of the design and the operational principles of the IS-95 CDMA cellular system and of related personal communication services (PCS) systems, such as the one specified as the standard J-STD-008. These CDMA communications systems are spread-spectrum systems and make use of most of the modern communication and information-theoretic techniques that have so far been discovered by so many scientists and engineers. The primary objective of this book is to explain *in a tutorial manner* the technical elements of these remarkable wireless communication systems *from the ground level up*. The book also provides in the beginning chapter all the *tools*, in the form of systems analysis basics, for those who need them to understand the main flow of the text in the succeeding chapters. In that sense, the book is self-contained. We have generated many *problems, each with a solution,* to aid the reader in gaining clear and complete understanding of the subjects presented. In order to keep the reader's attention focused on the main flow of the discussion, where necessary, involved mathematical derivations are put into an appendix in each chapter.

This book is based on materials used for extensive technical courses conducted by the first author of this book in Korea and the United States since 1993, under variations on the generic title of *Elements of the Technical Basis for CDMA Cellular System Design*. In Korea alone over 1100 hours of lectures on these topics were given at various organizations: the Electronics and Telecommunications Research Institute (ETRI); the Central Research Center of Korea Mobile Telecommunications Coporation (now SK Telecom); Shinsegi Telecommunications, Inc. (STI); Seoul Communication Technology Co. (SCT); Hyundai Electronics Industries Co., Ltd. (HEI); Hansol PCS; and Korea Radio Tower, Inc. (KRT). A tutorial on this subject was also given at the 2nd CDMA International Conference (CIC) held in Seoul in October, 1997. The style and manner of presentation of the technical issues were

Acknowledgments

The authors are grateful for the support of their families during the process of writing this book. We are also pleased to acknowledge the contributions of William A. Jesser, Jr. and Dr. Soon Young Kwon (former employees of J. S. Lee Associates, Inc.) for the research work on Walsh functions, interleaving techniques, convolutional codes, hash functions, and random number generators.

We also wish to acknowledge the support given to the first author of this book, during the period of giving CDMA lectures in Korea, by Dr. Jung Uck Seo (now President of SK Telecom), who was appointed by the Minister of Communications and Information to supervise the entire Korea CDMA Development Program; Dr. Seungtaik Yang, then President of Electronics and Telecommunications Research Institute (ETRI) (now President of the University of Information and Communications); Dr. Hang Gu Bahk, then Vice President of ETRI (now Vice President of Hyundai Electronics Industries Co., Ltd. (HEI)); Dr. Hyuck Cho Kwon, founding President of Shinsegi Telecom, Inc. (STI); Mr. Tai-Ki Chung, President of STI; Mr. Byung Joon Chang, Vice President of Telecommunications Systems Division of HEI; and Mr. Limond Grindstaff of AirTouch Communications, who served as fonding Technical Director of STI. These men in their respective roles did much to help Korea to become the world's first and most successful deployment of CDMA cellular technology, which as of this writing brought about nearly ten million CDMA system subscribers since the beginning of 1996. In addition, we want to recognize the leaders and engineers of the following organizations whose efforts made CDMA a practical reality in Korea and beyond: ETRI; Hansol PCS; HEI; Korea Telecom Freetel, Inc.; LG Information and Communications, Ltd.; LG Telecom, Ltd.; and Samsung Electronics Co., Ltd.

Jhong Sam Lee
Leonard E. Miller
Rockville, Maryland USA
September, 1998

Preface

The first North American digital cellular standard, based on time-division multiple-access (TDMA) technology, was adopted in 1989. Immediately thereafter, in 1990, Qualcomm, Inc. proposed a spread-spectrum digital cellular system based on code-division multiple-access (CDMA) technology, which in 1993 became the second North American digital cellular standard, known as the IS-95 system. This book is written for those who are interested in learning all about the technical basis of the design and the operational principles of the IS-95 CDMA cellular system and of related personal communication services (PCS) systems, such as the one specified as the standard J-STD-008. These CDMA communications systems are spread-spectrum systems and make use of most of the modern communication and information-theoretic techniques that have so far been discovered by so many scientists and engineers. The primary objective of this book is to explain *in a tutorial manner* the technical elements of these remarkable wireless communication systems *from the ground level up*. The book also provides in the beginning chapter all the *tools*, in the form of systems analysis basics, for those who need them to understand the main flow of the text in the succeeding chapters. In that sense, the book is self-contained. We have generated many *problems, each with a solution*, to aid the reader in gaining clear and complete understanding of the subjects presented. In order to keep the reader's attention focused on the main flow of the discussion, where necessary, involved mathematical derivations are put into an appendix in each chapter.

This book is based on materials used for extensive technical courses conducted by the first author of this book in Korea and the United States since 1993, under variations on the generic title of *Elements of the Technical Basis for CDMA Cellular System Design*. In Korea alone over 1100 hours of lectures on these topics were given at various organizations: the Electronics and Telecommunications Research Institute (ETRI); the Central Research Center of Korea Mobile Telecommunications Coporation (now SK Telecom); Shinsegi Telecommunications, Inc. (STI); Seoul Communication Technology Co. (SCT); Hyundai Electronics Industries Co., Ltd. (HEI); Hansol PCS; and Korea Radio Tower, Inc. (KRT). A tutorial on this subject was also given at the 2nd CDMA International Conference (CIC) held in Seoul in October, 1997. The style and manner of presentation of the technical issues were

motivated from the experience of teaching practicing engineers at these industrial facilities. The book is organized into eleven chapters:

Chapter 1, *Introduction and Review of System Analysis Basics*, begins by reviewing the fundamental concepts of SS and CDMA systems. The rest of the chapter contains tutorial coverage of systems analysis basics relevant to succeeding chapters, including sampling theory, waveshaping for spectrum control, and the use of probability functions in systems analysis.

Chapter 2, *Mobile Radio Propagation Considerations*, provides an overview of radio propagation loss models and mobile radio channel models, including the use of these models in cellular design. The material is given in some detail in order to enable the engineer to use such models as cell-design tools and to discern which models are useful in particular situations.

Chapter 3, *Basic Cellular Systems Engineering*, explains the fundamentals of telephone traffic theory, conventional cellular system architecture, and cellular engineering tradeoffs. Since it is important for engineers to know the reasoning behind any equation or table they use, each topic that is presented is given in complete form rather than as an unexplained "cookbook" ingredient. We have striven to make these topics clear so that engineers can "think cellular" on their own.

Chapter 4, *Overview of the IS-95 Standard*, gives a systematic summary of the main features of the CDMA common air interface standard, with more detailed discussions of selected aspects in the chapter's appendices. This chapter is the distillation of several hundred pages of documentation into a coherent summary that indicates not only what the system design is, but also the design philosophy behind it, including detailed explanations not available in the IS-95 document, such as the theory behind the interleaving and the hash functions used in the system.

Chapter 5, *Walsh Functions and CRC Codes*, sets forth the theory and application of the Walsh functions used for orthogonal multiplexing on the IS-95 forward link and for orthogonal modulation on the reverse link. The relations between Walsh, Hadamard, and Rademacher functions are shown, and several ways of generating and demodulating Walsh functions are given. The material presented on Walsh functions in this chapter is much more than what is required in understanding their application to IS-95 CDMA systems. The CRC codes used by the system to detect frame errors are explained in a tutorial manner to the extent needed to understand their use in IS-95.

Chapter 6, *Theory and Application of Pseudonoise Sequences*, gives the mathematical background of the PN sequence generators used in IS-95. It is shown how to derive the "mask" vectors that are used extensively in the

system to assign different PN code offsets to base stations and different PN code starting positions to mobile users. The correlation and spectral properties of PN code waveforms are also treated, with a view toward their application to code tracking in the following chapter.

Chapter 7, *Modulation and Demodulation of IS-95 Spread Spectrum Signals*, gives performance analyses of forward and reverse link modulations. The advantages of the QPSK spread-spectrum modulation used in IS-95 over BPSK spread-sprectrum modulation are thoroughly analyzed. The principles of PN code acquisition and tracking are explained. The effect of using shaped and unshaped PN code references are also quantitatively analyzed.

Chapter 8, *Convolutional Codes and Their Use in IS-95*, treats the theory and practice of convolutional codes in a tutorial manner, leading up to their use in the CDMA cellular system. The convolutional codes used in IS-95 are evaluated based on the theory and the formulas developed in the chapter.

Chapter 9, *Diversity Techniques and Rake Processing*, begins with the treatment of generic diversity techniques, such as selection diversity, equal gain diversity, and maximal ratio combining. The original Rake concept is explained. The chapter concludes with a description of the application of the Rake concept in the IS-95 system.

Chapter 10, *CDMA Cellular System Design and Erlang Capacity*, begins by examining the CDMA cellular system forward and reverse link power budgets in great detail, providing a systematic treatment of the signal and interference parameters, such as loading, that directly influence the operation of the system. Methods for characterizing CDMA cell size and for balancing forward and reverse link coverage areas are described, and the effect of CDMA soft handoff on link reliability is summarized. The merit of the CDMA system is assessed in terms of Erlang capacity. Methods are shown for analyzing the area coverage of the system.

Chapter 11, *CDMA Optimization Issues*, deals with the control of parameters related to system optimization in terms of the selection of base station PN code offsets and the allocation of power to forward link channels. The fade margins achievable on the forward link are derived as functions of the system parameters. A new concept of forward and reverse link "capacity balancing" is introduced. Finally, the implementation of dynamic forward power allocation to the signaling (pilot, sync, and paging) channels is discussed in conjunction with closed-loop forward traffic-channel power control.

Acknowledgments

The authors are grateful for the support of their families during the process of writing this book. We are also pleased to acknowledge the contributions of William A. Jesser, Jr. and Dr. Soon Young Kwon (former employees of J. S. Lee Associates, Inc.) for the research work on Walsh functions, interleaving techniques, convolutional codes, hash functions, and random number generators.

We also wish to acknowledge the support given to the first author of this book, during the period of giving CDMA lectures in Korea, by Dr. Jung Uck Seo (now President of SK Telecom), who was appointed by the Minister of Communications and Information to supervise the entire Korea CDMA Development Program; Dr. Seungtaik Yang, then President of Electronics and Telecommunications Research Institute (ETRI) (now President of the University of Information and Communications); Dr. Hang Gu Bahk, then Vice President of ETRI (now Vice President of Hyundai Electronics Industries Co., Ltd. (HEI)); Dr. Hyuck Cho Kwon, founding President of Shinsegi Telecom, Inc. (STI); Mr. Tai-Ki Chung, President of STI; Mr. Byung Joon Chang, Vice President of Telecommunications Systems Division of HEI; and Mr. Limond Grindstaff of AirTouch Communications, who served as fonding Technical Director of STI. These men in their respective roles did much to help Korea to become the world's first and most successful deployment of CDMA cellular technology, which as of this writing brought about nearly ten million CDMA system subscribers since the beginning of 1996. In addition, we want to recognize the leaders and engineers of the following organizations whose efforts made CDMA a practical reality in Korea and beyond: ETRI; Hansol PCS; HEI; Korea Telecom Freetel, Inc.; LG Information and Communications, Ltd.; LG Telecom, Ltd.; and Samsung Electronics Co., Ltd.

Jhong Sam Lee
Leonard E. Miller
Rockville, Maryland USA
September, 1998

4

Overview of the IS-95 Standard

This book is designed to explain the principles underlying CDMA digital cellular systems, and this chapter, by providing an overview of the IS-95 CDMA standard [1], functions as a "gateway" or point of departure for the contents in the rest of the book. The overview is intended for the reader to gain an overall familiarity with the system.

The full title of the IS-95 standard is "Mobile Station-Base Station Compatibility Standard for Dual-Mode Wideband Spread Spectrum Cellular System," which indicates the fact that the document is a *common air interface (CAI)*—it does not specify completely how a system is to be implemented, only the characteristics and limitations to be imposed on the signaling protocols and data structures. Different manufacturers may use different methods and hardware approaches, but they all must produce the waveforms and data sequences specified in IS-95.

Just as little is said in IS-95 about the implementation of a particular requirement, the theory motivating and justifying the various requirements is not given in any detail. Because in many cases the significance of a particular requirement is not obvious, there is a need for the type of background information provided in this book. Once the principles behind the requirements are understood, the operational significance of the requirements is often enhanced, and the implementation alternatives are apparent.

The IS-95 standard refers to a "dual-mode" system, one that is capable of both analog and digital operation to ease the transition between current analog cellular systems and digital systems. Therefore, there are sections of IS-95 for both analog and digital cellular systems. Although attention is paid in Chapter 3 to analog cellular systems engineering issues, in general this book concentrates on the CDMA cellular system, and in this chapter only the sections of IS-95 dealing with the digital system are summarized.

The IS-95 system, like all cellular systems, interfaces with the PSTN through an MTSO, as suggested in Figure 4.1. In that figure, the mobile stations are shown to communicate with base stations over "forward"

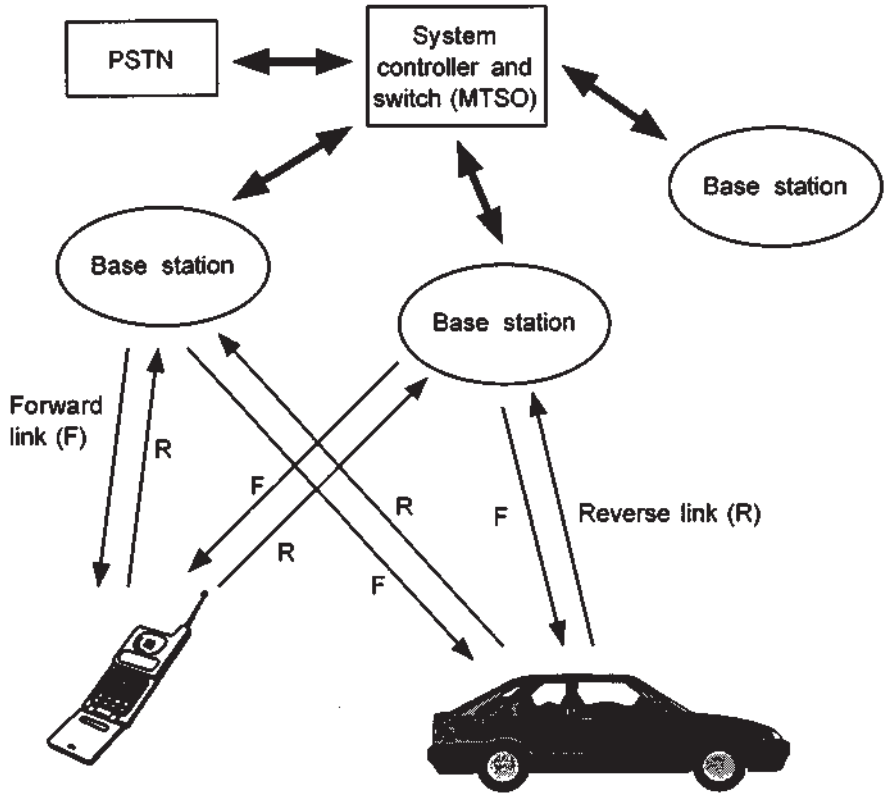

Figure 4.1 Cellular system architecture.

(base-to-mobile) and "reverse" (mobile-to-base) radio links, also sometimes called "downlink" and "uplink," respectively.

The radio communications over the forward and reverse links of the digital communications system that are specified by IS-95 are organized into "channels." Figure 4.2 illustrates the different channel types that are designated in IS-95: pilot, synchronization, paging, and traffic channels for the forward link; and access and traffic channels for the reverse link.

As will be shown, the modulation techniques and even the multiple access techniques are different on the forward and reverse links. Both links of the IS-95 system, however, depend on the conformity of all transmissions to strict frequency and timing requirements. Therefore, before proceeding to describe the forward and reverse link channels in Sections 4.2 and 4.3, respectively, we discuss the use of frequency and time in the system.

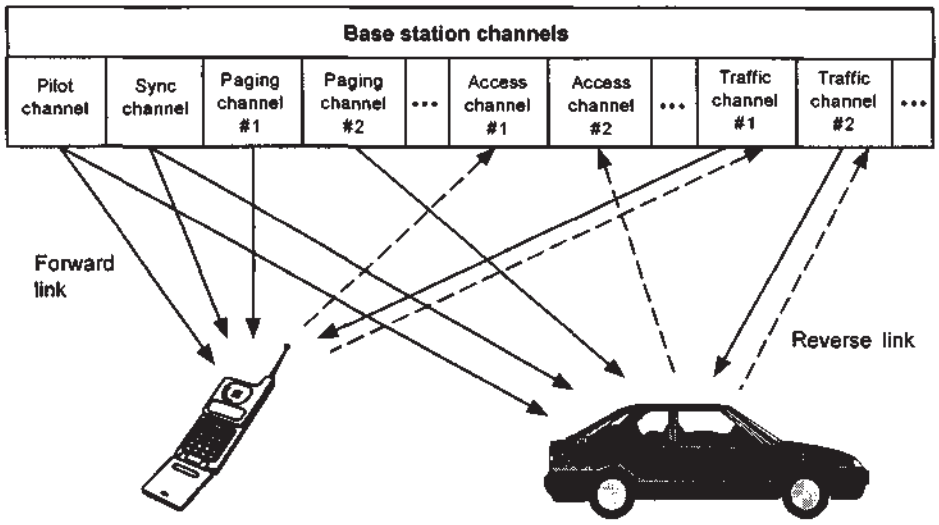

Figure 4.2 IS-95 forward and reverse link channels.

4.1 Coordination of Frequency and Time

The IS-95 standard concerns communications over the radio links between base station transceivers in one or more geographically dispersed fixed locations and subscriber transceivers in geographically dispersed mobile locations, as depicted previously in Figure 4.1. A number of base station sites are connected with and controlled by a base station controller that is associated with an MTSO, which interfaces with the PSTN through a mobile switching center (MSC). The several MTSOs in a region are in turn under the control of an operations management center (OMC). One of the critical functions of an MTSO in a CDMA system (also called a base station controller—BSC) is the maintenance of frequency and time standards. As suggested in Figure 4.3, each CDMA MTSO has a time and frequency coordination function, in addition to the normal cellular functions of the MTSO, that provides required timing and frequency signals such as a frequency reference, time of day, synchronization reference, and system clocks, based on reference signals broadcast by satellites in the Global Positioning System (GPS).

In this section, we review the aspects of the IS-95 standard that relate to the coordination of frequency and time resources and the maintenance of frequency and time standards.

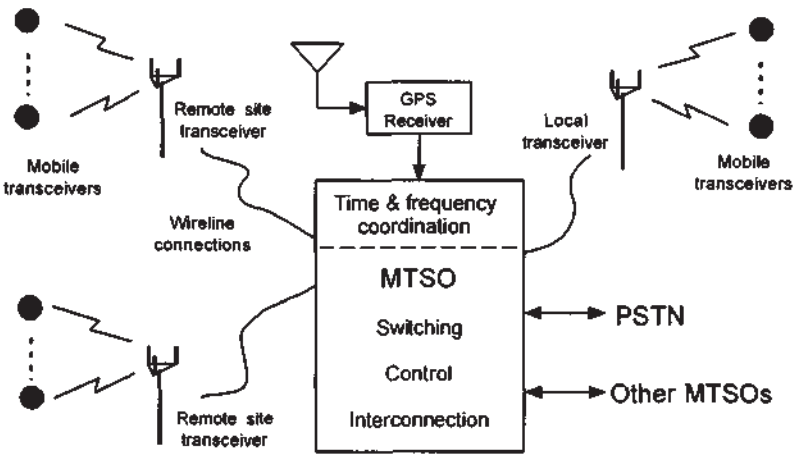

Figure 4.3 MTSO functions.

4.1.1 Cellular Frequency Bands and Channels

In North America, the first-generation analog cellular system, AMPS [2], uses FDMA to divide the allocated spectrum into 30-kHz analog FM voice channels. The frequency allocations for these voice channels are diagrammed in Figure 4.4. The "A" and "B" designations of the frequency bands refers to the Government's policy of licensing two cellular providers in a given geographical area: a carrier (A) whose business is primarily wireless systems, and a carrier (B) whose business traditionally has been wireline telephone communications. For historical, rather than technical, reasons the bands assigned to a particular provider are not contiguous—originally a contiguous band of 10 MHz was assigned to each provider; this allotment was later increased to 12.5 MHz by adding the smaller bands indicated in Figure 4.4. The dual-mode compatibility requirement dictates that the analog portion of equipment based on IS-95 be capable of operating in these bands and using these channels.

The correspondence between channel number N and center frequency is given for mobile and base station by

$$f_{\text{mobile}} = \begin{cases} 0.030\,N + 825.000\,\text{MHz}, & 1 \le N \le 799 \\ 0.030(N - 1023) + 825.000\,\text{MHz}, & 990 \le N \le 1023 \end{cases} \tag{4.1a}$$

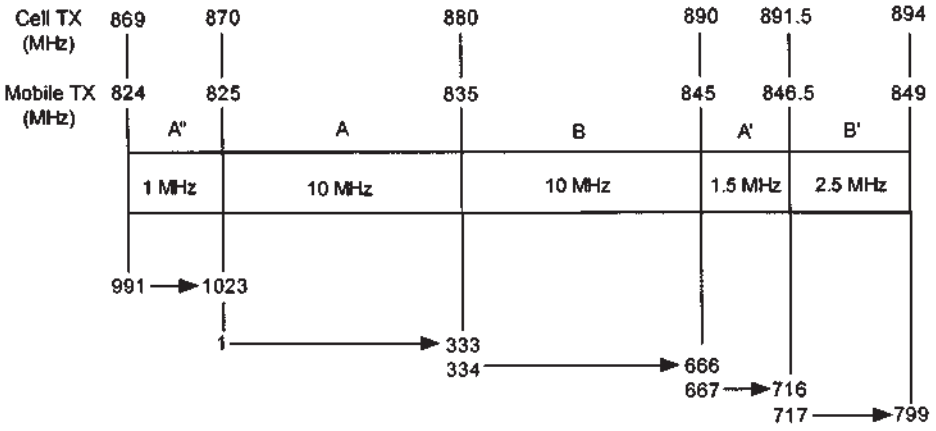

Figure 4.4 Cellular frequency allocations.

and

$$f_{\text{base}} = \begin{cases} 0.030\,N + 870.000\,\text{MHz}, & 1 \le N \le 799 \\ 0.030(N - 1023) + 870.000\,\text{MHz}, & 990 \le N \le 1023 \end{cases} \tag{4.1b}$$

For example, for channel 689, the forward link center frequency is $f_{\text{base}} = 890.670\,\text{MHz}$ and the reverse link center frequency is $f_{\text{mobile}} = 845.670\,\text{MHz}$.

Unlike an FDMA cellular system, a CDMA cellular system does not require the use of "clusters" of cells to enforce a minimum reuse distance between cells using the same frequency channels in order to control the amount of cochannel interference. Instead, adjacent CDMA cells reuse the identical spectrum and utilize spread-spectrum processing gain to overcome interference.

The nominal bandwidth of the IS-95 CDMA waveform is 1.25 MHz. Figure 4.4 shows that the smallest contiguous segment of bandwidth is 1.5 MHz. The IS-95 choice of chip rate was dictated in part by a desire to operate a CDMA system in the 1.5-MHz A′ band. In concept, the transition from analog to digital cellular in a given service area can be based on overlaying the CDMA waveform on a subset of the analog frequencies (simultaneous operation), or by arranging that the analog system does not use those frequencies (disjoint operation).

Because of the relatively wide bandwidth of the IS-95 digital waveform, its center frequencies are restricted to those cellular channels shown within the rectangles drawn in Figure 4.5. For example, the lowest mobile center frequency is 824.700 MHz (channel 1013), which is about half the CDMA signal bandwidth away from the lower edge of the A″ band. This restriction allows for up to five simultaneous CDMA waveforms at different center frequencies (frequency assignments or FAs) for operator A, and up to six for operator B, depending upon the size of the guard band used to separate CDMA waveforms in frequency.

4.1.2 System Time

While the maintenance of a systemwide time standard is not essential to the analog cellular system, it is a critical component of the CDMA digital cellular system design. Each base station of the IS-95 system is required to maintain a clock that is synchronized to GPS time signals. The known beginning of the GPS time count (time 00:00:00 on Jan. 6, 1980) is traceable to Universal Coordinated Time (UTC) and is required to be aligned in a particular fixed way with the PN codes used by every base station in the CDMA system—two "short" PN codes having 26.66-ms periods, and a "long" PN code that has a period that is over 41 days long, as we discuss in greater detail in what follows.

The particular alignment of base station PN codes with the beginning of GPS time is discussed in Section 6.3.4.2.

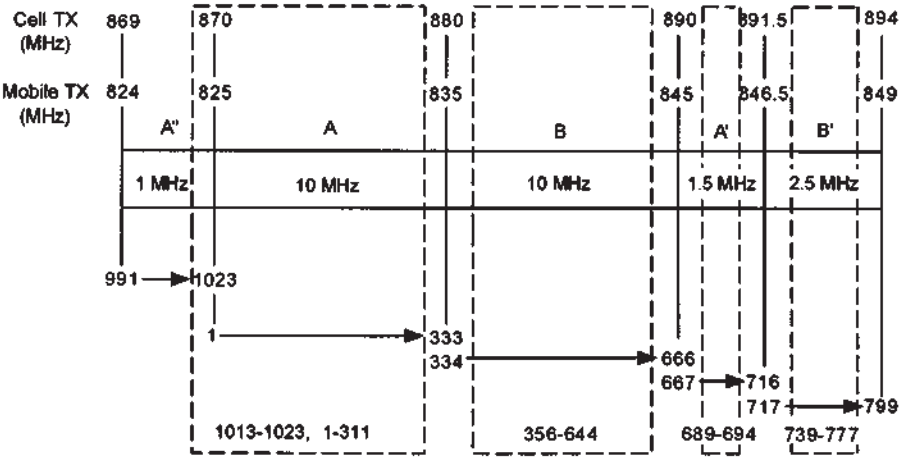

Figure 4.5 Allowed CDMA center frequency regions for A and B operators.

The synchronization of time standards for the several CDMA base stations in a cellular service area is necessary because each base station transmits on the same center frequency and uses the same two short PN codes to spread its (forward link) waveform, the different base station signals being distinguished at a mobile receiver only by their unique short PN code starting positions (phase offsets), as illustrated in Figure 4.6.

Although the base stations are synchronized to each other because each is synchronized to GPS, in general each mobile unit receives the base station signals with a different combination of propagation delays, because the mobile is usually at a different distance from each base station. (Traveling at the speed of light, signals are delayed by 3.336 ns/m or 1.017 ns/ft.) The system time reference for a particular mobile is established when it acquires a certain base station signal, usually that from the nearest base station, affiliates with that base station, and reads the sychronization message broadcast by that base station. The message contains information that enables the mobile unit to synchronize its long PN code and time reference with those of that particular base station—but slightly delayed, due to the distance of the mobile from the selected base station. Using this delayed version of system time, the mobile transmits on the reverse link, and its signal is received with additional delay at its affiliated base station.

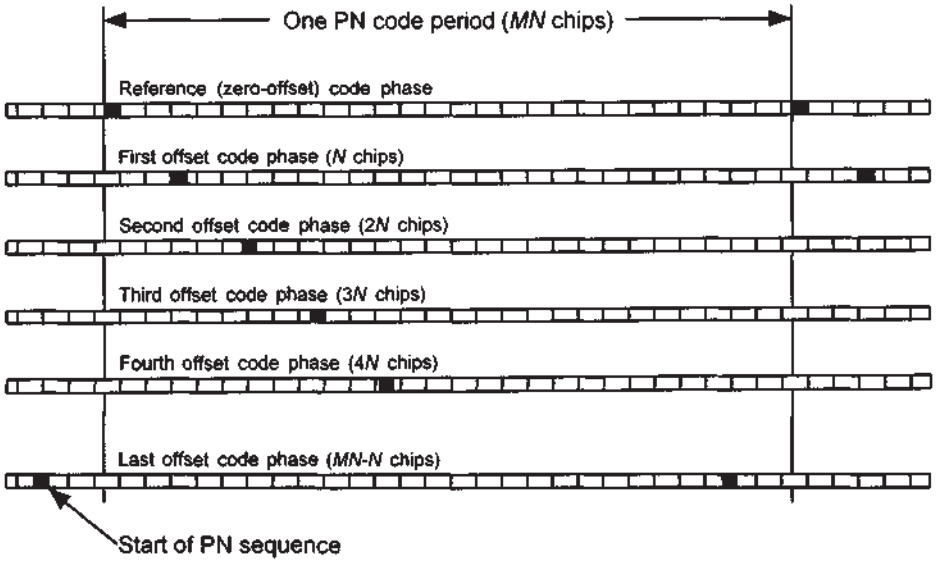

Figure 4.6 Short PN code offsets are assigned to different base stations.

4.2 Description of Forward Link Operations

The forward link channel structure consists of the transmission of up to 64 simultaneous, distinct channels with varying functions that are orthogonally multiplexed onto the same RF carrier. One of these channels is a high-power pilot signal that is transmitted continuously as a coherent phase reference for reception of carriers modulated by information. Another of these channels is a continuously transmitted synchronization channel that is used to convey system information to all users in the cell. Up to seven paging channels are used to signal incoming calls to mobiles in the cell and to convey channel assignments and other signaling messages to individual mobiles. The remainder of the channels are designated as traffic channels, each transmitting voice and data to an individual mobile user.

4.2.1 Forward Link CAI Summary

The IS-95 document [1] specifies a CAI for the CDMA cellular system that different manufacturers of equipment for the system can use to ensure that their design implementations (possibly different in some respects) work together. Before going into details of the various aspects of the IS-95 forward link design, we first provide a summary of the main features of the forward link CAI.

- *Multiplexing:* the forward link channelization is based on an orthogonal code-division multiplexing scheme using an orthogonal set of "subcarrier" digital waveforms known as Walsh functions. In this primary, multiple-access sense, the "C" in CDMA on the forward link refers to Walsh function multiplexing.
- *Interference rejection:* the forward link waveform is modulated by direct-sequence PN code spread-spectrum techniques to isolate the signals received from a particular base station and to discriminate against signals received from other base stations. In the sense that the mobile receiver uses PN code phase to distinguish base station signals (but not individual channels), the "C" in CDMA on the forward link refers to the PN code phase as well as the Walsh functions.
- *Modulation:* the forward link waveform features modulation of I (cosine) and Q (sine) RF carriers by different PN-coded bipolar ($\pm$) base-

band digital data streams, thereby generating a form of quaternary phase-shift keying (QPSK).

- *Pulse shaping:* the shape of the baseband digital pulses in the I and Q output channels is determined by a FIR filter that is designed to control the spectrum of the radiated power for minimal adjacent-frequency interference.
- *PN chip rate:* the PN code chip rate, which is 1.2288 Mcps, is 128 times the maximal source data rate of 9.6 kbps.
- *Effective bandwidth:* for the PN chip rate and spectrum control specified, the energy of the IS-95 forward link signal is almost entirely contained in a 1.25-MHz bandwidth.
- *Voice coding:* a variable-rate vocoder is specified, with data rates 1,200, 2,400, 4,800, and 9,600 bps depending on voice activity.
- *Error-control coding:* the forward link uses rate $\frac{1}{2}$ convolutional coding, with Viterbi decoding.
- *Interleaving:* to protect against burst error patterns (a distinct possibility on the fading mobile communications channel), the forward link interleaves code symbols before transmission, using a 20-ms span.

4.2.2 Orthogonal Multiplexing Scheme

On the forward link, each channel is distinguished by a distinct orthogonal Walsh sequence modulated by the encoded data, much like an individual telemetry subcarrier that is modulated by one of several data sources. Walsh sequences are the rows of Hadamard matrices whose dimensions are powers of 2 and are orthogonal when correlated over their period. Data on the paging and traffic channels are scrambled using an assigned phase offset of a long PN code that provides a degree of privacy, but is not used to distinguish the channels. The channel assignments are shown in Figure 4.7 with their corresponding Walsh sequence "covers," H_i, where $i = 0, 1, \ldots, 63$. Hadamard and Walsh sequences are discussed in detail in Chapter 5.

The baseband data rate from each of the channels being multiplexed varies, as discussed below, with the highest rate being 19.2 kilosymbols per second (ksps). Each channel's baseband data stream is combined with an assigned 64-chip Walsh sequence that repeats at the 19.2-ksps rate. Thus, the orthogonally multiplexed combination of forward link channels forms a baseband data stream with a rate of 64×19.2 ksps $= 1.2288$ Mcps.

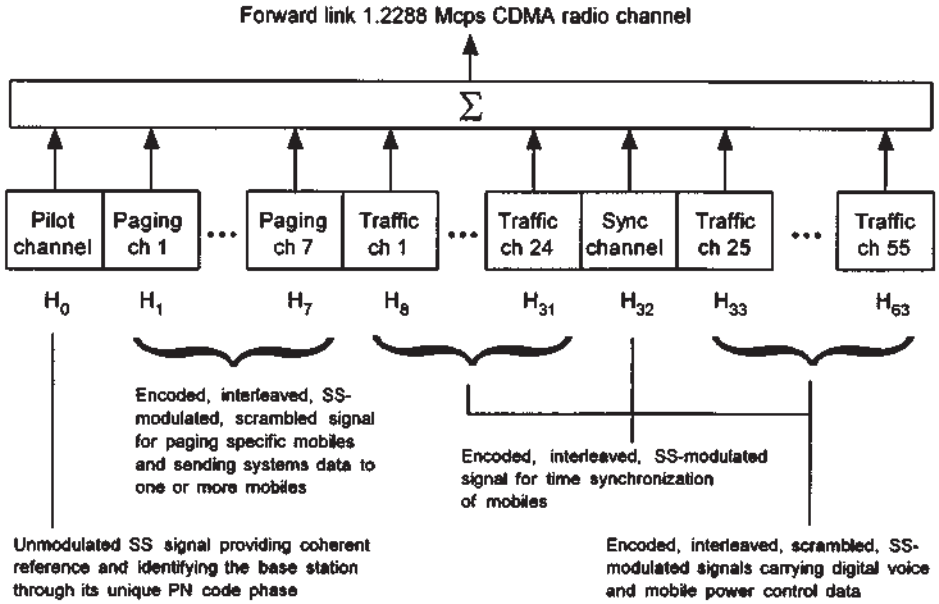

Figure 4.7 Forward link channel assignments.

As indicated in Figure 4.8, the multiplexed data stream for a particular channel is combined separately with two different short PN codes that are identified with I- and Q-quadrature carrier components. The I- and Q-channel PN codes are denoted by $\mathrm{PN}_I(t, \theta_i)$ and $\mathrm{PN}_Q(t, \theta_i)$, respectively, which are generated by fifteen ($n = 15$) stage linear feedback shift registers (LFSR). The notation θ_i denotes the *PN code offset* phase assigned to a particular base station, which is selected from 512 possible values. We discuss the details of how 512 values come about shortly. Thus, unlike conventional QPSK, which assigns alternate baseband symbols to the I- and Q-quadratures, the IS-95 system assigns the same data to each quadrature channel. There is a good reason for the IS-95 system to adopt this particular scheme—an analytical explanation of the rationale is given in Section 7.3. It is common to speak of the operations depicted in Figure 4.8 as "quadrature spreading" [3]. The two quadrature digital baseband waveforms are *shaped* using FIR filters, as shown Figure 4.8, in order to control the shape of the emitted spectrum, which we discussed in Section 1.4.2. The shaped I- and Q-channel signals are modulated by in-phase carrier ($\cos 2\pi f_c t$) and quadrature-phase carrier ($\sin 2\pi f_c t$) and are then combined and transmitted.

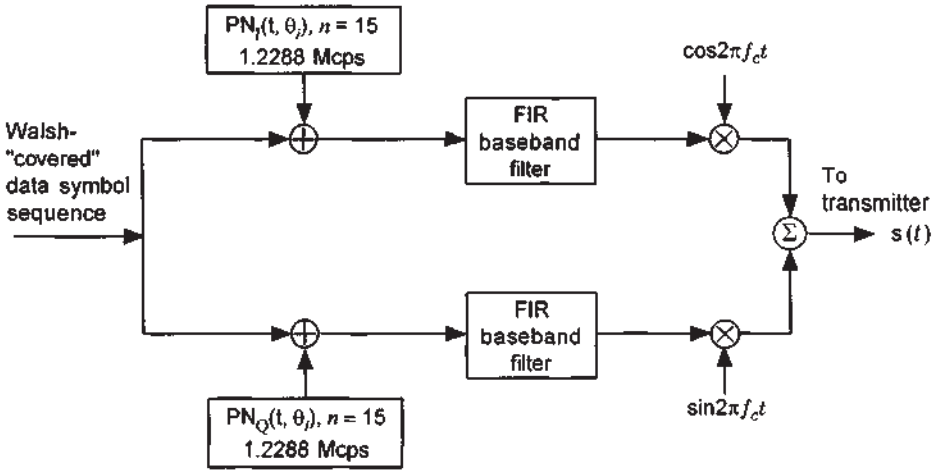

Figure 4.8 Quadrature spreading for the forward link.

4.2.3 Forward Link Channels

The orthogonal multiplexing operations on the forward link are shown in Figure 4.9. The forward link channels consist of pilot channel, sync channel, paging channels, and traffic channels as indicated in the figure. Each channel is modulated by a channel-specific Walsh sequence, denoted H_i, $i = 0, 1, \ldots, 63$. The IS-95 standard assigns H_0 for the pilot channel, H_{32} for the synchronization channel, H_1 to H_7 for the paging channels, and the remainder of the H_i to the traffic channels. Note that we use the notation H_i to designate Walsh function i, which is also denoted as W_i. In this book, we use H_i and W_i synonymously. The reasons behind this notation are fully explained in Chapter 5. Note that the I-channel PN sequence and the Q-channel PN sequence simultaneously quadrature-modulate each of the forward link channels. The quadrature spreading circuit for each channel is as shown in Figure 4.8.

For modularity and the ability to give each channel a different gain and RF power, each channel is separately filtered for RF modulation (Chapter 11 covers this aspect in detail). Each channel is spread-sprectrum modulated by quadrature PN codes. We now discuss the channel types.

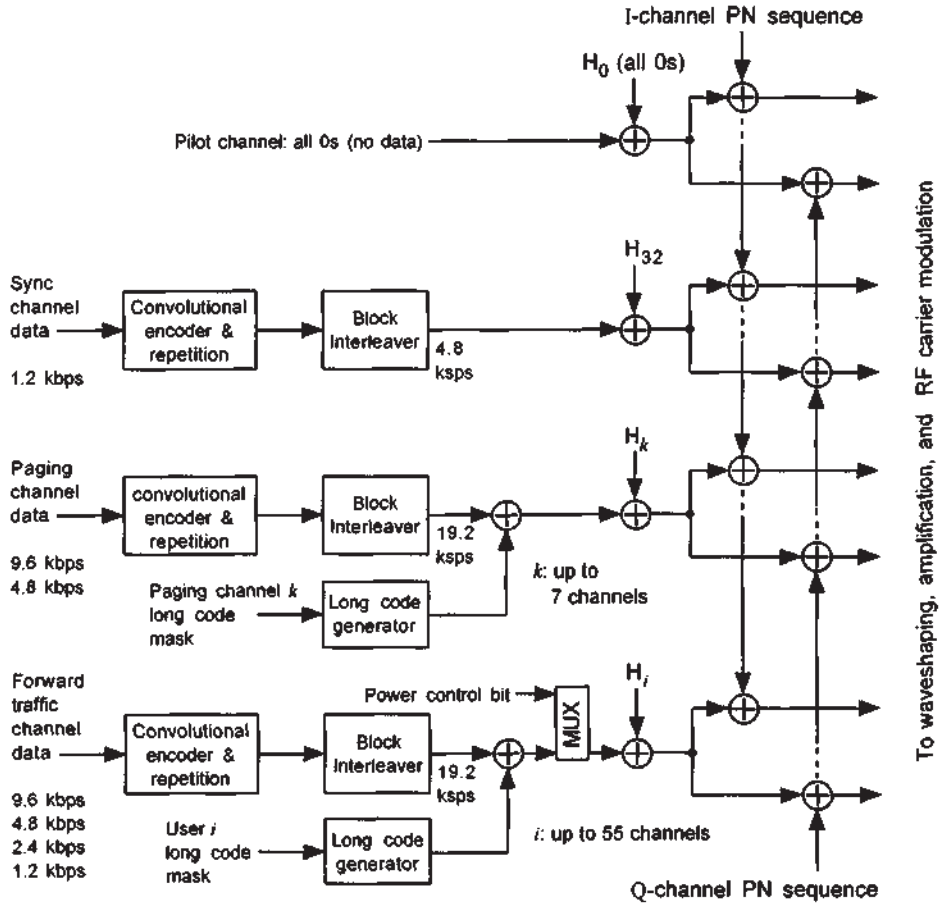

Figure 4.9 Forward link multiplexing operations.

4.2.3.1 Pilot Channel and Quadrature PN Codes

The *pilot channel* is used primarily as a coherent phase reference for demodulating the other channels; for this reason, IS-95 requires that the chip timing and carrier phase of each forward link channel be in very close agreement. The pilot channel is easily acquired by the mobile receiver because it has no data modulation, only the quadrature PN codes shown above in Figure 4.8 and Figure 4.9. Because the pilot channel is necessary for crucial timing information, it is transmitted at a higher power level than the other channels.

The engineering principles involved in choosing the relative powers of the forward link channels for optimal CDMA systems operation are fully discussed in Chapter 11.

The pilot baseband "data" (which are a constant logical 0) are modulated at a Walsh chip rate of 1.2288 Mcps by H_0, the 0th row of the 64×64 Hadamard matrix, which is the Walsh sequence consisting of 64 zeros—thus, in effect, it is not modulated at all. The multiplexed baseband data input from the pilot channel to the forward link quadrature spreading modulator of Figure 4.8 is a constant logical 0.[1]

The two distinct short PN codes in Figures 4.8 and 4.9 are maximal-length sequences generated by 15-stage shift registers and lengthened by the insertion of one chip per period in a specific location in the PN sequence. Thus, these modified short PN codes have periods equal to the normal sequence length of $2^{15} - 1 = 32,767$ plus one chip, or 32,768 chips. As indicated previously in Figures 4.6 and 4.8, each base station is distinguished by a different phase offset θ_i of the in-phase (I) and quadrature-phase (Q) PN sequences. Each offset is a multiple of 64 PN chips, which yields $32,768/64 = 512$ possible 64-chip offsets.

At a rate of 1.2288 Mcps, the I- and Q-sequences repeat every 26.66 ms, or 75 times every 2 sec. The characteristic polynomials of the in-phase and quadrature sequence are given by[2]

$$f_I(x) = 1 + x^2 + x^6 + x^7 + x^8 + x^{10} + x^{15} \tag{4.2}$$

$$f_Q(x) = 1 + x^3 + x^4 + x^5 + x^9 + x^{10} + x^{11} + x^{12} + x^{15} \tag{4.3}$$

which can be generated using the modular shift register generator (MSRG) shown in Figures 4.10 and 4.11. The figures show how a "mask" vector can be used to select a shift of the sequence that is different for each base station.

---

[1] Note that a logical 0 is equivalent to a positive voltage in a ± 1 binary system, and a logical 1 is equivalent to negative voltage, so that the modulo-2 addition operation in logic (also known as exclusive OR) is equivalent to multiplication. Therefore the modulo-2 combination of baseband data and a Walsh function in (0, 1) logic can be implemented by a product of the two in $(+1, -1)$ logic.

[2] The characteristic polynomials $P(x)$ given in IS-95 are the *reciprocal* polynomials for the *sequences* specified. In our treatment of this subject, we consistently refer to the characteristic polynomial $f(x) = x^n P(x^{-1})$ as that whose inverse $1/f(x)$ generates the sequence algebraically. See Chapter 6.

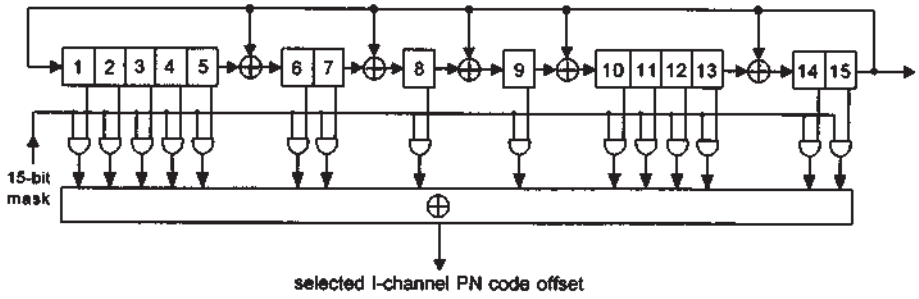

Figure 4.10 In-phase PN generator and offset-selecting mask.

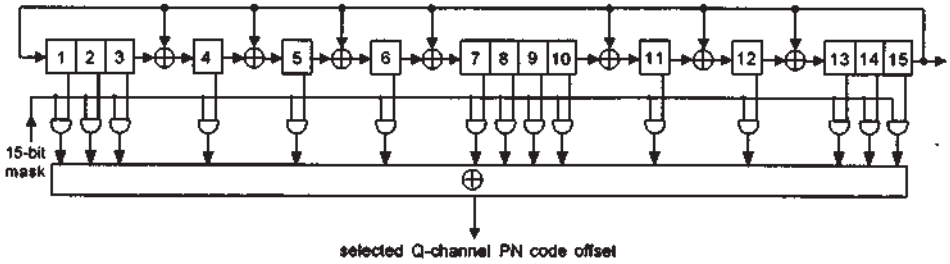

Figure 4.11 Quadrature-phase PN generator and mask.

The theory and practice of generating PN codes is discussed at length in Chapter 6, including the use of masks to control PN code phase and the significance of the insertion of an extra zero in a PN sequence.

In the absence of baseband filtering, the quadrature PN modulated data streams are binary-valued. If the logic values are mapped from (0, 1) to (+1, −1), the PN modulation produces the two-dimensional constellation with the transitions shown in Figure 4.12. Ideally, because the unfiltered data modulation has only two values (± 1), the resulting RF waveform has a constant envelope, and the transitions in Figure 4.12 would be constrained by that fact. In practice, however, the binary data streams are filtered to produce a baseband waveshape whose spectrum is more concentrated than the ideal baseband data, as discussed in Chapter 1, resulting in an RF signal envelope that is not constant. We give detailed explanations on QPSK and offset QPSK (OQPSK) modulations in Section 7.2.1.

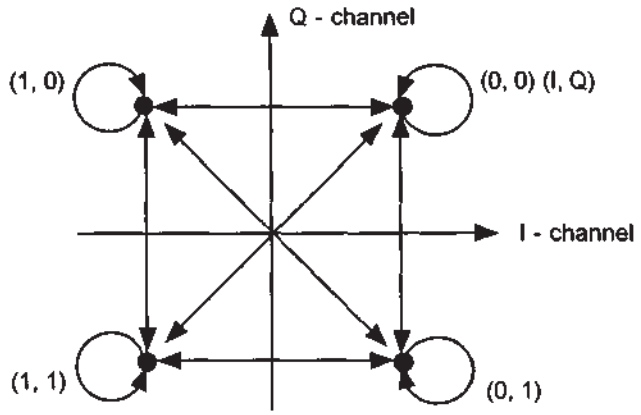

Figure 4.12 Signal constellation for the forward link quadrature modulation.

4.2.3.2 Synchronization Channel

The *synchronization channel* is demodulated by all mobiles and contains important system information conveyed by the *sync channel message*, which is broadcast repeatedly. This signal identifies the particular transmitting base station and conveys long PN code synchronization information, at a rate of 1.2 kbps, or 32 sync channel data bits per $80/3 = 26.66$-ms sync channel frame and 96 bits per 80-ms sync channel "superframe." Note that the sync channel frame length is equal to one period of the short PN codes, and the sync channel frames are in fact aligned with those periods so that, once the mobile has acquired a particular base station's pilot signal, the mobile automatically knows the basic timing structure of the sync channel. As shown in Figure 4.13, this information is provided error-control coding protection by being convolutionally encoded by a rate 1/2 encoder; this operation results in a coded binary symbol rate of $2 \times 1.2\,\text{kbps} = 2.4\,\text{kilosymbols/sec}$ (ksps), or 64 code symbols per frame; the state of the convolutional encoder is not reset after each frame, so that no encoder tail is used. The theory and practice of convolutional coding are reviewed in Chapter 8, where special attention is paid to the particular convolutional codes used in IS-95.

For further protection against possible bursts of errors, such as can occur during signal fading on the mobile channel, a combination of time diversity and interleaving is used on the sync channel. By rearranging the

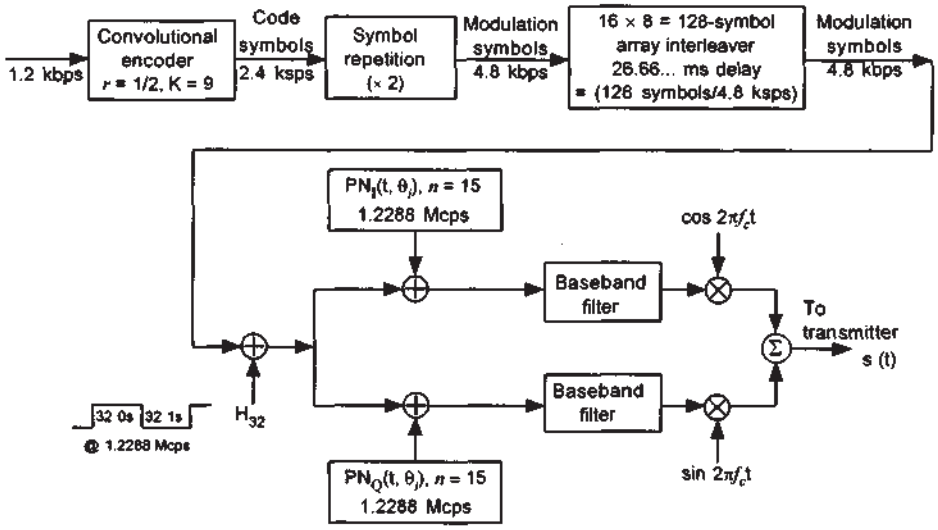

Figure 4.13 Sync channel modulation.

order of the binary symbols before transmission (interleaving them) and then restoring the correct order at the receiver (deinterleaving them), patterns of consecutive, dependent bit errors can be broken into isolated, independent errors for more reliable error detection and correction. On the sync channel, each symbol is repeated once, giving 128 coded symbols per sync channel frame. The block of 128 symbols per frame then is interleaved using a special technique designed to provide as much separation as possible between adjacent bits received in error when they are deinterleaved at the receiver. The interleaving process introduces a delay of one frame duration, or 26.66 ms. Principles of the IS-95 interleaving are explained in Section 4.4.

The interleaved sync channel data are then modulated by H_{32}, the 32nd row of the Hadamard matrix, which is the Walsh sequence consisting of 32 zeros followed by 32 ones—a "square wave"—with the chip rate of 1.2288 Mcps. The use of this particularly simple Walsh sequence facilitates acquisition of the sync channel by the mobile. The period of this square wave (64 chips) is $64/1.2288 = 52.083\,\mu s$, which is one-fourth the period of one data symbol; the combining of the sync data and this Walsh sequence can be viewed as the data's modulating the polarity of a square wave, four periods at a time.

The Walsh-multiplexed sync channel data are spread in bandwidth by the quadrature PN code modulator, as shown above in Figure 4.13. The effective spreading factor (processing gain) for the coding, diversity, multiplexing, and PN modulation is the ratio 1.2288 Mcps/1,200 bps = 1,024. A summary of sync channel modulation parameters is given in Table 4.1.

The sync channel message provides the information that is necessary for the mobile to obtain synchronization to the system timing. After this synchronization has been accomplished, the mobile can receive the paging channel and transmit on the access channel. Because all channels except the pilot and sync channels are scrambled using the long PN code, the sync message is necessary to correctly demodulate any other channel. As mentioned previously, the sync channel is divided into 26.66-ms frames, conveniently made identical to the period of the short PN codes, of which three form an 80-ms superframe. Every sync channel frame and hence sync channel superframe begins at the same instant as the short PN sequence. Thus, when the pilot channel is obtained, the beginning of the PN sequence is known as is the beginning of the sync channel frame. The sync channel message begins at the start of a sync channel superframe. The system time and long code state given in the message are valid at the start of the fourth superframe after the last superframe containing the message. The message is padded to be contained in an integer number of superframes. The interleaver, symbol repetition, and convolutional encoding used by the sync channel are also synchronized to the beginning of the frame. The valid system time is referenced to the zero-offset superframe, as shown in Figure 4.14. In other words, the offset of the base station is subtracted from the received frame time to yield the zero-offset time. The base station's offset is explicitly transmitted as part of the sync channel message to identify the base station.

Table 4.1 Sync channel modulation parameters

Parameter	Value	Units
Data rate	1,200	bps
PN chip rate	1.2288	Mcps
Code rate	1/2	bits/code symbol
Code repetition	2	mod symbols/code symbols
Modulation symbol rate	4,800	sps
PN chips/mod symbol	256	
PN chips/bit	1,024	

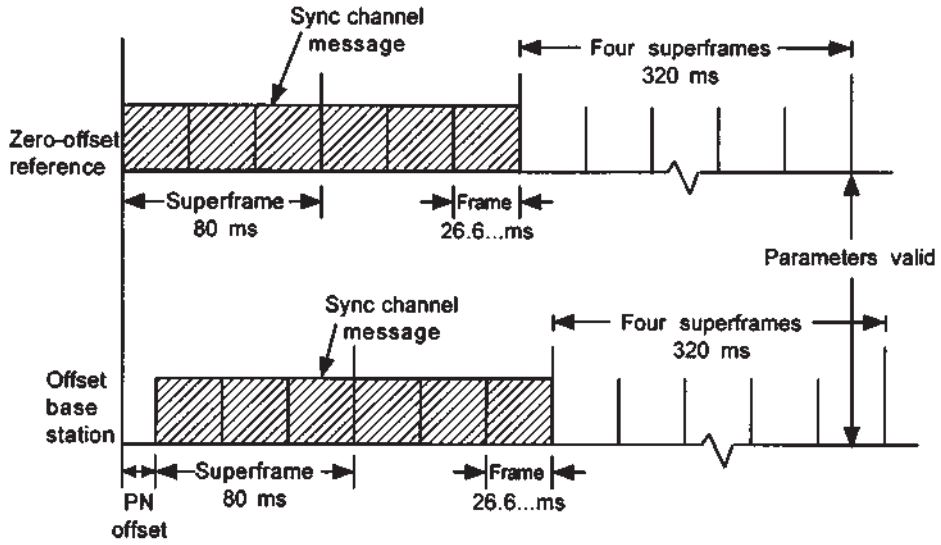

Figure 4.14 Time at which sync channel parameters become valid.

After receiving the sync channel message, the initial loading of the long code register is known. These data are loaded by the mobile into its long-code shift register, which is started at the precise moment the parameters become valid. With the long-code generator running, it can be accessed when needed. It is also useful to note that the beginning of the paging and traffic channel frames coincide with the start of a sync channel superframe.

4.2.3.3 Paging Channels

The *paging channels* are used to alert the mobile to incoming calls, to convey channel assignments, and to transmit system overhead information. Paging information is generated at either 9.6 kbps or 4.8 kbps, as shown in Figure 4.15. The information is convolutionally encoded, repeated, and interleaved. Note that the repetition of the code symbols is adapted to the data rate to fix the rate of symbols being interleaved at 19.2 ksps. Other than for the sync channel, the data frames for the IS-95 channels are 20 ms in length, and the interleaving is performed on a frame-by-frame basis. The 19.2-ksps rate requires the interleaver to process 384 coded symbols. It does so by forming the incoming data into 16 columns of 24 consecutive symbols, then reading them out in such a way as to maximize the distance between symbols that

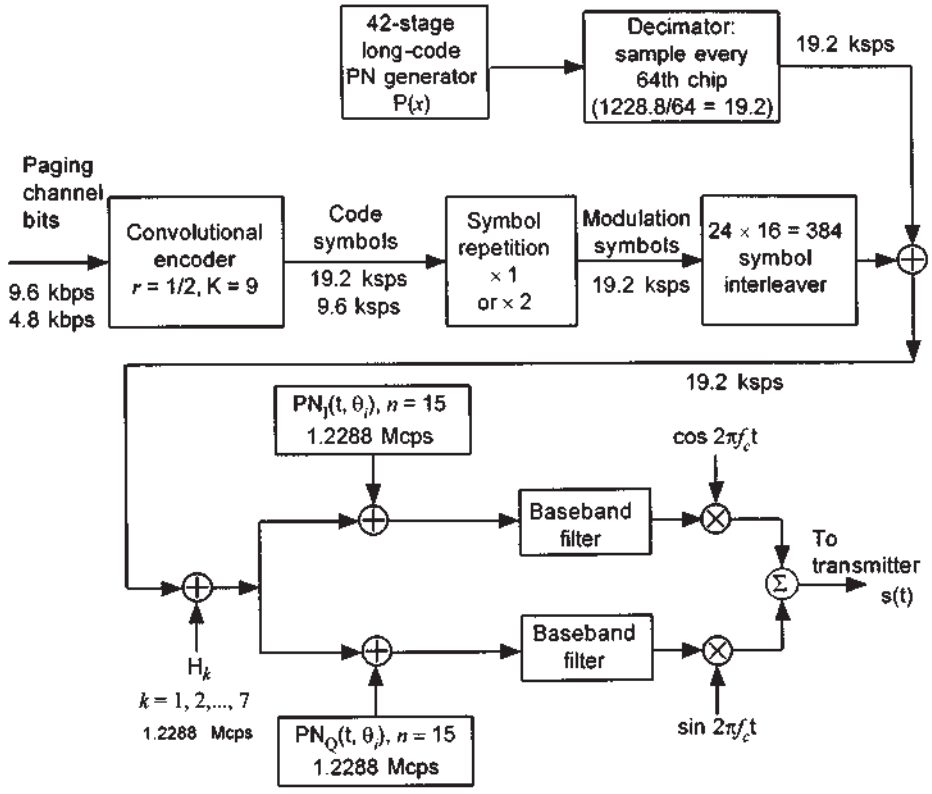

Figure 4.15 Paging channel modulation.

formerly were adjacent, as explained in detail in Section 4.4. All the paging channel modulation symbols are transmitted at the same power and baseband data rate for a given CDMA system, in contrast to the frame-by-frame variation of voice data rate and reduced power for lower rate symbols in the forward traffic channel, as is discussed below.

As with the sync channel, the convolutional encoder for a paging channel is not reset after each frame; thus, for both types of channel, symbols at the end of one interleaver block affect the symbols at the beginning of the next block. Unlike the sync channel, the encoded and interleaved paging channel symbols are scrambled with a 42-stage long-code PN sequence running at 1.2288 Mcps that is decimated to a 19.2-ksps rate by sampling every 64th PN code chip. The long PN code is generated by a 42-stage shift

register, with a period of $2^{42} - 1 \approx 4.4 \times 10^{12}$ chips (lasting over 41 days at 1.2288 Mcps), that implements the recursion that is specified by the characteristic polynomial

$$f(x) = 1 + x^7 + x^9 + x^{11} + x^{15} + x^{16} + x^{17} + x^{20} + x^{21} + x^{23} + x^{24} + x^{25} + x^{26} + x^{32} + x^{35} + x^{36} + x^{37} + x^{39} + x^{40} + x^{41} + x^{42} \quad (4.4)$$

A phase offset of the original long PN code sequence that is unique to the particular paging channel and base station is obtained by combining the outputs of the shift register stages selected by a 42-bit mask, as illustrated in Figure 4.16. For paging channels, the mask is derived from the paging channel number and and the base station ID in the form of its pilot PN code offset; that is, the paging channel mask (beginning with the most significant bit) is given by

$$110001100110100000xxx000000000000yyyyyyyyyy \quad (4.5)$$

where xxx is the paging channel number and yyyyyyyyyy is the base station pilot PN sequence offset index.

The decimated PN sequence is some shift of the original sequence, running at 1/64 times the rate. Because the sampled PN code has the same rate as the encoded data, the data waveform is not spread in bandwidth by combining with this particular PN code. The factors affecting the selection of the long-code masks used on the forward and reverse links are discussed in Chapter 6, as is the effect of decimating a PN sequence.

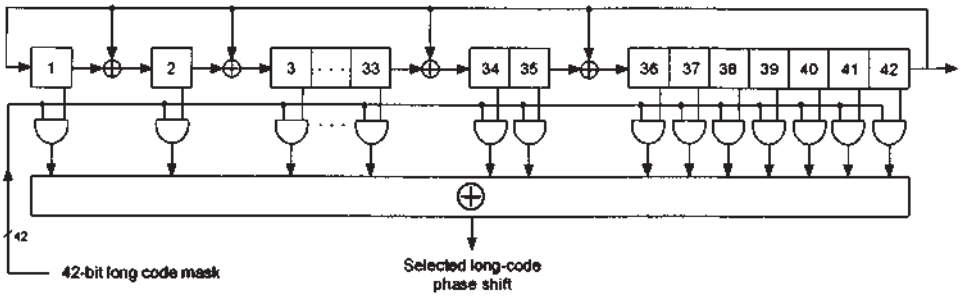

Figure 4.16 42-Stage long-code PN generator with user-distinct mask.

Each paging channel symbol data stream is spread by its designated Walsh sequence, corresponding to one of the first through seventh rows of the Hadamard matrix H_1–H_7, then spread in quadrature by the short PN codes. Paging channel modulation parameters are summarized in Table 4.2.

A paging message directed to a particular mobile unit could be broadcast periodically on one of the paging channels, requiring mobile *n* to scan the active paging channels for a possible message addressed to mobile *n*. Or, to relieve the mobile of the burden of scanning the different paging channels, the paging message could be broadcast periodically on all paging channels; however, this procedure is wasteful of paging channel capacity. In IS-95, each active paging channel has a number of periodically recurring message slots (e.g., 2,048 slots) available for transmitting pages and other base-to-mobile messages. When a message is queued up for a particular mobile, using a *hash function*, the base station pseudorandomly selects one of the paging channels and pseudorandomly selects one of the message slots in that paging channel for transmission to the particular mobile. The mobile knows exactly which paging channel and message slot to monitor for possible messages because the pseudorandom selection is based on its own identification number and known system parameters. The purpose of the hash function is to distribute the message traffic evenly among the paging channels and message slots. The IS-95 hash functions are discussed in Appendix 4B.

4.2.3.4 Traffic Channels

There are nominally up to 55 forward *traffic channels* that carry the digital voice or data to the mobile user. It is possible to use one or more of the seven Walsh sequences normally assigned to paging channels for traffic channels, for a total of up to 62 traffic channels, if the system becomes heavily loaded.

Table 4.2 Paging channel modulation parameters

Parameter	Value		Units
Data rate	9600	4800	bps
PN chip rate	1.2288	1.2288	Mcps
Code rate	1/2	1/2	bits/code symbol
Code repetition	1	2	mod symbols/code symbols
Modulation symbol rate	19,200	19,200	symbols/sec (sps)
PN chips/mod symbol	64	64	
PN chips/bit	128	256	

It is usually the case, however, that mutual interference on the reverse link limits the number of simultaneous calls to fewer than 55 calls, so the forward link's capacity is more than adequate for the traffic that can be supported by the system. Walsh sequences designated for use on the traffic channels are H_8–H_{31} and H_{33}–H_{63}. A block diagram for the forward traffic channel modulation is given in Figure 4.17. As shown in the diagram, voice data for the mth user is encoded on a frame-by-frame basis using a variable-rate voice coder, which generates data at 8.6, 4.0, 2.0, or 0.8 kbps depending on voice activity, corresponding respectively to 172, 80, 40, or 16 bits per 20-ms frame. A cyclic redundancy check (CRC) error-detecting code calculation is made at the two highest rates, adding 12 bits per frame for the highest rate and 8 bits per frame at the second highest rate. At the mobile receiver, which voice

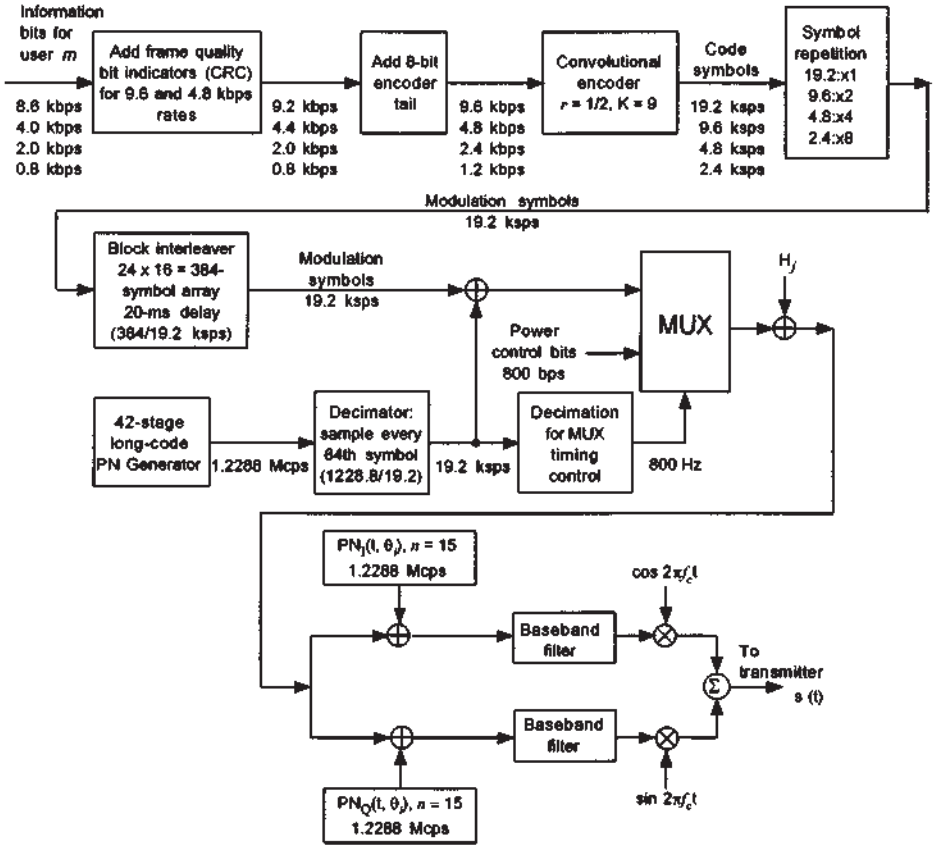

Figure 4.17 Traffic channel modulation.

data rate is being received is determined in part from performing similar CRC calculations, which also provide frame error reception statistics for forward link power control purposes. The theory and use of CRC codes are discussed in Chapter 5.

In anticipation of convolutional coding on a block basis (code symbols in one frame not affecting those in adjacent frames), a convolutional encoder "tail" of 8 bits is added to each block of data to yield blocks of 192, 96, 48, or 24 bits per frame, corresponding to the data rates of 9.6, 4.8, 2.4, and 1.2 kbps going into the encoder, which are defined as full, one-half, one-quarter, and one-eighth rates, respectively. Convolutional encoding is performed using a rate 1/2, constraint length 9 code, resulting in coded symbol rates of 19.2, 9.6, 4.8, and 2.4 ksps.

Coded symbols are repeated as necessary to give a constant number of coded symbols per frame, giving a constant symbol data rate of 19.2 ksps (i.e., 19.2 ksps × 1, 9.6 ksps × 2, 4.8 ksps × 4, 2.4 ksps × 8). The 19.2 ksps × 20 ms = 384 symbols within the same 20-ms frame are interleaved to combat burst errors due to fading, using the same interleaving scheme as on the paging channels.

Each traffic channel's encoded voice or data symbols are scrambled to provide voice privacy by a different phase offset of the long PN code, decimated to yield a code rate of 19.2 kcps. Note that different mobile users are distinguished on the forward link by the orthogonal Walsh sequence associated with the particular traffic channel, not by the user-specific long-code phase offset.

The scrambled data are punctured (overwritten) at an average rate of 800 bps by symbols that are used to control the power of the mobile station; the details of this "power control subchannel" are discussed in Section 4.4.

One of 64 possible Walsh-Hadamard periodic sequences is modulo-2 added to the data stream at 1.2288 Mcps, thus increasing the rate by a factor of 64 chips/modulation symbol (scrambled code symbol). Each symbol for a given traffic channel is represented by the same assigned 64-chip Walsh sequence for a data symbol value of 0 and the sequence's complement for a data symbol value of 1. Walsh-Hadamard sequences of order 64 have the property that all 64 of the sequences are mutually orthogonal. A unique sequence is assigned to each traffic channel so that upon reception at their respective mobile stations, the traffic channels can be distinguished (demultiplexed) based on the orthogonality of the assigned sequences. This orthogonally spread data stream is passed to the quadrature modulator for PN spreading and RF transmission.

Note from Figure 4.17 that, regardless of the data rate, the modulated channel symbol rate must be 19.2 ksps. This is accomplished by means of code symbol repetition for rates less than the 9.6-ksps data rate. The relationship between code symbol energy and the information bit rate is specified in Table 4.3 for different data rates.

4.3 Description of Reverse Link Operations

The IS-95 reverse link channel structure consists of two types of channels: access and traffic channels. To reduce interference and save mobile power, a pilot channel is not transmitted on the reverse link. A mobile transmits on either an access or a traffic channel but never both at the same time. Thus, as far as the mobile is concerned, the reverse link "channel" is an operating mode.

4.3.1 Reverse Link CAI Summary

Before going into details of the various aspects of the IS-95 reverse link design, we first provide a summary of the main features of the reverse link CAI.

- *Multiple access:* the reverse link channelization is based on a conventional spread-spectrum PN code-division multiple-access scheme in which different mobile users are distinguished by distinct phase offsets of the 42-stage long PN code, which serve as user addresses. Thus, the "C" in CDMA on the reverse link refers to spread-spectrum multiple access by means of PN codes.

Table 4.3 Forward traffic channel modulation parameters

Parameter	Value				Units
Parameter	9,600	4,800	2,400	1,200	bps
PN chip rate	1.2288	1.2288	1.2288	1.2288	Mcps
Code rate	1/2	1/2	1/2	1/2	bits/code symbol
Code repetition	1	2	4	8	mod sym/code sym
Mod symbol rate	19,200	19,200	19,200	19,200	sps
Code sym energy	$E_b/2$	$E_b/4$	$E_b/8$	$E_b/16$	
PN chips/symbol	64	64	64	64	
PN chips/bit	128	256	512	1,024	

- *Quadrature spreading:* in addition to the long PN code, the reverse link data stream is direct-sequence modulated in quadrature by the same two short PN codes as on the forward link; each mobile station in each cell uses the reference or zero-offset phases of these two codes.
- *Modulation:* the reverse link waveform features 64-ary orthogonal modulation using sequences of 64 chips to represent six binary data symbols. The quadrature modulation of I (cosine) and Q (sine) RF carriers by the two different PN-coded bipolar ($\pm$) baseband digital data streams, with the Q-quadrature stream delayed by half a PN chip, generates a form of offset quaternary phase-shift keying (OQPSK).
- *Pulse shaping:* the shape of the baseband digital pulses in the I and Q output channels is determined by a FIR filter that is designed to control the spectrum of the radiated power for minimal adjacent-frequency interference.
- *PN chip rate:* the PN code chip rate, which is 1.2288 Mcps, is 128 times the maximal source data rate of 9.6 kbps.
- *Acquisition:* the base station's acquisition and tracking of mobile signals is aided by the mobile's transmission of a preamble containing no data.
- *Voice coding:* a variable-rate vocoder is specified, with data rates 1,200, 2,400, 4,800, and 9,600 bps depending on voice activity in a particular 20-ms frame. The transmission duty cycle of the reverse link signal during a call is proportional to the data rate.
- *Error-control coding:* the reverse link uses rate 1/3 convolutional coding, with Viterbi decoding.
- *Interleaving:* to protect against possible burst-error patterns, the reverse link interleaves code symbols before transmission, using a 20-ms span.

4.3.2 Multiple Access Scheme

There is at least one reverse link access channel for every paging channel on the forward link, with a maximum of 32 access channels per paging channel. The access channels are used for the mobile to initiate a call or respond to a page or information request from the base station.

The number of traffic channels on the reverse link, transmitting voice and data to the base station, is equal to the number of traffic channels on the forward link. When no paging channels are used on the forward link, the

maximum number of traffic channels is 62. In practice, the number of channels is limited by interference from users on the reverse link.

Each reverse link channel is distinguished by a user-distinct phase offset of the same 42-stage long-code PN sequence used on the forward link. Therefore, the "C" in CDMA on the reverse link is the user-distinct PN code, while on the forward link, it is the set of mutually orthogonal Walsh sequences. The channels as received at the base station are shown in Figure 4.18, where n (the number of paging channels) and m (the number of traffic channels) are limited by interference.

The reverse link transmitter consists of a convolutional encoder and modulator, and a quadrature modulator and RF circuitry, shown conceptually in Figure 4.19. Each of these components is used during mobile transmissions on both reverse link channels. Note that the quadrature modulator for the reverse link is different from that used on the forward link in that a half-chip delay is inserted in the quadrature-phase (Q) channel to achieve a form of OQPSK modulation. The effect of this delay is to constrain the I and Q chip data transitions to one quadrature at a time, rather than allowing them to be simultaneous as on the forward link. The one-half chip offset

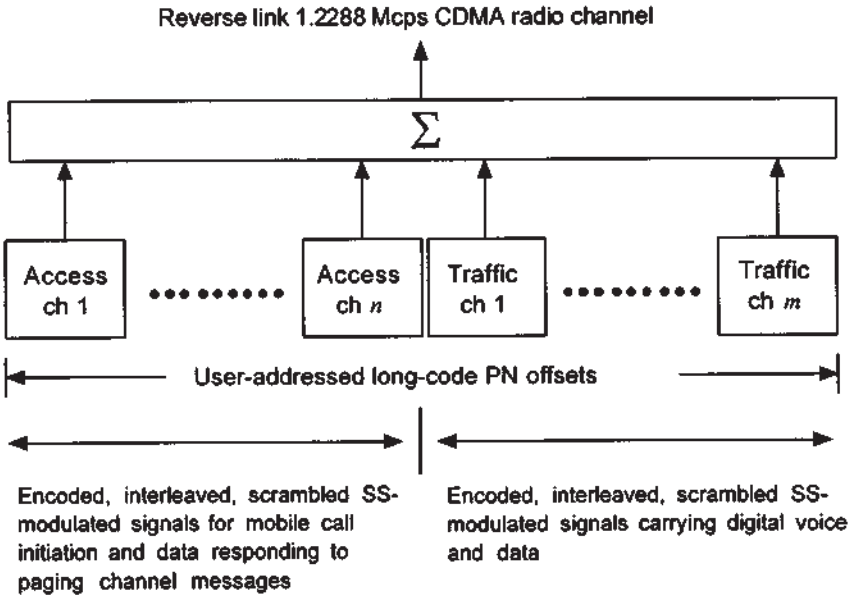

Figure 4.18 Reverse link channel assignments at the base station.

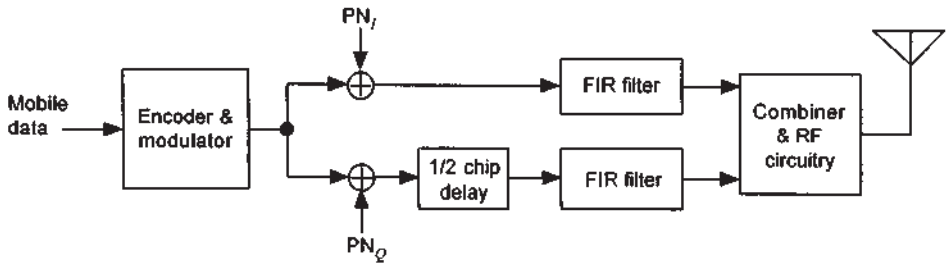

Figure 4.19 Block diagram of the reverse link transmitter.

eliminates phase transitions through the origin to provide a modulation scheme that gives a relatively constant envelope. The binary I and Q signals are mapped into phase producing the signal constellation shown in Figure 4.20. The transitions shown in the figure do not reflect the influence of the waveshaping filters that constrain the phase trajectory through their effect on the quadrature waveforms. Note, however, that there is no transition through the origin. We have more to say about OQPSK signaling in Section 7.2.

The transmission of the same data by means of a two-quadrature modulation scheme is a form of diversity. As explained in Section 7.3, its analytical justification shows that the QPSK CDMA system has a 3-dB advantage over BPSK CDMA system in terms of intersymbol interference performance and also has cochannel interference advantages.

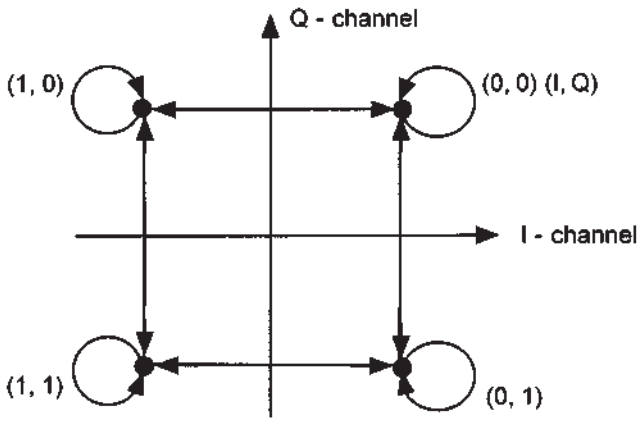

Figure 4.20 Phase transitions for OQPSK.

4.3.3 Reverse Link Channels

There are two categories of channels in the reverse link: access channel and traffic channel. The access channel is used by the mobile station to initiate communication with the base station and to respond to messages that are sent to the mobile by the base station on the paging channels. As for the forward link, the reverse link also has variable data rates for traffic channels, ranging from 1.2 to 9.6 kbps. The transmission of different data rates is accomplished by the *data burst randomizer*, as is discussed in detail below.

4.3.3.1 Access Channel

Access channel data are generated at a rate of 88 bits per 20-ms frame, to which eight encoder tail bits are appended because the encoder state is reset after each frame. The rate into the encoder then is $(88 + 8)/.02 = 4{,}800$ bps, as illustrated in Figure 4.21. These data are encoded with a rate 1/3, constraint length 9 convolutional encoder. The rate from the encoder is $3 \times 4.8 = 14.4$ ksps.

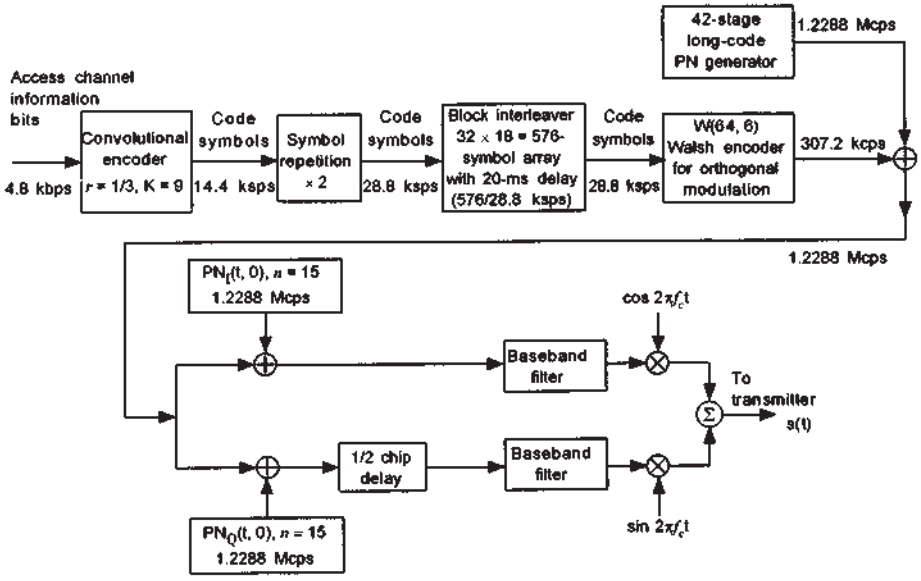

Figure 4.21 Access channel modulation.

To accommodate the same block-interleaving scheme on the access and reverse traffic channels, the access channel code symbols are repeated, making the rate into the interleaver $2 \times 14.4 = 3 \times 9.6 = 28.8$ ksps, the same as the rate into the interleaver for the highest reverse traffic channel data rate, 9,600 bps. The interleaving scheme, described more fully in Section 4.4, reads a frame's worth of data ($28.8 \times 20 = 576$ code symbols) by column into an array of 18 columns of 32 consecutive symbols, which are read out by rows in a certain order to separate the data symbols in time.

The interleaved code symbols are passed to a (64, 6) Walsh encoder. The Walsh encoding consists of using each group of six encoded symbols (c_0, c_1, ..., c_5) to select one of $2^6 = 64$ Walsh sequences H_i of order 64. The selection is performed by computing the index i according to the rule

$$i = c_0 + 2c_1 + 4c_2 + 8c_3 + 16c_4 + 32c_5 \tag{4.6}$$

where i is the row of the 64×64 Hadamard matrix, and the $\{c_j\}$ are encoded binary (0, 1) symbols. The symbol rate is therefore increased by 64/6, from 28,800 sps to 307,200 cps, in units of "Walsh chips" per second. This step can be thought of as the encoding sequence of an ($n = 64$, $k = 6$) error-correcting code. It also is readily interpreted as a form of 64-ary orthogonal modulation using binary channel symbols. An analysis of the reverse link's 64-ary orthogonal modulation scheme is presented in Section 7.2.2.5.

The access channel signal is further spread by a factor of four using a particular phase offset of the 42-stage long PN code clocked at the rate of 1.2288 Mcps. A phase offset of the original sequence is obtained by forming the inner product of the vector consisting of the output of each shift register stage with a user-distinct 42-bit mask sequence. For access channels, the mask is constructed using pseudorandomly calculated access channel and associated paging channel numbers, and by base-station identification parameters.

The long PN code-spread baseband data stream is combined separately with I- and Q-quadrature short PN code sequences prior to waveshaping and transmission, with the Q channel combination delayed by one-half chip to implement OQPSK modulation and quadrature diversity. Note that the signal is not further spread by this operation, because the short PN codes are clocked at the same rate, 1.2288 Mcps. Note also that Figure 4.21 indicates that the zero-offset code phases of the short PN codes are used for all mobiles in all cells; the different user signals are distinguished only by their unique long PN code phases. Table 4.4 summarizes the modulation parameters of the access channel.

Table 4.4 Access channel modulation parameters

Parameter	Value	Units
Data rate	4800	bps
PN chip rate	1.2288	Mcps
Code rate	1/3	Bits/code symbol
Code symbol repetition	2	Symbols/code symbol
Transmit duty cycle	100	%
Code symbol rate	28,800	sps
Modulation	6	Code sym/mod sym
Modulation rate	4800	sps
Walsh chip rate	307.2	kcps
Mod symbol duration	208.33	μs
PN chips/code symbol	42.67	
PN chips/mod symbol	256	
PN chips/Walsh chip	4	

Access channel transmissions by particular mobiles are permitted during assigned intervals called *access channel slots*, which are an integer number of 20-ms frames in length. Each transmission within an access channel slot begins with a short random delay to distribute the transmission start times of the various mobiles that may be transmitting in the same slot on different channels, and with a preamble of 96 data zeros to aid the base station in acquiring the signal. The first time that a mobile uses an access channel, its transmissions are confined to "probe" messages formatted according to a certain procedure until the proper power level for that particular mobile has been determined.

4.3.3.2 Reverse Traffic Channel

Up to 62 traffic channels receive voice or data from the mobile at the base station. A block diagram of traffic channel processing is given in Figure 4.22. A variable rate vocoder is used to generate a digital voice signal at rate varying from 0.8 to 8.6 kbps in a given 20-ms traffic channel frame. Depending on the data rate, the data frame is encoded with a CRC block code to enable the base station receiver to determine if the frame has been received with error. An 8-bit encoder tail is added to the frame to ensure that the convolutional encoder, which follows, is reset to the all-zero state at the end of the frame. These operations result in data rates of 9,600 (full rate), 4,800 (half rate),

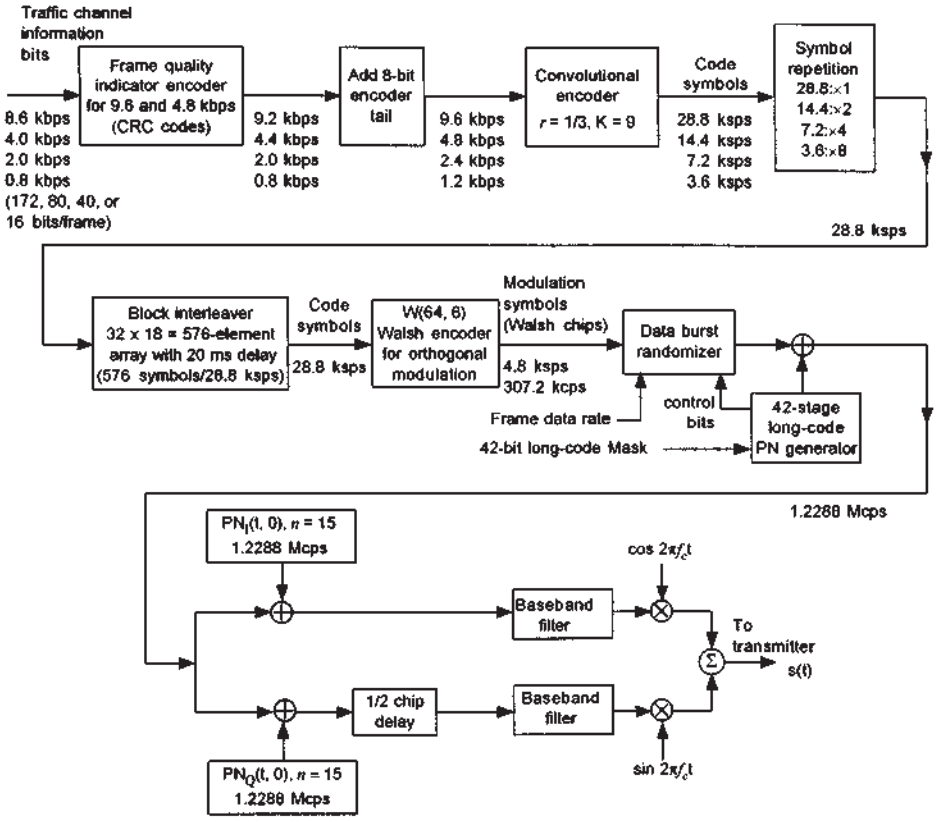

Figure 4.22 Reverse traffic channel modulation.

2,400 (1/4 rate), or 1,200 (1/8 rate) bps with, respectively, 192, 96, 48, or 24 bits per frame. The frame is then convolutionally encoded at a 1/3 rate, resulting in $3 \times 192 = 576$ code symbols per frame at full rate, or 28.8 ksps. For other voice data rates, the code symbols are repeated as necessary to cause each rate to input the same number of code symbols to the interleaver in a frame. The interleaver reads the data consecutively by column into an array of 32 rows and 18 columns; this procedure causes symbol repetitions to be located in different rows. As described more fully in Section 4.4, the rows of the interleaver array, each containing 18 code symbols, are read out in an order that depends on how many times the code symbols are repeated.

For example, if the symbols are repeated twice (i.e., the voice data rate is 4,800 bps), then every other symbol in a column of 32 symbols is a repeated symbol, making every other row in the array a repeated row. In this case, IS-

95 specifies that the rows be read out as follows: the first two odd-numbered rows, then their repeated rows; the second two odd-numbered rows, then their repetitions; and so forth. This procedure results in a sequence of two rows' worth of code symbols (36 symbols), their 36 repeated symbols, another 36 symbols followed by their 36 repeated symbols, and so on. In other words, the data repetitions are rearranged to occur by groups of 36 symbols. The purpose of this regrouping of the repeated symbols is to enable deletion of repeated symbols by groups. The motivation for such deletion is explained below.

Every six consecutive encoded symbols out of the interleaver are used to select a 64-chip Walsh sequence for orthogonal modulation according to the rule given in (4.6), with a chip rate of $28.8 \times 64/6 = 307.2$ kcps. Thus, each row of 18 symbols out of the interleaver generates three Walsh-encoded orthogonal modulation symbols, and each frame of 576 code symbols generates 96 orthogonal modulation symbols; because of the way that the symbols are read out from the interleaver array, these modulation symbols occur in alternating groups of six modulation symbols and $6(n-1)$ repeated modulation symbols, where n is the order of repetition. Altogether in a frame interval there are $96/6 = 16$ groups of six orthogonal modulation symbols, each composed of $6 \times 64 = 384$ Walsh chips. Table 4.5 summarizes the grouping of these symbols in terms of their repetitions.

To reduce the average amount of reverse link interference and thereby increase user capacity, on reverse link transmissions, repeated symbols are gated off. A "data burst randomizer" is used to select in a pseudorandom

Table 4.5 Grouping of orthogonal modulation symbols

Voice rate	Repetition	Modulation symbol grouping
9,600 bps	× 1	6 symbols (96/6 = 16 groups of 6); 6 symbols; etc. (no repetitions)
4,800 bps	× 2	6 symbols, 6 repeats (96/12 = 8 groups of 12); 6 symbols, 6 repeats; etc.
2,400 bps	× 4	6 symbols, 3 groups of 6 repeats (96/24 = 4 groups of 24); etc.
1,200 bps	× 8	6 symbols, 7 groups of 6 repeats (96/48 = 2 groups of 48); etc.

manner which of the groups of six symbols are transmitted, based on "control bits" that are values of long PN code sequence bits at a certain time. Figure 4.23 illustrates the concept of "filling" six-symbol slots of the frame with pseudorandomly selected transmissions.

The user-distinct offset of the 42-stage long PN code is then used to further spread the signal and ensure that the channels can be distinguished. The offset is implemented using a mask that depends on the electronic serial number (ESN) of the mobile. The masks and offsets on both forward and reverse traffic channels are identical for a given mobile user.

The modulation parameters of the reverse traffic channel are summarized in Table 4.6.

Transmissions on the reverse traffic channel begin with a preamble of all-zero data frames to aid the base station in acquiring the signal. Signaling messages from the mobile to the base station may be sent on the reverse traffic channel as well as the access channel. When a message is to be sent, it can be sent in a "dim and burst" mode during periods of active speech, in which a portion of the voice data in a frame is overwritten by the message data, or in a "blank and burst" mode during periods of speech inactivity, in which all the data in the frame are message data.

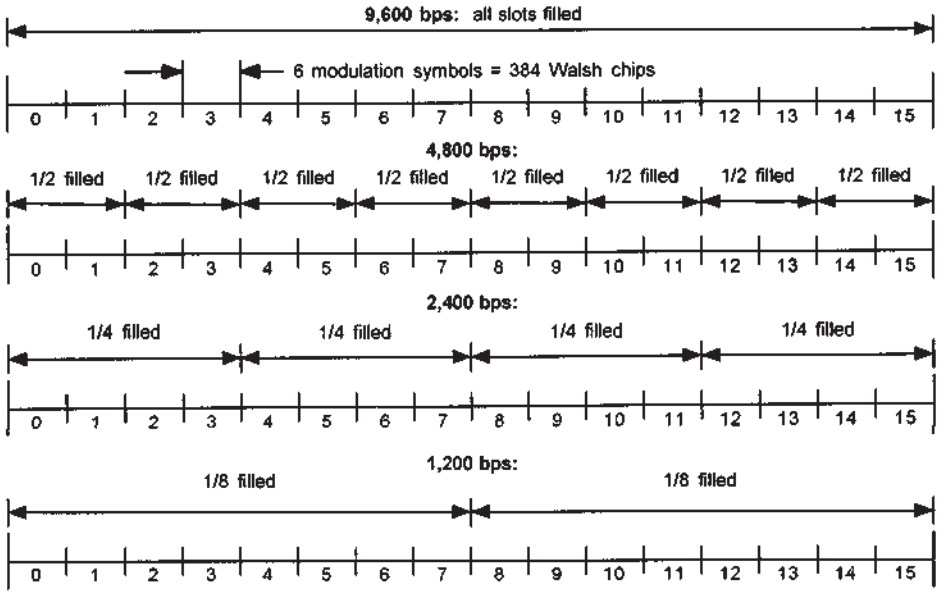

Figure 4.23 Data-burst randomizer operation.

Table 4.6 Reverse traffic channel modulation parameters

Parameter	Value				Units
Data rate	9,600	4,800	2,400	1,200	bps
PN chip rate	1.2288	1.2288	1.2288	1.2288	Mcps
Code rate	1/3	1/3	1/3	1/3	$\frac{\text{bits}}{\text{code symbol}}$
Transmit duty cycle	100	50	25	12.5	%
Code symbol rate	28,800	28,800	28,800	28,800	sps
Modulation rate	6	6	6	6	$\frac{\text{code sym}}{\text{mod sym}}$
Mod symbol rate	4,800	4,800	4,800	4,800	sps
Walsh chip rate	307.2	307.2	307.2	307.2	kcps
Mod symbol duration	208.33	208.33	208.33	208.33	μs
PN chips/code symbol	42.67	42.67	42.67	42.67	
PN chips/mod symbol	256	256	256	256	
PN chips/Walsh chip	4	4	4	4	

4.3.4 Comparison of Forward and Reverse Links

We can see that many similarities and differences exist between the operation of the forward and reverse links. Most of these differences can be traced to the fact that the forward link is a one-to-many transmission that is conducive to the transmission of a pilot for coherent demodulation. On the reverse link, a many-to-one transmission, a pilot is impractical and noncoherent demodulation must be employed. Thus, on the reverse link, it becomes difficult to ensure that the received signals from all mobiles are orthogonal. Instead, many interference-reducing techniques are used on the reverse link to ensure that capacity is maximized.

The voice-coding process for both links is identical up to the point of convolutional coding. Both links use powerful constraint-length 9 convolutional codes, but the forward link uses rate 1/2 and the reverse link uses rate 1/3. The asymptotic coding gain is 4.77 dB for both codes; however, the rate 1/3 code exhibits approximately 0.3 dB more coding gain over most ranges of SNR. Symbol repetition on both links is used to bring the data rate up to that of the 9.6-kbps code. Block interleaving is performed over a single 20-ms frame, which contains 384 symbols on the forward link and 576 on the reverse.

The mobile-to-base link uses Walsh-Hadamard sequences to form 64-ary modulation symbols. On the base-to-mobile link, the Walsh sequences are

assigned by the base station based on the usage of the channel. Thus, on the reverse link, the Walsh sequences are chosen by the encoded data symbols, and on the forward link, they are chosen by the use of the channel.

The forward link uses the Walsh sequences to distinguish among different users, with one period of a Walsh sequence per scrambled code symbol. The reverse link employs a distinct phase offset of the long PN code to distinguish among users. The long PN code on the forward channel is decimated to scramble the data for voice privacy, because the scrambling has to be done at the modulation symbol rate to preserve Walsh sequence orthogonality among users. The reverse long code chip rate can be greater than the Walsh chip rate because Walsh symbol orthogonality is not used to distinguish users on the reverse link.

All repeated symbols on a forward traffic channel are transmitted, while repeated symbols on a reverse traffic channel are gated off using a randomization process. The forward channels employ QPSK modulation, but the reverse channels use OQPSK modulation. The comparison of the two links can be summarized as shown in Table 4.7.

4.4 Special Features of the IS-95 System

In this subsection, we detail some of the modulation features mentioned briefly in the summaries of the IS-95 forward and reverse links that are given above, including details of the interleaving and power control schemes. Also, we draw attention to special features of the system operation not mentioned previously, including the various uses of diversity made by the system and the handoff procedures employed.

Table 4.7 Comparison between forward and reverse traffic channels

	Forward link	Reverse link
Coding	Rate 1/2, constraint length 9	Rate 1/3, constraint length 9
Interleaving	1 frame, 384 symbols	1 frame, 576 symbols
Walsh modulation	Distinguishes a particular user	Provides 64-ary modulation
Long PN code	Scrambles data	Distinguishes users
	Decimated to symbol rate	No need to change rate
Repeated symbols	All symbols transmitted	Repeated symbols gated off
Modulation	QPSK	OQPSK

4.4.1 Power Control

One of the goals in a multiple-access system, such as the IS-95 CDMA digital cellular telephone system, is to maximize the number of simultaneous users it can accommodate. If each mobile unit's transmitter is adjusted so that the signal-to-interference ratio received at the base station is at the minimal acceptable level, the capacity of the system will be maximized. Any increase in mobile power raises the interference in the system, and capacity is compromised. A highly complex and dynamic scheme must be used to control the received power and thus maximize the channel capacity.

In a cellular system, one mobile may be close to the base station, while another may be several miles away. The distance between different mobiles and the base station can vary by a factor of 100. Because propagation path loss is governed approximately by an inverse fourth-power law, variations of up to 80 dB can be found between different users. A method of power control with a high dynamic range must be used.

Another characteristic of the cellular channel is fading caused by the signal's being reflected off various objects, creating a signal whose multipath components mutually interfere in a manner that is very sensitive to the position of the antenna. The average rate of the fades as a mobile travels in an area characterized by multipath fading is a function of mobile speed, being approximately one fade per second per mile per hour of mobile speed in the 850-MHz frequency range. These fades can cause the signal to be attenuated by more than 30 dB in extreme cases. The power control method must be able to track the majority of these fades. Figure 4.24 illustrates the effect of fast fading on the received mobile signal power. The principles underlying propagation path loss, fading, and their mathematical modeling were the subject of Chapter 2.

The IS-95 system uses a combination of open-loop and closed-loop power control. In the open-loop scheme, the measured received signal strength from the base station is used to determine the transmit power for the mobile; a decrease in the average received base station signal power is a real-time indication of a degradation in the mobile channel that can be caused by variations in the characteristics of the signal path, such as terrain and manmade structures that introduce "shadowing" of the signal. Assuming that the reverse link is subject to the same changes in average path loss as the forward link, under open-loop power control the mobile's average transmit power is adjusted accordingly. This open-loop method of power control provides a quick response to changes in signal conditions. Because the

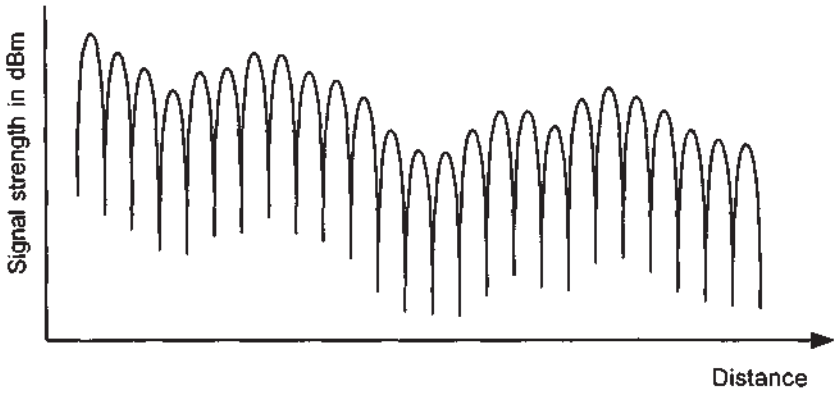

Figure 4.24 Effect of fast fading on signal strength.

forward and reverse links are separated in frequency (45 MHz for cellular and 80 MHz for PCS), however, they tend to fade independently. The correct setting of mobile transmitter power cannot be derived exactly using only the base station's average signal strength as measured at the mobile; feedback from the base station on its measurement of received mobile power must be also used.

In the IS-95 system, the base station measures the mobile signal strength and then transmits a power control command for the mobile to raise or lower its transmit power, thus providing a closed-loop refinement to the individual mobile's setting for its transmit power level.

4.4.1.1 Open-Loop Power Control

As mentioned above, each mobile station measures the received signal strength of the pilot signal. From this measurement and from information on the link power budget that is transmitted during initial synchronization, the forward link path loss is estimated. Assuming a similar path loss for the reverse link, the mobile uses this information to determine its transmitter power. A simplified link budget equation for the reverse link can be written

$$\text{Received SNR (dB)} = \text{mobile power (dBm)} - \text{net reverse losses (dB)} - \text{total reverse link noise and interference (dBm)} \quad (4.7a)$$

so that the mobile power to be transmitted is determined by

$$\text{Mobile power (dBm)} = \text{received SNR (dB)} + \text{net reverse losses (dB)} + \text{total reverse noise and interference (dBm)} \quad (4.7b)$$

where dBm denotes dB with respect to 1 mW and the net losses on the reverse link include propagation and other losses offset by antenna gains. For the forward link, the received base station power can be written

$$\text{Received power (dBm)} = \text{base power (dBm)} - \text{net forward losses (dB)} \quad (4.8a)$$

which can be solved for the net losses on the forward link:

$$\text{Net forward losses (dB)} = \text{base power (dBm)} - \text{received power (dBm)} \quad (4.8b)$$

This equation neglects the fact that the mobile measurement of received base station power is corrupted by forward link noise and interference. Substituting the net forward loss of (4.8b) in (4.7b) as an estimate of the net reverse loss and substituting a target value of the reverse link received SNR result in the equation

$$\text{Mobile power (dBm)} = \text{target SNR (dB)} + \text{base station power (dBm)} + \text{total reverse noise and interference (dBm)} - \text{received power (dBm)} \quad (4.9a)$$

$$= \text{constant (dB)} - \text{received power (dBm)} \quad (4.9b)$$

In IS-95, the nominal value of the constant in (4.9b) is specified to be −73 dB. This value can be attributed to the nominal values of −13 dB for the target SNR, −100 dBm for the reverse link noise and interference, and 40 dBm (10 W) for the base station power. The actual values of these parameters may be different, however—the point is that the required amount of mobile transmitter power is inversely proportional to the amount of received forward link power, as expressed by the relationship in (4.9b). Data for calibrating the constant in (4.9b) are broadcast to the mobiles on the sync channel.

By design, the temporal response of the mobile to this information is nonlinear. If the pilot is suddenly received with a high signal strength, the mobile transmitter power is reduced immediately, within several microseconds, on the principle that a higher received value of forward link power is a better estimate of *average* link loss, apart from fading. But if the measured

signal strength drops, the mobile power is increased slowly, on the order of a millisecond. The reason for this procedure is that if the power is not decreased quickly when a improvement in the path is encountered, the mobile will cause an increase in interference for the other users until the problem is corrected. Similarly, if the power is increased rapidly, the path loss may in fact be less than inferred from the forward link, perhaps because the base station signal faded and the mobile signal did not, and again the mobile would cause interference for the other users. Therefore, the system accepts a degradation in a single user's signal to prevent increased interference for all users.

Figure 4.25 shows the mobile transmit power corresponding to the channel in Figure 4.24 as controlled only by the open-loop nonlinear method. The dashed line in Figure 4.25 represents the transmit power if the received signal were traced without the nonlinear filter, and the solid line represents the transmit power with the filter.

4.4.1.2 Closed-Loop Power Control

Because the forward and reverse links may fade independently, closed-loop power control is employed in IS-95. The calculation of forward link path loss through the measurement of the base station received signal strength can be used as a rough estimate of the path loss on the reverse link. The true value, however, must be measured at the base station upon reception of the mobile's signal.

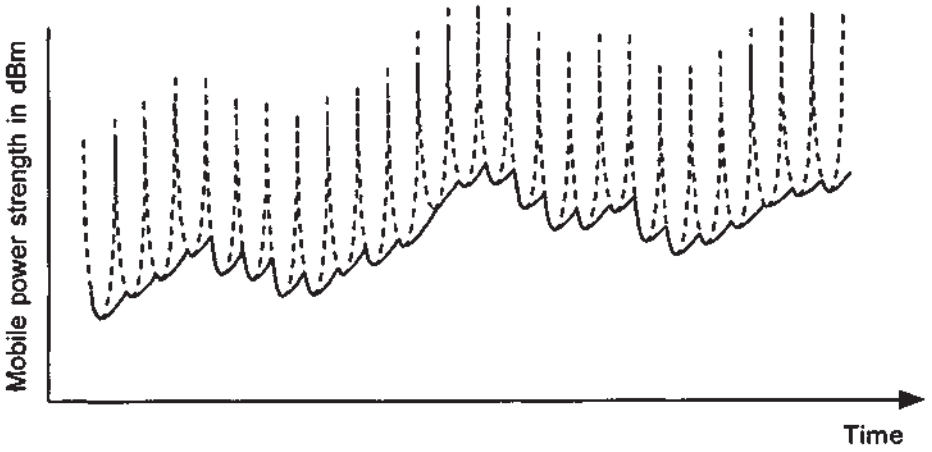

Figure 4.25 Mobile transmitter power as governed by the open-loop power control only.

At the base station, the measured signal strength is compared with the desired strength, and a power adjustment command is generated. The signal strength is estimated from intermediate outputs in the reverse link 64-ary orthogonal demodulator and is averaged over a "power control group" period of 1.25 ms (six Walsh 64-ary symbols). This power estimate is compared with the desired mobile received power level. If the average power level is greater than the threshold, the power command generator generates a "1" to instruct the mobile to decrease power. If the average power is less than the desired level, a "0" is generated to instruct the mobile to increase power. These commands instruct the mobile to adjust transmitter power by a predetermined amount, usually 1 dB.

On the forward link, in each 1.25-ms interval are $19.2 \times 1.25 = 24$ modulation symbols (i.e., scrambled and interleaved code symbols), as discussed previously in connection with the forward link traffic channel modulation diagram in Figure 4.17. The power control command is inserted into the forward traffic channel data stream following the interleaving and the scrambling by "puncturing" (overwriting) two consecutive modulation symbols with the power control bit. Because the code rate is 1/2, a power control symbol has an energy equivalent to one information bit. The position of the power control command in the data stream is pseudorandomly selected using values of the long-code chips in the preceding 1.25-ms interval.

Because the power control commands should affect the mobile transmitter power level as soon as possible, they are added to the data stream after the encoding and interleaving in order to eliminate the more than 20-ms delay associated with deinterleaving and decoding. The first 16 of the 24 modulation symbols in a 1.25-ms interval are possible starting positions for the power control bit. The starting position of the power control bit is determined by the values of the last four long-code chips used for scrambling in the preceding 1.25-ms period, as illustrated in Figure 4.26. Therfore, the separation between the start of consecutive power control bits is random, ranging from 9 to 39 modulation symbols. The 24th PN code chip from the last 1.25-ms period is the most significant bit in determining the position, and the 21st chip is the least significant bit. In the figure, the values of the chips 24, 23, 22, 21 are $1\ 0\ 1\ 1 = 11$; thus, in this case, the power control bit starts at the 11th modulation symbol.

The closed-loop power control also employs what is termed an *outer loop power control*. This mechanism ensures that the power control strategy is operating correctly. The frame error rate at the base station is measured and compared with the desired error rate. If the difference between error

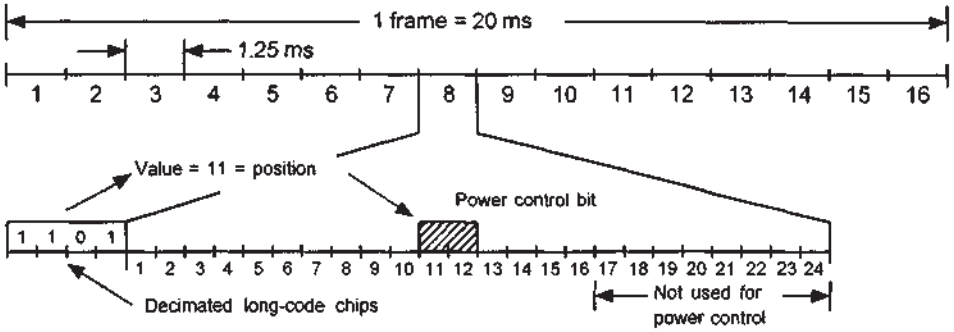

Figure 4.26 Example of power control bit position.

rates is large, then the power command threshold is adjusted to yield the desired FER.

4.4.1.3 Forward Link Power Control

In some mobile locations, the forward link may be subject to poor reception conditions, as evidenced at the mobile by an unacceptably high frame error rate. The mobile in such a situation can request an increase in the power transmitted to it by the base station.

When forward link power control is enabled, the base station periodically reduces the power transmitted to an individual mobile unit. This process continues until the mobile senses an increase in the forward link frame error rate. The mobile reports the number of frame errors to the base. With this information the base station can decide whether to increase power by an small amount, nominally 0.5 dB. Before the base station complies with the request, it must consider other requests, loading, and the current transmitted power.

The rate of forward link power adjustment is slower than that of reverse link power control, increments being made on the order of the frame interval, 20 ms. Also, the dynamic range of forward link power adjustments is limited to about $\pm$ 6 dB about the nominal power.

The effect of forward link power control is studied in Chapter 11 in connection with the optimal allocation of forward link power.

4.4.2 Interleaving Techniques

Used in conjunction with repetition or coding, interleaving is a form of time diversity that is employed to disperse bursts of errors in time. A sequence of symbols is permuted or interleaved before transmission over a bursty channel. If a burst of errors occurs during transmission, restoring the original sequence to its original ordering has the effect of spreading the errors over time. If the interleaver is designed well, then the errors have a more random pattern that can more easily be corrected by coding techniques.

The most commonly employed interleaving techniques fall into two classes. The more common type is *block interleaving*. This form is used when the data are divided into blocks or frames, such as in the IS-95 system. *Convolutional interleaving*, on the other hand, is more practical for a continuous data stream. Block interleaving is known for its ease of implementation, whereas convolutional interleaving has performance advantages. Continuous operation allows the original overhead associated with convolutional interleaving to become insignificant. IS-95 uses other forms of interleaving that are based on block-like techniques and are described further. A brief review of the general subject of interleaving is given in Appendix 4A of this chapter.

Several parameters describe interleaver performance. One of the most important is the minimum separation, S, which is the minimum distance by which consecutive errors in a burst are dispersed. Naturally this parameter depends on the length of the burst, decreasing as burst length increases. As an extreme, consider the case where the burst length is the same as the entire sequence. The minimum separation will be one because no matter how the data are permuted, an error always resides next to another error. Because interleaving involves storing some symbols in memory elements while reading others from memory elements, a delay is experienced. In general, this same delay is also experienced upon deinterleaving. The delay D is expressed as the number of additional read/write operations required to perform both interleaving and deinterleaving. As just mentioned, the process requires a number of memory elements for implementation denoted by the parameter M. To achieve good interleaver performance, the minimum separation should be as great as possible, while the delay and memory requirement should be as small as possible. This fact often leads to performance described by ratios of minimum separation-to-delay S/D and minimum separation-to-memory S/M.

An (I, J) block interleaver can be viewed as an array of storage locations which contains I columns and J rows. The data are written into

the array by columns and read out by rows, as demonstrated in Figure 4.27. The first symbol written into the array is written into the top left corner, but the first symbol read out is from the bottom left corner. Continuous processing of data requires two arrays: one has data written into it, the other has data being read from it. The deinterleaving process simply requires duplicate arrays in order to reverse the interleaving procedure.

Properties of the block interleaver are readily apparent by observing the array. Let the length of a burst of errors be given by B. The minimum separation of any two errors in the burst of length B is given by

$$S = \begin{cases} J & B \leq I \\ 1 & B > I \end{cases} \tag{4.10}$$

The interleaver delay is IJ at the transmitter and IJ at the receiver. Thus, the total delay is

$$D = 2IJ \tag{4.11}$$

For continuous operation, two arrays are required, giving a memory requirement of

$$M = 2IJ \tag{4.12}$$

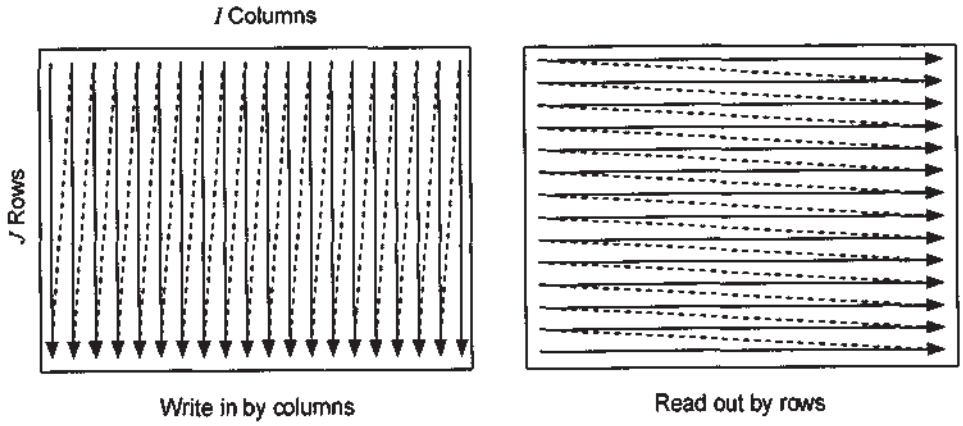

Figure 4.27 Reading to and writing from an (I, J) block interleaver.

The minimum separation of the interleaver can be changed by reading the rows out in a different order. The delay and memory requirement are essentially unchanged by this action. The largest minimum separation for $B \leq I$ is achieved by reading the rows in the order described above. However, this method yields $S = 1$ for $B > I$. Other reading strategies can reduce the minimum separation for $B \leq I$ while increasing it for $B > I$. The IS-95 system employs such techniques. Unless the reading strategy is determined carefully, the minimum separation is generally reduced.

The IS-95 system interleaves data from single data frames, which have durations of 20 ms for all channels except the sync channel, which has a frame duration of 26.66 ms. Thus, all the IS-95 interleavers operate on blocks of symbols. Strictly speaking, however, block interleaving is not employed, but the type of interleaving depends on the channel and original data rate. For example, the reverse link gates the power amplifier on and off to remove repeated symbols, and the interleaver is designed to facilitate this action. The forward link reads the rows from the array in a nonconventional order to modify the minimum-separation properties.

Interleaving on the sync channel uses a nonconventional technique that is best described as *bit reversal*. As diagrammed previously in Figure 4.13, sync channel code symbols at 2.4 ksps are repeated once, resulting in a 4.8-ksps rate into the interleaver. The symbols are interleaved over a 26.667-ms period, which gives a total of 26.667 ms $\times$ 4.8 ksps = 128 symbols per frame. Let the first symbol into the interleaver be assigned position 0, and the last be 127. The read order is given by changing the position to a 7-bit number, reversing the order of the bits, and changing the binary number back to decimal form.

For example, suppose a 16-bit sequence is to be interleaved, and the first bit is assigned position 0, and the last bit is 15. The original ordering is thus

0, 1, 2, 3, 4, 5, 6, 7, 8, 9, 10, 11, 12, 13, 14, 15

Expressing this ordering in binary format yields

0000, 0001, 0010, 0011, 0100, 0101, 0110, 0111,
1000, 1001, 1010, 1011, 1100, 1101, 1110, 1111

Reversing the order of the bits in each binary number gives

0000, 1000, 0100, 1100, 0010, 1010, 0110, 1110,
0001, 1001, 0101, 1101, 0011, 1011, 0111, 1111

Converting the binary representation back to decimal form gives the order with which the symbols are read

$$0, 8, 4, 12, 2, 10, 6, 14, 1, 9, 5, 13, 3, 11, 7, 15$$

Through observation, the minimum spacing for symbols in a burst of length B is

$$S = \begin{cases} 4, & B = 2 \\ 2, & 3 \leq B \leq 4 \\ 1, & B \geq 5 \end{cases}$$

IS-95 uses the bit reversal technique over the 128 symbols in the sync channel frame. The input array is in Figure 4.28(a), and the output array in Figure 4.28(b), where the symbols are read into the input array by columns are read out of the output array by columns. As an example, the 38th symbol in the input array would occupy position 37, which is 0100101. Reversing the order gives 1010010, which is decimal 82. Note that symbol 37 in the input array shares the same position as 82 in the output array. The minimum separation can be found by observation and ranges from $S = 32$ for $B = 2$ to $S = 1$ for $B \geq 33$. The memory requirement is twice the number of symbols in a block for continuous operation: $M = 2 \times 128 = 256$. The delay is also equivalent to twice the number of symbols in the array:

$$D = 256 = \frac{256 \text{ sym}}{4{,}800 \text{ sym/s}} = 53.333 \text{ ms} \tag{4.13}$$

The paging and traffic channels use the same interleaver structure on a single 20-ms frame, which contains 384 symbols. As with the sync channel, IS-95 specifies the interleaver using input and output arrays. The paging channel can generate data at 9.6 or 4.8 kbps, but the traffic channel can operate at four rates. The full-rate 9.6-kbps interleaver is shown in Figure 4.29. The 4.8-, 2.4-, and 1.2-kbps interleavers are shown in Figures 4.30, 4.31, and 4.32, respectively. Note that all of the interleavers are identical, and the difference between the four is only the repetition of the input symbols. Thus, the true structure, without repetition, is shown by the full-rate scheme. The arrays corresponding to less than full rate show the symbol repetition. Note that adjacent symbol repetitions going into the interleaver are converted to block repetitions coming out of the interleaver.

By observing the first six symbols of the full-rate output array, we find that the symbols are separated by 64 positions. The second group of six,

0	16	32	48	64	80	96	112
1	17	33	49	65	81	97	113
2	18	34	50	66	82	98	114
3	19	35	51	67	83	99	115
4	20	36	52	68	84	100	116
5	21	37	53	69	85	101	117
6	22	38	54	70	86	102	118
7	23	39	55	71	87	103	119
8	24	40	56	72	88	104	120
9	25	41	57	73	89	105	121
10	26	42	58	74	90	106	122
11	27	43	59	75	91	107	123
12	28	44	60	76	92	108	124
13	29	45	61	77	93	109	125
14	30	46	62	78	94	110	126
15	31	47	63	79	95	111	127

(a) Interleaver input array

0	4	2	6	1	5	3	7
64	68	66	70	65	69	67	71
32	36	34	38	33	37	35	39
96	100	98	102	97	101	99	103
16	20	18	22	17	21	19	23
80	84	82	86	81	85	83	87
48	52	50	54	49	53	51	55
112	116	114	118	113	117	115	119
8	12	10	14	9	13	11	15
72	76	74	78	73	77	75	79
40	44	42	46	41	45	43	47
104	108	106	110	105	109	107	111
24	28	26	30	25	29	27	31
88	92	90	94	89	93	91	95
56	60	58	62	57	61	59	63
120	124	122	126	121	125	123	127

(b) Interleaver output array

Figure 4.28 Forward link sync channel interleaving.

1	25	49	73	97	121	145	169	193	217	241	265	289	313	337	361
2	26	50	74	98	122	146	170	194	218	242	266	290	314	338	362
3	27	51	75	99	123	147	171	195	219	243	267	291	315	339	363
4	28	52	76	100	124	148	172	196	220	244	268	292	316	340	364
5	29	53	77	101	125	149	173	197	221	245	269	293	317	341	365
6	30	54	78	102	126	150	174	198	222	246	270	294	318	342	366
7	31	55	79	103	127	151	175	199	223	247	271	295	319	343	367
8	32	56	80	104	128	152	176	200	224	248	272	296	320	344	368
9	33	57	81	105	129	153	177	201	225	249	273	297	321	345	369
10	34	58	82	106	130	154	178	202	226	250	274	298	322	346	370
11	35	59	83	107	131	155	179	203	227	251	275	299	323	347	371
12	36	60	84	108	132	156	180	204	228	252	276	300	324	348	372
13	37	61	85	109	133	157	181	205	229	253	277	301	325	349	373
14	38	62	86	110	134	158	182	206	230	254	278	302	326	350	374
15	39	63	87	111	135	159	183	207	231	255	279	303	327	351	375
16	40	64	88	112	136	160	184	208	232	256	280	304	328	352	376
17	41	65	89	113	137	161	185	209	233	257	281	305	329	353	377
18	42	66	90	114	138	162	186	210	234	258	282	306	330	354	378
19	43	67	91	115	139	163	187	211	235	259	283	307	331	355	379
20	44	68	92	116	140	164	188	212	236	260	284	308	332	356	380
21	45	69	93	117	141	165	189	213	237	261	285	309	333	357	381
22	46	70	94	118	142	166	190	214	238	262	286	310	334	358	382
23	47	71	95	119	143	167	191	215	239	263	287	311	335	359	383
24	48	72	96	120	144	168	192	216	240	264	288	312	336	260	384

(a) Interleaver input array

1	9	5	13	3	11	7	15	2	10	6	14	4	12	8	16
65	73	69	77	67	75	71	79	66	74	70	78	68	76	72	80
129	137	133	141	131	139	135	143	130	138	134	142	132	140	136	144
193	201	197	205	195	203	199	207	194	202	198	206	196	204	200	208
257	265	261	269	259	267	263	271	258	266	262	270	260	268	264	272
321	329	325	333	323	331	327	335	322	330	326	334	324	332	328	336
33	41	37	45	35	43	39	47	34	42	38	46	36	44	40	48
97	105	101	109	99	107	103	111	98	106	102	110	100	108	104	112
161	169	165	173	163	171	167	175	162	170	166	174	164	172	168	176
225	233	229	237	227	235	231	239	226	234	230	238	228	236	232	240
289	297	293	301	291	299	295	303	290	298	294	302	292	300	296	304
353	361	357	365	355	363	359	367	354	362	358	366	356	364	360	368
17	25	21	29	19	27	23	31	18	26	22	30	20	28	24	32
81	89	85	93	83	91	87	95	82	90	86	94	84	92	88	96
145	153	149	157	147	155	151	159	146	154	150	158	148	156	152	160
209	217	213	221	211	219	215	223	210	218	214	222	212	220	216	224
273	281	277	285	275	283	279	287	274	282	278	286	276	284	280	288
337	345	341	349	339	347	343	351	338	346	342	350	340	348	344	352
49	57	53	61	51	59	55	63	50	58	54	62	52	60	56	64
113	121	117	125	115	123	119	127	114	122	118	126	116	124	120	128
177	185	181	189	179	187	183	191	178	186	182	190	180	188	184	192
241	249	245	253	243	251	247	255	242	250	246	254	244	252	248	256
305	313	309	317	307	315	311	319	306	314	310	318	308	316	312	320
369	377	373	381	371	379	375	383	370	378	374	382	372	380	376	384

(b) Interleaver output array

Figure 4.29 Forward traffic and paging channels interleaving at 9,600 bps.

1	13	25	37	49	61	73	85	97	109	121	133	145	157	169	181
1	13	25	37	49	61	73	85	97	109	121	133	145	157	169	181
2	14	26	38	50	62	74	86	98	110	122	134	146	158	170	182
2	14	26	38	50	62	74	86	98	110	122	134	146	158	170	182
3	15	27	39	51	63	75	87	99	111	123	135	147	159	171	183
3	15	27	39	51	63	75	87	99	111	123	135	147	159	171	183
4	16	28	40	52	64	76	88	100	112	124	136	148	160	172	184
4	16	28	40	52	64	76	88	100	112	124	136	148	160	172	184
5	17	29	41	53	65	77	89	101	113	125	137	149	161	173	185
5	17	29	41	53	65	77	89	101	113	125	137	149	161	173	185
6	18	30	42	54	66	78	90	102	114	126	138	150	162	174	186
6	18	30	42	54	66	78	90	102	114	126	138	150	162	174	186
7	19	31	43	55	67	79	91	103	115	127	139	151	163	175	187
7	19	31	43	55	67	79	91	103	115	127	139	151	163	175	187
8	20	32	44	56	68	80	92	104	116	128	140	152	164	176	188
8	20	32	44	56	68	80	92	104	116	128	140	152	164	176	188
9	21	33	45	57	69	81	93	105	117	129	141	153	165	177	189
9	21	33	45	57	69	81	93	105	117	129	141	153	165	177	189
10	22	34	46	58	70	82	94	106	118	130	142	154	166	178	190
10	22	34	46	58	70	82	94	106	118	130	142	154	166	178	190
11	23	35	47	59	71	83	95	107	119	131	143	155	167	179	191
11	23	35	47	59	71	83	95	107	119	131	143	155	167	179	191
12	24	36	48	60	72	84	96	108	120	132	144	156	168	180	192
12	24	36	48	60	72	84	96	108	120	132	144	156	168	180	192

(a) Interleaver input array

1	5	3	7	2	6	4	8	1	5	3	7	2	6	4	8
33	37	35	39	34	38	36	40	33	37	35	39	34	38	36	40
65	69	67	71	66	70	68	72	65	69	67	71	66	70	68	72
97	101	99	103	98	102	100	104	97	101	99	103	98	102	100	104
129	133	131	135	130	134	132	136	129	133	131	135	130	134	132	136
161	165	163	167	162	166	164	168	161	165	163	167	162	166	164	168
17	21	19	23	18	22	20	24	17	21	19	23	18	22	20	24
49	53	51	55	50	54	52	56	49	53	51	55	50	54	52	56
81	85	83	87	82	86	84	88	81	85	83	87	82	86	84	88
113	117	115	119	114	118	116	120	113	117	115	119	114	118	116	120
145	149	147	151	146	150	148	152	145	149	147	151	146	150	148	152
177	181	179	183	178	182	180	184	177	181	179	183	178	182	180	184
9	13	11	15	10	14	12	16	9	13	11	15	10	14	12	16
41	45	43	47	42	46	44	48	41	45	43	47	42	46	44	48
73	77	75	79	74	78	76	80	73	77	75	79	74	78	76	80
105	109	107	111	106	110	108	112	105	109	107	111	106	110	108	112
137	141	139	143	138	142	140	144	137	141	139	143	138	142	140	144
169	173	171	175	170	174	172	176	169	173	171	175	170	174	172	176
25	29	27	31	26	30	28	32	25	29	27	31	26	30	28	32
57	61	59	63	58	62	60	64	57	61	59	63	58	62	60	64
89	93	91	95	90	94	92	96	89	93	91	95	90	94	92	96
121	125	123	127	122	126	124	128	121	125	123	127	122	126	124	128
153	157	155	159	154	158	156	160	153	157	155	159	154	158	156	160
185	189	187	191	186	190	188	192	185	189	187	191	186	190	188	192

(b) Interleaver output array

Figure 4.30 Forward traffic and paging channels interleaving at 4,800 bps.

1	7	13	19	25	31	37	43	49	55	61	67	73	79	85	91
1	7	13	19	25	31	37	43	49	55	61	67	73	79	85	91
1	7	13	19	25	31	37	43	49	55	61	67	73	79	85	91
1	7	13	19	25	31	37	43	49	55	61	67	73	79	85	91
2	8	14	20	26	32	38	44	50	56	62	68	74	80	86	92
2	8	14	20	26	32	38	44	50	56	62	68	74	80	86	92
2	8	14	20	26	32	38	44	50	56	62	68	74	80	86	92
2	8	14	20	26	32	38	44	50	56	62	68	74	80	86	92
3	9	15	21	27	33	39	45	51	57	63	69	75	81	87	93
3	9	15	21	27	33	39	45	51	57	63	69	75	81	87	93
3	9	15	21	27	33	39	45	51	57	63	69	75	81	87	93
3	9	15	21	27	33	39	45	51	57	63	69	75	81	87	93
4	10	16	22	28	34	40	46	52	58	64	70	76	82	88	94
4	10	16	22	28	34	40	46	52	58	64	70	76	82	88	94
4	10	16	22	28	34	40	46	52	58	64	70	76	82	88	94
4	10	16	22	28	34	40	46	52	58	64	70	76	82	88	94
5	11	17	23	29	35	41	47	53	59	65	71	77	83	89	95
5	11	17	23	29	35	41	47	53	59	65	71	77	83	89	95
5	11	17	23	29	35	41	47	53	59	65	71	77	83	89	95
5	11	17	23	29	35	41	47	53	59	65	71	77	83	89	95
6	12	18	24	30	36	42	48	54	60	66	72	78	84	90	96
6	12	18	24	30	36	42	48	54	60	66	72	78	84	90	96
6	12	18	24	30	36	42	48	54	60	66	72	78	84	90	96
6	12	18	24	30	36	42	48	54	60	66	72	78	84	90	96

(a) Interleaver input array

1	3	2	4	1	3	2	4	1	3	2	4	1	3	2	4
17	19	18	20	17	19	18	20	17	19	18	20	17	19	18	20
33	35	34	36	33	35	34	36	33	35	34	36	33	35	34	36
49	51	50	52	49	51	50	52	49	51	50	52	49	51	50	52
65	67	66	68	65	67	66	68	65	67	66	68	65	67	66	68
81	83	82	84	81	83	82	84	81	83	82	84	81	83	82	84
9	11	10	12	9	11	10	12	9	11	10	12	9	11	10	12
25	27	26	28	25	27	26	28	25	27	26	28	25	27	26	28
41	43	42	44	41	43	42	44	41	43	42	44	41	43	42	44
57	59	58	60	57	59	58	60	57	59	58	60	57	59	58	60
73	75	74	76	73	75	74	76	73	75	74	76	73	75	74	76
89	91	92	94	89	91	92	94	89	91	92	94	89	91	92	94
5	7	6	8	5	7	6	8	5	7	6	8	5	7	6	8
21	23	22	24	21	23	22	24	21	23	22	24	21	23	22	24
37	39	38	40	37	39	38	40	37	39	38	40	37	39	28	40
53	55	54	56	53	55	54	56	53	55	54	56	53	55	54	56
69	71	70	72	69	71	70	72	69	71	70	72	69	71	70	72
85	87	86	88	85	87	86	88	85	87	86	88	85	87	86	88
13	15	14	16	13	15	14	16	13	15	14	16	13	16	14	16
29	31	30	32	29	31	30	32	29	31	30	32	29	31	30	32
45	47	26	28	45	47	46	48	45	47	46	48	45	47	46	48
61	63	62	64	61	63	62	64	61	63	62	64	61	63	62	64
77	79	78	80	77	79	78	80	77	79	78	80	77	79	78	80
93	95	94	96	93	95	94	96	96	95	94	96	93	95	94	96

(b) Interleaver output array

Figure 4.31 Forward traffic channel interleaving at 2,400 bps.

1	4	7	10	13	16	19	22	25	28	31	34	37	40	43	46
1	4	7	10	13	16	19	22	25	28	31	34	37	40	43	46
1	4	7	10	13	16	19	22	25	28	31	34	37	40	43	46
1	4	7	10	13	16	19	22	25	28	31	34	37	40	43	46
1	4	7	10	13	16	19	22	25	28	31	34	37	40	43	46
1	4	7	10	13	16	19	22	25	28	31	34	37	40	43	46
1	4	7	10	13	16	19	22	25	28	31	34	37	40	43	46
1	4	7	10	13	16	19	22	25	28	31	34	37	40	43	46
2	5	8	11	14	17	20	23	26	29	32	35	38	41	44	47
2	5	8	11	14	17	20	23	26	29	32	35	38	41	44	47
2	5	8	11	14	17	20	23	26	29	32	35	38	41	44	47
2	5	8	11	14	17	20	23	26	29	32	35	38	41	44	47
2	5	8	11	14	17	20	23	26	29	32	35	38	41	44	47
2	5	8	11	14	17	20	23	26	29	32	35	38	41	44	47
2	5	8	11	14	17	20	23	26	29	32	35	38	41	44	47
2	5	8	11	14	17	20	23	26	29	32	35	38	41	44	47
3	6	9	12	15	18	21	24	27	30	33	36	39	42	45	48
3	6	9	12	15	18	21	24	27	30	33	36	39	42	45	48
3	6	9	12	15	18	21	24	28	30	33	36	39	42	45	48
3	6	9	12	15	18	21	24	28	30	33	36	39	42	45	48
3	6	9	12	15	18	21	24	28	30	33	36	39	42	45	48
3	6	9	12	15	18	21	24	28	30	33	36	39	42	45	48
3	6	9	12	15	18	21	24	28	30	33	36	39	42	45	48
3	6	9	12	15	18	21	24	28	30	33	36	39	42	45	48

(a) Interleaver input array

1	2	1	2	1	2	1	2	1	2	1	2	1	2	1	2
9	10	9	10	9	10	9	10	9	10	9	10	9	10	9	10
17	18	17	18	17	18	17	18	17	18	17	18	17	18	17	18
25	26	25	26	25	26	25	26	25	26	25	26	25	26	25	26
33	34	33	34	33	34	33	34	33	34	33	34	33	34	33	34
41	43	41	42	41	42	41	42	41	42	41	42	41	42	41	42
5	6	5	6	5	6	5	6	5	6	5	6	5	6	5	6
13	14	13	14	13	14	13	14	13	14	13	14	13	14	13	14
21	22	21	22	21	22	21	22	21	22	21	22	21	22	21	22
29	30	29	30	29	30	29	30	29	30	29	30	29	30	29	30
37	38	37	38	37	38	37	38	37	38	37	38	37	38	37	38
45	46	45	46	45	46	45	46	45	46	45	46	45	46	45	46
3	4	3	4	3	4	3	4	3	4	3	4	3	4	3	4
11	12	11	12	11	12	11	12	11	12	11	12	11	12	11	12
19	20	19	20	19	20	19	20	19	20	19	20	19	20	19	20
27	28	27	28	27	28	27	28	27	28	27	28	27	28	27	28
35	36	35	36	35	36	35	36	35	36	35	36	35	36	35	36
43	44	43	44	43	44	43	44	43	44	43	44	43	44	43	44
7	8	7	8	7	8	7	8	7	8	7	8	7	8	7	8
15	16	15	16	15	16	15	16	15	16	15	16	15	16	15	16
23	24	23	24	23	24	23	24	23	24	23	24	23	24	23	24
31	32	31	32	31	32	31	32	31	32	31	32	31	32	31	32
39	40	39	40	39	40	39	40	39	40	39	40	39	40	39	40
47	48	47	48	47	48	47	48	47	48	47	48	47	48	47	48

(b) Interleaver output array

Figure 4.32 Forward traffic channel interleaving at 1,200 bps.

as well as subsequent groups of six, exhibit the same property. This is a characteristic of an ($I = 6$, $J = 64$) block interleaver. These observations demonstrate that the paging and traffic channels use a (6, 64) block interleaver, which is shown in Figure 4.33.

The read array for the 9,600-bps traffic and paging channels (Figure 4.29) does correspond to the (6, 64) array of Figure 4.33, but the rows are read out in a permuted order. Upon closer observation, it becomes evident that the rows are read from the (6, 64) array in bit-reversal order. The first six symbols are from row 0. The next six are from row 32. The next six are those in row 16, and so forth. Reading the rows in bit-reversal order changes the properties of the interleaver. For a conventional (6, 64) array, the minimum spacing is given by $S = 64$ for $B \leq 6$ and $S = 1$ for $B > 6$. With this permuted structure, the minimum-separation profile is found to be

$$S = \begin{cases} 64, & B \leq 5 \\ 32, & B = 6 \\ 16, & B = 7 \\ 3, & 8 \leq B \leq 48 \\ 2, & 49 \leq B \leq 96 \\ 1, & B \geq 97 \end{cases} \tag{4.14}$$

Using the bit-reversal row reading, the minimum separation for $B > I$ is increased at the expense of the separation for $B \leq I$. The memory and delay requirements are equal to those of conventional block interleavers:

$$M = 2IJ = 2 \times 6 \times 64 = 768 \tag{4.15}$$

$$D = 2IJ = 768 = \frac{768 \text{ sym}}{19{,}200 \text{ sym/s}} = 40 \text{ ms} \tag{4.16}$$

The encoding and interleaving process for the reverse link was shown previously in Figure 4.21 for the access channel and 4.22 for the reverse traffic channel. Similar to the forward traffic channel, the access channel reads the rows from the input array in bit-reversal order. On the reverse traffic channel, symbols at the lower data rates (1.2, 2.4, and 4.8 kbps) are repeated after convolutional encoding. The transmitter pseudorandomly gates the amplifier on and off to eliminate the repeated symbols. The traffic channel interleaver is designed to operate in conjunction with the amplifier gating.

Row 0	1	65	129	193	257	321	Row 32	33	97	161	225	289	353
Row 1	2	66	130	194	258	322	Row 33	34	98	162	226	290	354
Row 2	3	67	131	195	259	323	Row 34	35	99	163	227	291	355
Row 3	4	68	132	196	260	324	Row 35	36	100	164	228	292	356
Row 4	5	69	133	197	261	325	Row 36	37	101	165	229	293	357
Row 5	6	70	134	198	262	326	Row 37	38	102	166	230	294	358
Row 6	7	71	135	199	263	327	Row 38	39	103	167	231	295	359
Row 7	8	72	136	200	264	328	Row 39	40	104	168	232	296	360
Row 8	9	73	137	201	265	329	Row 40	41	105	169	233	297	361
Row 9	10	74	138	202	266	330	Row 41	42	106	170	234	298	362
Row 10	11	75	139	203	267	331	Row 42	43	107	171	235	299	363
Row 11	12	76	140	204	268	332	Row 43	44	108	172	236	300	364
Row 12	13	77	141	205	269	333	Row 44	45	109	173	237	301	365
Row 13	14	78	142	206	270	334	Row 45	46	110	174	238	302	366
Row 14	15	79	143	207	271	335	Row 46	47	111	175	239	303	367
Row 15	16	80	144	208	272	336	Row 47	48	112	176	240	304	368
Row 16	17	81	145	209	273	337	Row 48	49	113	177	241	305	369
Row 17	18	82	146	210	274	338	Row 49	50	114	178	242	306	370
Row 18	19	83	147	211	275	339	Row 50	51	115	179	243	307	371
Row 19	20	84	148	212	276	340	Row 51	52	116	180	244	308	372
Row 20	21	85	149	213	277	341	Row 52	53	117	181	245	309	373
Row 21	22	86	150	214	278	342	Row 53	54	118	182	246	310	374
Row 22	23	87	151	215	279	343	Row 54	55	119	183	247	311	375
Row 23	24	88	152	216	280	344	Row 55	56	120	184	248	312	376
Row 24	25	89	153	217	281	345	Row 56	57	121	185	249	313	377
Row 25	26	90	154	218	282	346	Row 57	58	122	186	250	314	378
Row 26	27	91	155	219	283	347	Row 58	59	123	187	251	315	379
Row 27	28	92	156	220	284	348	Row 59	60	124	188	252	316	380
Row 28	29	93	157	221	285	349	Row 60	61	125	189	253	317	381
Row 29	30	94	158	222	286	350	Row 61	62	126	190	254	318	382
Row 30	31	95	159	223	287	351	Row 62	63	127	191	255	319	383
Row 31	32	96	160	224	288	352	Row 63	64	128	192	256	320	384

Figure 4.33 Forward traffic and paging channel interleaving is observed to be equivalent to a (6, 64) array.

Data from the access channel are generated at 4.8 kbps, repeated once, and $R_c = 1/3$ convolutionally encoded to 28.8 ksps. Interleaving is performed within a single 20-ms frame containing 20 ms $\times$ 28.8 ksps = 576 symbols. Symbols are read from the ($I = 18$, $J = 32$) array by rows in bit-reversal order. No gating is used on the access channel, and thus, both identical symbols are transmitted. The order of the rows is given by

0, 16, 8, 24, 4, 20, 12, 28, 2, 18, 10, 26, 6, 22, 14, 30,
1, 17, 9, 25, 5, 21, 13, 29, 3, 19, 11, 27, 7, 23, 15, 31

where 0 is the first row and 31 is the last row. The (18, 32) array with the symbols read out by consecutive rows is shown in Figure 4.34. The access channel minimum-separation profile can be found to be

$$S = \begin{cases} 32, & B \leq 17 \\ 16, & B = 18 \\ 8, & B = 19 \\ 3, & 20 \leq B \leq 72 \\ 2, & 73 \leq B \leq 144 \\ 1, & B \geq 145 \end{cases} \tag{4.17}$$

As with conventional block interleavers, the memory requirement is twice the number of symbols in the array:

1	33	65	97	129	161	193	225	257	289	321	353	385	417	449	481	513	545
17	49	81	113	145	177	209	241	273	305	337	369	401	433	465	497	529	561
9	41	73	105	137	169	201	233	265	297	329	361	393	425	457	489	521	553
25	57	89	121	153	185	217	249	281	313	345	377	409	441	473	505	537	569
5	37	69	101	133	165	197	229	261	293	325	357	389	421	453	485	517	549
21	53	85	117	149	181	213	245	277	309	341	373	405	437	469	501	533	565
13	45	77	109	141	173	205	237	269	301	333	365	397	429	461	493	525	557
29	61	93	125	157	189	221	253	285	317	349	381	413	445	477	509	541	573
3	35	67	99	131	163	195	227	259	291	323	355	387	419	451	483	515	547
19	51	83	115	147	179	211	243	275	307	339	371	403	435	467	499	531	563
11	43	75	107	139	171	203	235	267	299	331	363	395	427	459	491	523	555
27	59	91	123	155	187	219	251	283	315	347	379	411	443	475	507	539	571
7	39	71	103	135	167	199	231	263	295	327	359	391	423	455	487	519	551
23	55	87	119	151	183	215	247	279	311	343	375	407	439	471	503	535	567
15	47	79	111	143	175	207	239	271	303	335	367	399	431	463	495	527	559
31	63	95	127	159	191	223	255	287	319	351	383	415	447	479	511	543	575
2	34	66	98	130	162	194	226	258	290	322	354	386	418	450	482	514	546
18	50	82	114	146	178	210	242	274	306	338	370	402	434	466	498	530	562
10	42	74	106	138	170	202	234	266	298	330	362	394	426	258	490	522	554
26	58	90	122	154	186	218	250	282	314	346	378	410	442	474	506	538	570
6	38	70	102	134	166	198	230	262	294	326	358	390	422	454	486	518	550
22	54	86	118	150	182	214	246	278	310	342	374	406	438	470	502	534	566
14	46	78	110	142	174	206	238	270	302	334	366	398	430	462	494	526	558
30	62	94	126	158	190	222	254	286	318	350	382	414	446	478	510	542	574
4	36	68	100	132	164	196	228	260	292	324	356	388	420	452	484	516	548
20	52	84	116	148	180	212	244	276	308	340	372	404	436	468	500	532	564
12	44	78	108	140	172	204	236	268	300	332	364	396	428	460	492	524	556
28	60	92	124	156	188	220	252	284	316	348	380	412	444	476	508	540	572
8	40	72	104	136	168	200	232	264	296	328	360	392	424	456	488	520	552
24	56	88	120	152	184	216	248	280	312	344	376	408	440	472	504	536	568
16	48	80	112	144	176	208	240	272	304	336	368	400	432	464	496	528	560
32	64	96	128	160	192	224	256	288	320	352	384	416	448	480	512	544	576

Figure 4.34 Output of the access channel interleaver.

$$M = 2IJ = 2 \times 18 \times 32 = 1152 \tag{4.18}$$

Likewise, the delay is

$$D = 2IJ = 1{,}152 = \frac{1{,}152 \text{ sym}}{28{,}800 \text{ sym/s}} = 40 \text{ ms} \tag{4.19}$$

The reverse traffic channel performs interleaving over a single 20-ms frame period. The data rate into the interleaver is 28.8 ksps, and the block size is therefore 20 ms × 28.8 ksps = 576 symbols. As with the forward traffic channel, the reverse traffic channel uses symbol repetition.

Unlike the forward link, however, the reverse link gates the amplifier to eliminate the repeated symbols. Each 20-ms frame is divided into 16 equally spaced timeslots, called "power control groups." Each timeslot has a duration of 1.25 ms or 36 symbols, as shown previously in Figure 4.23. At an original data rate of 9.6 kbps, all timeslots contain symbols, and none is gated. At 4.8 kbps, one-half of the symbols would be gated, which would be either position 0 or 1, either position 2 or 3, and so on. At 2.4 kbps, only 1/4 are filled, and at 1.2 kbps, 1/8 are filled. Which positions contain symbols is determined pseudorandomly, a process termed *data burst randomizing*.

The reverse traffic channel interleaver for all rates is an ($I = 18$, $J = 32$) array, and thus, two rows are needed to fill one power control group. The rows of the interleaver are read out in an order that ensures that groups of 36 symbols (two rows) do not contain any duplicate symbols. The reverse traffic channel interleaver write arrays showing the symbol repetition are given in Figures 4.35, 4.36, 4.37, and 4.38 for 9.6, 4.8, 2.4, and 1.2 kbps, respectively.

The symbols are read out of the interleaver by rows in the order that is given in Table 4.8.

The combination of the 576-symbol interleaver and amplifier gating forms block interleavers whose minimum separation characteristics are dependent on the original data rate. The memory requirement and delay are independent of data rate because the original array has 576 symbols. Note that the arrays are read from the top to bottom instead of bottom to top, which reduces the minimum spacing by one. The 9.6-kbps interleaver is an ($I = 18$, $J = 32$) block interleaver. The 4.8-kbps interleaver is effectively ($I = 18$, $J = 16$). The 2.4-kbps array is effectively ($I = 18$, $J = 8$), and the 1.2-kbps interleaver is effectively ($I = 18$, $J = 4$). The term *effective* implies that only the minimum-spacing parameter is affected, and not the memory or delay. The minimum separation is thus given by

1	33	65	97	129	161	193	225	257	289	321	353	385	417	449	481	513	545
2	34	66	98	130	162	194	226	258	290	322	354	386	418	450	482	514	546
3	35	67	99	131	163	195	227	259	291	323	355	387	419	451	483	515	547
4	36	68	100	132	164	196	228	260	292	324	356	388	420	452	484	516	548
5	37	69	101	133	165	197	229	261	293	325	357	389	421	453	485	517	549
6	38	70	102	134	166	198	230	262	294	326	358	390	422	454	486	518	550
7	39	71	103	135	167	199	231	263	295	327	359	391	423	455	487	519	551
8	40	72	104	136	168	200	232	264	296	328	360	392	424	456	488	520	552
9	41	73	105	137	169	201	233	265	297	329	361	393	425	457	489	521	553
10	42	74	106	138	170	202	234	266	298	330	362	394	426	458	490	522	554
11	43	75	107	139	171	203	235	267	299	331	363	395	427	459	491	523	555
12	44	76	108	140	172	204	236	268	300	332	364	396	428	460	492	524	556
13	45	77	109	141	173	205	237	269	301	333	365	397	429	461	493	525	557
14	46	78	110	142	174	206	238	270	302	334	366	398	430	462	494	526	558
15	47	79	111	143	175	207	239	271	303	335	367	399	431	463	495	527	559
16	48	80	112	144	176	208	240	272	304	336	368	400	432	464	496	528	560
17	49	81	113	145	177	209	241	273	305	337	369	401	433	465	497	529	561
18	50	82	114	146	178	210	242	274	306	338	370	402	434	466	498	530	562
19	51	83	115	147	179	211	243	275	307	339	371	403	435	467	499	531	563
20	52	84	116	148	180	212	244	276	308	340	372	404	436	468	500	532	564
21	53	85	117	149	181	213	245	277	309	341	373	405	437	469	501	533	565
22	54	86	118	150	182	214	246	278	310	342	374	406	438	470	502	534	566
23	55	87	119	151	183	215	247	279	311	343	375	407	439	471	503	535	567
24	56	88	120	152	184	216	248	280	312	344	376	408	440	472	504	536	568
25	57	89	121	153	185	217	249	281	313	345	377	409	441	473	505	537	569
26	58	90	122	154	186	218	250	282	314	346	378	410	442	474	506	538	570
27	59	91	123	155	187	219	251	283	315	347	379	411	443	475	507	539	571
28	60	92	124	156	188	220	252	284	316	348	380	412	444	476	508	540	572
29	61	93	125	157	189	221	253	285	317	349	381	413	445	477	509	541	573
30	62	94	126	158	190	222	254	286	318	350	382	414	446	478	510	542	574
31	63	95	127	159	191	223	255	287	319	351	383	415	447	479	511	543	575
32	64	96	128	160	192	224	256	288	320	352	384	416	448	480	512	544	576

Figure 4.35 Reverse traffic channel interleaving at 9,600 bps.

$$S = \begin{cases} J - 1 & B \leq I \\ 1 & B > I \end{cases} \tag{4.20}$$

where the I and J are the effective values. As with conventional block interleavers, the memory requirement is twice the number of symbols in the array

$$M = 2IJ = 2 \times 18 \times 32 = 1152 \tag{4.21}$$

Likewise, the delay is

1	17	33	49	65	81	97	113	129	145	161	177	193	209	225	241	257	273
1	17	33	49	65	81	97	113	129	145	161	177	193	209	225	241	257	273
2	18	34	50	66	82	98	114	130	146	162	178	194	210	226	242	258	274
2	18	34	50	66	82	98	114	130	146	162	178	194	210	226	242	258	274
3	19	35	51	67	83	99	115	131	147	163	179	195	211	227	243	259	275
3	19	35	51	67	83	99	115	131	147	163	179	195	211	227	243	259	275
4	20	36	52	68	84	100	116	132	148	164	180	196	212	228	244	260	276
4	20	36	52	68	84	100	116	132	148	164	180	196	212	228	244	260	276
5	21	37	53	69	85	101	117	133	149	165	181	197	213	229	245	261	277
5	21	37	53	69	85	101	117	133	149	165	181	197	213	229	245	261	277
6	22	38	54	70	86	102	118	134	150	166	182	198	214	230	246	262	278
6	22	38	54	70	86	102	118	134	150	166	182	198	214	230	246	262	278
7	23	39	55	71	87	103	119	135	151	167	183	199	215	231	247	263	279
7	23	39	55	71	87	103	119	135	151	167	183	199	215	231	247	263	279
8	24	40	56	72	88	104	120	136	152	168	184	200	216	232	248	264	280
8	24	40	56	72	88	104	120	136	152	168	184	200	216	232	248	264	280
9	25	41	57	73	89	105	121	137	153	169	185	201	217	233	249	265	281
9	25	41	57	73	89	105	121	137	153	169	185	201	217	233	249	265	281
10	26	42	58	74	90	106	122	138	154	170	186	202	218	234	250	266	282
10	26	42	58	74	90	106	122	138	154	170	186	202	218	234	250	266	282
11	27	43	59	75	91	107	123	139	155	171	187	203	219	235	251	267	283
11	27	43	59	75	91	107	123	139	155	171	187	203	219	235	251	267	283
12	28	44	60	76	92	108	124	140	156	172	188	204	220	236	252	268	284
12	28	44	60	76	92	108	124	140	156	172	188	204	220	236	252	268	284
13	29	45	61	77	93	109	125	141	157	173	189	205	221	237	253	269	285
13	29	45	61	77	93	109	125	141	157	173	189	205	221	237	253	269	285
14	30	46	62	78	94	110	126	142	158	174	190	206	222	238	254	270	286
14	30	46	62	78	94	110	126	142	158	174	190	206	222	238	254	270	286
15	31	47	63	79	95	111	127	143	159	175	191	207	223	239	255	271	287
15	31	47	63	79	95	111	127	143	159	175	191	207	223	239	255	271	287
16	32	48	64	80	96	112	128	144	160	176	192	208	224	240	256	272	288
16	32	48	64	80	96	112	128	144	160	176	192	208	224	240	256	272	288

Figure 4.36 Reverse traffic channel interleaving at 4,800 bps.

$$D = 2IJ = 1{,}152 = \frac{1{,}152 \text{ sym}}{28{,}800 \text{ sym/s}} = 40 \text{ ms} \tag{4.22}$$

4.4.3 Diversity and Handoff

The digital spread-spectrum design of the IS-95 forward and reverse link waveforms permits the use of several forms of diversity in addition to the time diversity inherent in the repetition, encoding, and interleaving of the data symbols. These forms of diversity include multipath diversity and base station diversity, the latter being available with or without the prospect of handing off the call to a different base station.

1	9	17	25	33	41	49	57	65	73	81	89	97	105	113	121	129	137
1	9	17	25	33	41	49	57	65	73	81	89	97	105	113	121	129	137
1	9	17	25	33	41	49	57	65	73	81	89	97	105	113	121	129	137
1	9	17	25	33	41	49	57	65	73	81	89	97	105	113	121	129	137
2	10	18	26	34	42	50	58	66	74	82	90	98	106	114	122	130	138
2	10	18	26	34	42	50	58	66	74	82	90	98	106	114	122	130	138
2	10	18	26	34	42	50	58	66	74	82	90	98	106	114	122	130	138
2	10	18	26	34	42	50	58	66	74	82	90	98	106	114	122	130	138
3	11	19	27	35	43	51	59	67	75	83	91	99	107	115	123	131	139
3	11	19	27	35	43	51	59	67	75	83	91	99	107	115	123	131	139
3	11	19	27	35	43	51	59	67	75	83	91	99	107	115	123	131	139
3	11	19	27	35	43	51	59	67	75	83	91	99	107	115	123	131	139
4	12	20	28	36	44	52	60	68	76	84	92	100	108	116	124	132	140
4	12	20	28	36	44	52	60	68	76	84	92	100	108	116	124	132	140
4	12	20	28	36	44	52	60	68	76	84	92	100	108	116	124	132	140
4	12	20	28	36	44	52	60	68	76	84	92	100	108	116	124	132	140
5	13	21	29	37	45	53	61	69	77	85	93	101	109	117	125	133	141
5	13	21	29	37	45	53	61	69	77	85	93	101	109	117	125	133	141
5	13	21	29	37	45	53	61	69	77	85	93	101	109	117	125	133	141
5	13	21	29	37	45	53	61	69	77	85	93	101	109	117	125	133	141
6	14	22	30	38	46	54	62	70	78	86	94	102	110	118	126	134	142
6	14	22	30	38	46	54	62	70	78	86	94	102	110	118	126	134	142
6	14	22	30	38	46	54	62	70	78	86	94	102	110	118	126	134	142
6	14	22	30	38	46	54	62	70	78	86	94	102	110	118	126	134	142
7	15	23	31	39	47	55	63	71	79	87	95	103	111	119	127	135	143
7	15	23	31	39	47	55	63	71	79	87	95	103	111	119	127	135	143
7	15	23	31	39	47	55	63	71	79	87	95	103	111	119	127	135	143
7	15	23	31	39	47	55	63	71	79	87	95	103	111	119	127	135	143
8	16	24	32	40	48	56	64	72	80	88	96	104	112	120	128	136	144
8	16	24	32	40	48	56	64	72	80	88	96	104	112	120	128	136	144
8	16	24	32	40	48	56	64	72	80	88	96	104	112	120	128	136	144
8	16	24	62	40	48	56	64	72	80	88	96	104	112	120	128	136	144

Figure 4.37 Reverse traffic channel interleaving at 2,400 bps.

Because the forward link waveform for a particular channel is a dual-quadrature direct-sequence spread-spectrum signal, it is possible to employ spread-spectrum correlation techniques to isolate a single multipath component of that channel's signal and to discriminate not only against signals from other base stations but also against multipath components of the same channel's received signal. Using the Rake technique, in which the receiver uses several parallel receiver "fingers" to isolate multipath components, on the forward link it is possible to extract several multipath components from the total received signal and to align them for optimal combining.

In the implementation of the IS-95 system, the mobile receiver employs a "searcher" receiver and three digital data receivers that act as fingers of a rake in that they may be assigned to track and isolate particular multipath

1	5	9	13	17	21	25	29	33	37	41	45	49	53	57	61	65	69
1	5	9	13	17	21	25	29	33	37	41	45	49	53	57	61	65	69
1	5	9	13	17	21	25	29	33	37	41	45	49	53	57	61	65	69
1	5	9	13	17	21	25	29	33	37	41	45	49	53	57	61	65	69
1	5	9	13	17	21	25	29	33	37	41	45	49	53	57	61	65	69
1	5	9	13	17	21	25	29	33	37	41	45	49	53	57	61	65	69
1	5	9	13	17	21	25	29	33	37	41	45	49	53	57	61	65	69
1	5	9	13	17	21	25	29	33	37	41	45	49	53	57	61	65	69
2	6	10	14	18	22	26	30	34	38	42	46	50	54	58	62	66	70
2	6	10	14	18	22	26	30	34	38	42	46	50	54	58	62	66	70
2	6	10	14	18	22	26	30	34	38	42	46	50	54	58	62	66	70
2	6	10	14	18	22	26	30	34	38	42	46	50	54	58	62	66	70
2	6	10	14	18	22	26	30	34	38	42	46	50	54	58	62	66	70
2	6	10	14	18	22	26	30	34	38	42	46	50	54	58	62	66	70
2	6	10	14	18	22	26	30	34	38	42	46	50	54	58	62	66	70
2	6	10	14	18	22	26	30	34	38	42	46	50	54	58	62	66	70
3	7	11	15	19	23	27	31	35	39	43	47	51	55	59	63	67	71
3	7	11	15	19	23	27	31	35	39	43	47	51	55	59	63	67	71
3	7	11	15	19	23	27	31	35	39	43	47	51	55	59	63	67	71
3	7	11	15	19	23	27	31	35	39	43	47	51	55	59	63	67	71
3	7	11	15	19	23	27	31	35	39	43	47	51	55	59	63	67	71
3	7	11	15	19	23	27	31	35	39	43	47	51	55	59	63	67	71
3	7	11	15	19	23	27	31	35	39	43	47	51	55	59	63	67	71
3	7	11	15	19	23	27	31	35	39	43	47	51	55	59	63	67	71
4	8	12	16	20	24	28	32	36	40	44	48	52	56	60	64	68	72
4	8	12	16	20	24	28	32	36	40	44	48	52	56	60	64	68	72
4	8	12	16	20	24	28	32	36	40	44	48	52	56	60	64	68	72
4	8	12	16	20	24	28	32	36	40	44	48	52	56	60	64	68	72
4	8	12	16	20	24	28	32	36	40	44	48	52	56	60	64	68	72
4	8	12	16	20	24	28	32	36	40	44	48	52	56	60	64	68	72
4	8	12	16	20	24	28	32	36	40	44	48	52	56	60	64	68	72
4	8	12	16	20	24	28	32	36	40	44	48	52	56	60	64	68	72

Figure 4.38 Reverse traffic channel interleaving at 1,200 bps.

components of a base station signal; the block diagram in Figure 4.39 illustrates this parallel receiver concept. The search receiver scans the time domain about the desired signal's expected time of arrival for multipath pilot signals from the same cell site and pilot signals (and their multipath components) from other cell sites. Searching the time domain on the forward link is simplified because the pilot channel permits the coherent detection of signals. The search receiver indicates to the mobile phone's control processor where, in time, the strongest replicas of the signal can be found, and their respective signal strengths. In turn, the control processor provides timing and PN code information to the three digital data receivers, enabling each of them to track and demodulate a different signal.

Table 4.8 Order of the traffic channel read operation

Rate	Row Number
9.6 kbps	0, 1, 2, 3, 4, 5, 6, 7, 8, 9, 10, 11, 12, 13, 14, 15, 16, 17, 18, 19, 20, 21, 22, 23, 24, 25, 26, 27, 28, 29, 30, 31
4.8 kbps	0, 2, 1, 3, 4, 6, 5, 7, 8, 10, 9, 11, 12, 14, 13, 15, 16, 18, 17, 19, 20, 22, 21, 23, 24, 26, 25, 27, 28, 30, 29, 31
2.4 kbps	0, 4, 1, 5, 2, 6, 3, 7, 8, 12, 9, 13, 10, 14, 11, 15, 16, 20, 17, 21, 18, 22, 19, 23, 24, 28, 25, 29, 26, 30, 27, 31
1.2 kbps	0, 8, 1, 9, 2, 10, 3, 11, 4, 12, 5, 13, 6, 14, 7, 15, 16, 24, 17, 25, 18, 26, 19, 27, 20, 28, 21, 29, 22, 30, 23, 31

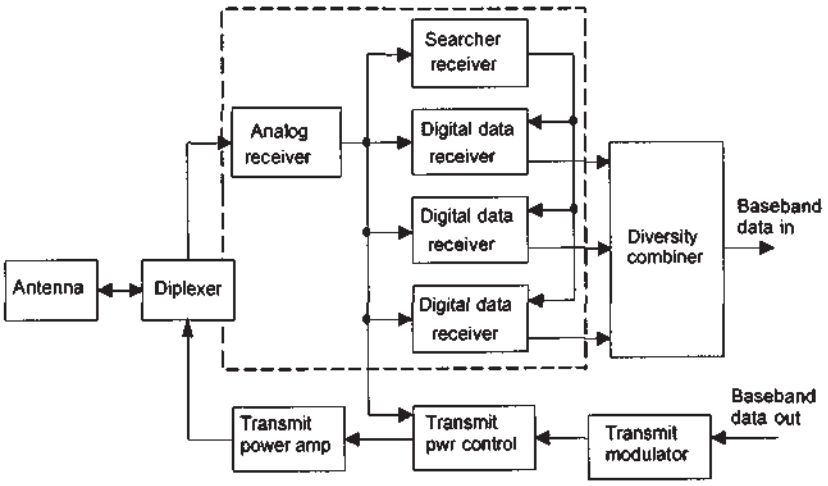

Figure 4.39 Mobile station block diagram.

The principles of diversity combining and Rake receiver processing are explained in Chapter 9.

If another cell site pilot signal becomes significantly stronger than the current pilot signal, the control processor initiates handoff procedures during which the forward links of both cell sites transmit the same call data on all their traffic channels. When both sites handle the call, additional space diversity is obtained. When handoff is not contemplated, in a cell site diversity mode the strongest paths from multiple cell sites are determined by the search receiver, and the digital data receivers are assigned to demodulate

these paths. As shown conceptually in Figure 4.40, the data from all three digital receivers are combined for improved resistance to fading; in the figure, the fact that different base stations or sectors are distinguished by different short PN code offsets is highlighted by identifying the two adjacent base stations with different offsets of $64i$ PN code chips and $64j$ PN chips, respectively.

The forward link performs coherent postdetection (after demodulation) combining after ensuring that the data streams are time-aligned; performance is not compromised by using postdetection combining because the modulation technique is linear. Coherent combining, illustrated in Figure 4.41, is possible because the pilot signal from each base station provides a coherent phase reference that can be tracked by the digital data receivers.

On the reverse link, the base station receiver uses two antennas for space diversity reception, and there are four digital data receivers available for tracking up to four multipath components of a particular subscriber's signal, as depicted in Figure 4.42. During "soft" handoff from one base station site to another, the voice data that are selected could result from combining up to eight multipath components, four at each site, as illustrated in Figure 4.43. The reverse link transmissions, not having a coherent phase reference like the forward link's pilot signal, must be demodulated and combined non-coherently; "maximal ratio" (optimum) combining can be done by weighting each path's symbol statistics in proportion to the path's relative power prior

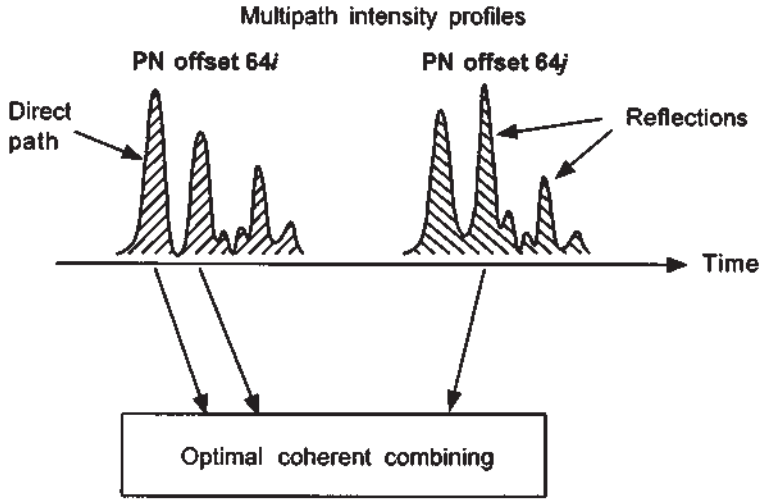

Figure 4.40 Forward link multipath/base station diversity.

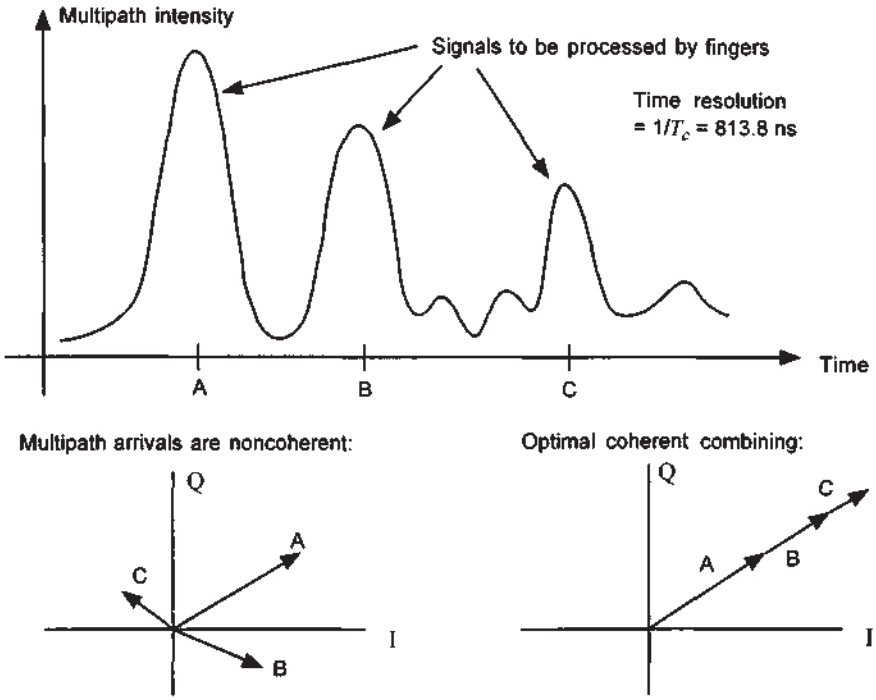

Figure 4.41 Concept of coherent combining.

to demodulation and decoding decisions. At the MTSO, the frames of data from the two base stations are selection-diversity "combined"; that is, the frame with the better quality is chosen. (These diversity combining methods are treated in Chapter 9.)

The soft handoff depicted as in progress in Figure 4.43 is termed "soft" because the connection of the mobile with one station is not broken off until one is established with the new station, rather than the "hard" handoff procedure that is necessary in analog FDMA cellular systems because the receiver must tune to a new frequency. Because the combining is done at the MTSO, however, under soft handoff, it is necessary to make hard data decisions to transmit the data frame to the MTSO. A "softer" handoff can occur in an IS-95 CDMA system when the mobile is in transition between two sectors of the same cell site. As illustrated in Figure 4.44, up to four multipath components of the mobile's transmission, as received at up to four antennas, can be combined before making a hard data decision. The figure indicates that the handoff process involves a gradually increasing preference for multipath

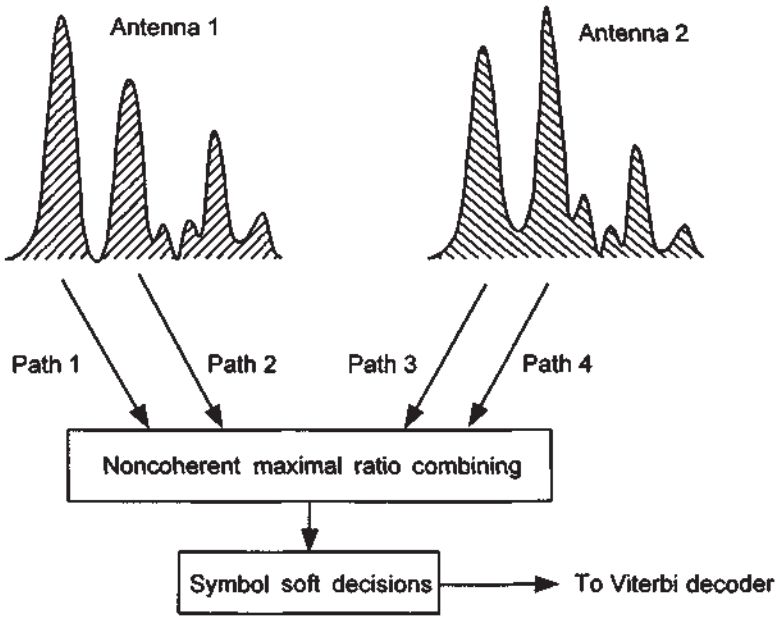

Figure 4.42 Reverse link multipath/antenna diversity.

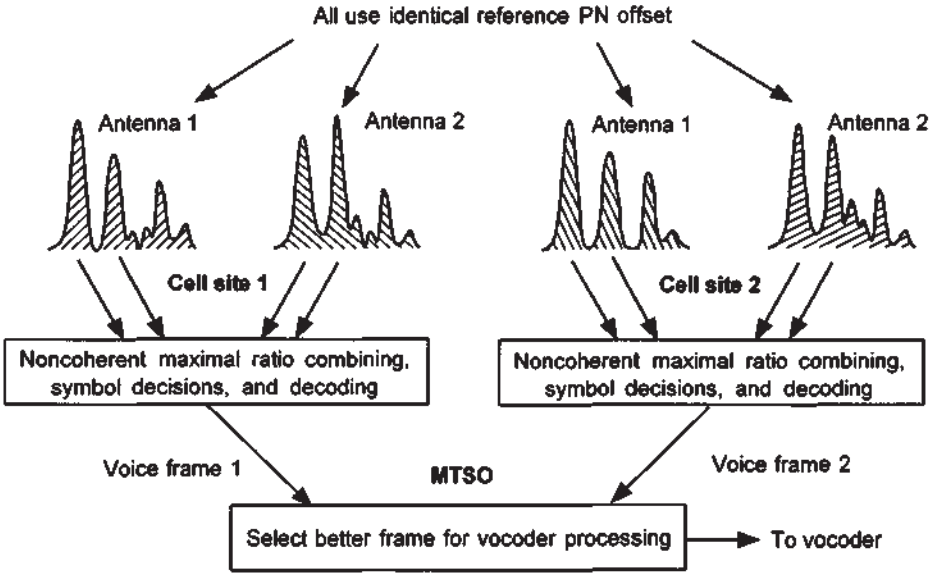

Figure 4.43 Reverse link soft handoff/multipath/base station diversity.

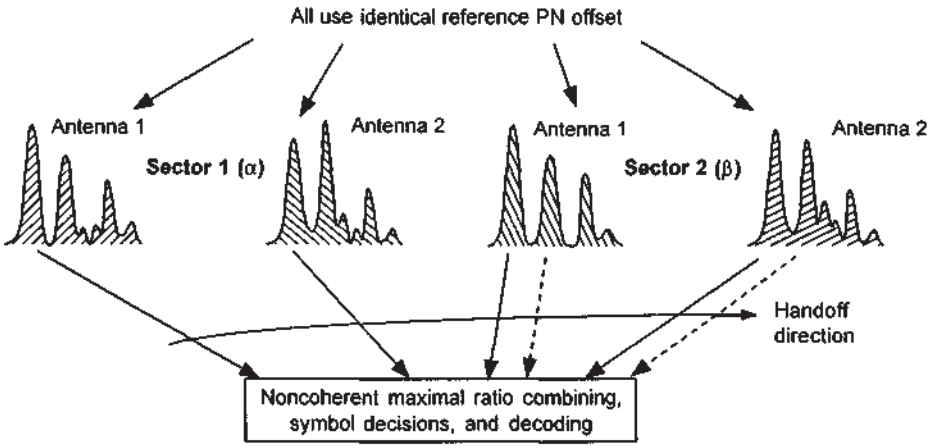

Figure 4.44 Reverse link "softer" handoff between sectors of a cell site.

components received in one sector, until the mobile signal is being processed by just one sector.

Note that on reverse link transmissions, the mobile transmits using zero-offset short PN codes; during handoff, each base station must align its receiver to the unique value of propagation delay experienced by the mobile signal, using the preamble sent on reverse link access channel and traffic channel transmissions as an aid to acquisition. On the forward link, during handoff each base station or sector uses its usual short PN code offset.

As shown previously in Figures 4.8 and 4.9, the IS-95 system modulates the same data on both the in-phase and quadrature-phase channels. This modulation is different from conventional QPSK where different data are modulated on the I and Q channels. The IS-95 scheme is not conventional QPSK but a form of diversity transmission that reduces multiple access interference relative to a conventional BPSK scheme. A derivation of this fact is presented in Chapter 7.

The IS-95 CDMA system "soft handoff" greatly reduces the number of failed handoffs. As a call is initiated, the base station sends the mobile, among other parameters, a set of handoff thresholds and candidate base stations for handoff. The mobile tracks all possible pilot phase offsets in the system, with the emphasis on the candidates and the current base station. Those base stations that have a signal above the candidate threshold are kept on a periodically updated list. The list is updated when (1) a new candidate exceeds the "add threshold," (2) an old candidate remains below the "drop threshold" for

a predetermined time, (3) the list becomes too large, or (4) a handoff forces a change in the candidates.

When the pilot signal level of another base station exceeds the currently active base station's signal by a specified amount, the mobile relays this information to the active base station. The system controller then assigns a modem in the new cell to handle the call and the original base station transmits the information necessary for the mobile to acquire the new base station. The mobile continues to monitor the the E_c/I_0 of the original base station and assigns at least one digital data receiver to demodulate data from the other base station. Digital data receivers are assigned to the strongest multipath components from either base station, providing a form of space diversity as discussed above in Section 4.4.2.

An example of soft handoff can be seen in Figure 4.45, where the mobile is originally communicating through base station A. When the pilot signal of base station B exceeds the add threshold, the mobile informs base station A, and base station B is put on the candidate list. Once the signal strength of base B exceeds the signal strength of base A by a specified margin, base B is put on the active list and begins to handle the call also. The signals to and from both base stations are diversity combined. As soon as the signal

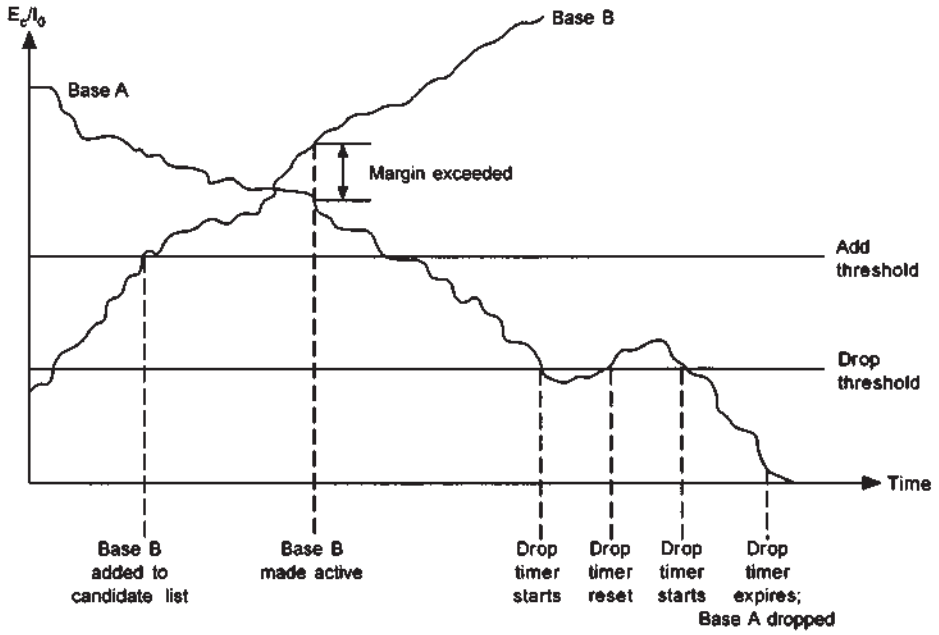

Figure 4.45 Signal levels during soft handoff.

from base station A crosses the drop threshold, the drop timer is started. The timer is reset when the signal exceeds the drop threshold. When the signal falls below the drop threshold, the drop timer is restarted. After the drop timer expires, base station A is dropped from active service.

Soft handoff methods have several advantages over conventional hard handoff methods. Contact with the new base station is made before the call is switched, which prevents the mobile from losing contact with the system if the handoff signal is not heard or incorrectly interpreted. Diversity combining is used between multiple cell sites, allowing for additional resistance to fading. Because more than one base station is used in the soft handoff region, the ping-ponging effect can be virtually eliminated. Thus, the system is relieved from unnecessary switching operations. The system is further relieved from determining signal strengths, because this processing is done at the mobile. If the new cell is loaded to capacity, handoff can still be performed if all users accept a small increase in the bit-error rate. This type of handoff can be likened to make-before-break switching. Note that in soft handoff, neither the mobile nor the base station is required to change frequency. Conventional hard handoff is performed if the mobile is required to switch to an analog system or change to another CDMA frequency. Frequency changes may be necessary if the current frequency is crowded or the mobile enters a new CDMA network.

References

[1] "Mobile Station-Base Station Compatibility Standard for Dual-Mode Wideband Spread Spectrum Cellular System," TIA/EIA Interim Standard 95 (IS-95), Washington, D.C.: Telecommunications Industry Association, July 1993 (amended as IS-95-A in May 1995).

[2] "Cellular System Dual-Mode Mobile Station-Base Station Compatibility Standard," TIA/EIA Interim Standard 54 (IS-54-B), Washington, D.C.: Telecommunications Industry Association, April 1992.

[3] Viterbi, A. J., *Principles of Spread Spectrum Multiple Access Communication*, New York: Addison-Wesley, 1995.

[4] Carlson, B. C., *Special Functions of Applied Mathematics*, New York: Academic Press, 1977.

[5] Knuth, D. N., *Sorting and Searching*, vol. 3 of *The Art of Computer Programming*, Reading, MA: Addison-Wesley, 1973.

[6] Lehmer, D. H. "Mathematical Methods in Large Scale Computing Units," *Annals Computation Laboratory Harvard Univ.*, Vol. 26, pp. 141–146, 1951.

Appendix 4A Theory of Interleaving

The most commonly employed interleaving techniques fall into two classes. The more common type is *block interleaving*, which is often used when the data is divided into blocks or frames, such as in the IS-95 system. *Convolutional interleaving*, on the other hand, is more practical for a continuous data stream. Block interleaving is known for its ease of implementation, whereas convolutional interleaving has performance advantages. Continuous operation allows the original overhead associated with convolutional interleaving to become insignificant.

4A.1 Block Interleaving

The fundamentals of block interleaving are covered in Section 4.4.2. This section simply gives an example demonstrating the fact that the minimum separation is affected by reading out the rows in another order. Assume that the block contains 20 symbols and is read into an $I = 5$, $J = 4$ interleaver. Let a number be assigned to each symbol that indicates its original order in the transmission sequence. After reading into the interleaver, it can be represented by the following array:

$$\begin{bmatrix} 1 & 5 & 9 & 13 & 17 \\ 2 & 6 & 10 & 14 & 18 \\ 3 & 7 & 11 & 15 & 19 \\ 4 & 8 & 12 & 16 & 20 \end{bmatrix}$$

If the symbols are read out in a conventional manner, then the output of the interleaver would be

4, 8, 12, 16, 20, 3, 7, 11, 15, 19, 2, 6, 10, 14, 18, 1, 5, 9, 13, 17

Note that the minimum separation of any burst of $B \leq I = 5$ symbols is $J = 4$, and that for $B > I = 5$, $S = 1$.

Now suppose that the symbols are read out by rows in the following order: first row, third row, second row, and then the last row. The symbols would be ordered

1, 5, 9, 13, 17, 3, 7, 11, 15, 19, 2, 6, 10, 14, 18, 4, 8, 12, 16, 20

The minimum-separation profile becomes

$$S = \begin{cases} 4 & B \leq 4 \text{ (e.g., between 1 and 5)} \\ 2 & B = 5 \text{ (e.g., between 1 and 3)} \\ 1 & B > 5 \text{ (e.g., between 3 and 2)} \end{cases}$$

In this particular case, the minimum separation was reduced from 4 to 2 for $B = 5$. Increasing the minimum separation for $B > I$ becomes easier with larger interleaver sizes. Note also that the memory requirement and delay remain essentially unchanged.

4A.2 Convolutional Interleaving

Convolutional interleavers have a series of K parallel lines with an input commutator moving between each line much like an encoder for a convolutional code. Each of the K lines contains various numbers of storage elements, as shown in Figure 4A.1. The first line is a short from the input to output, and the second has L storage elements. Each successive line has L more units than the previous, and thus, the last contains $K(L-1)$ storage registers. The storage elements must be loaded with some initial symbols, which are shifted out into channel and increase overhead. This loading is similar to tail bits in convolutional coding. An output commutator moves in synchronization with the input commutator to extract a symbol every time one is entered. The deinterleaver performs the complementary operations are requires a corresponding structure, depicted in Figure 4A.2.

An example, using a $K = 4$, $L = 2$ interleaver, will help illustrate the convolutional interleaving process. Let the initial loading of each register be represented by any symbol "i," and the 48 input symbols be represented by x_j, where j is the initial ordering ($j = 1, 2, \ldots, 47$). The initial conditions

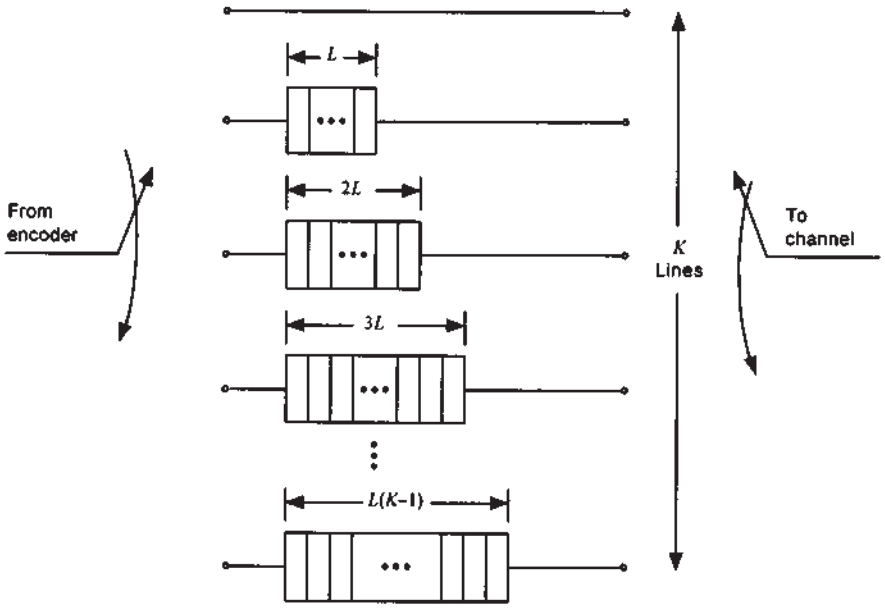

Figure 4A.1 (K, L) **Convolutional interleaver structure.**

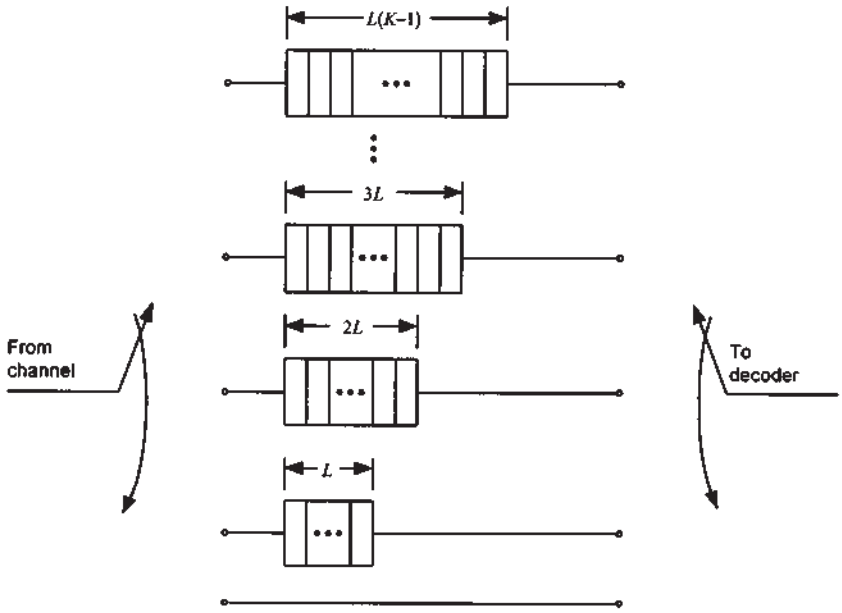

Figure 4A.2 The deinterleaver performs the reverse operation.

and the interleaving process for the first three commutator periods are shown in Figures 4A.3, 4A.4, 4A.5, and 4A.6.

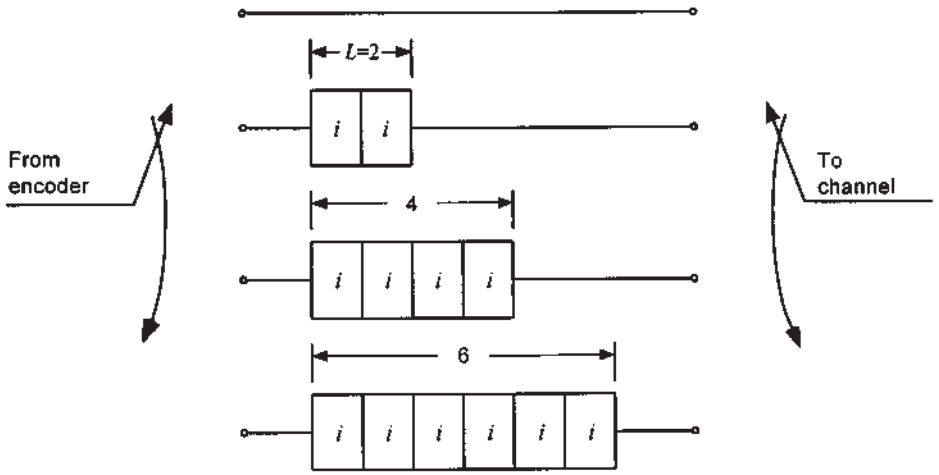

Figure 4A.3 Initial conditions of the interleaver example.

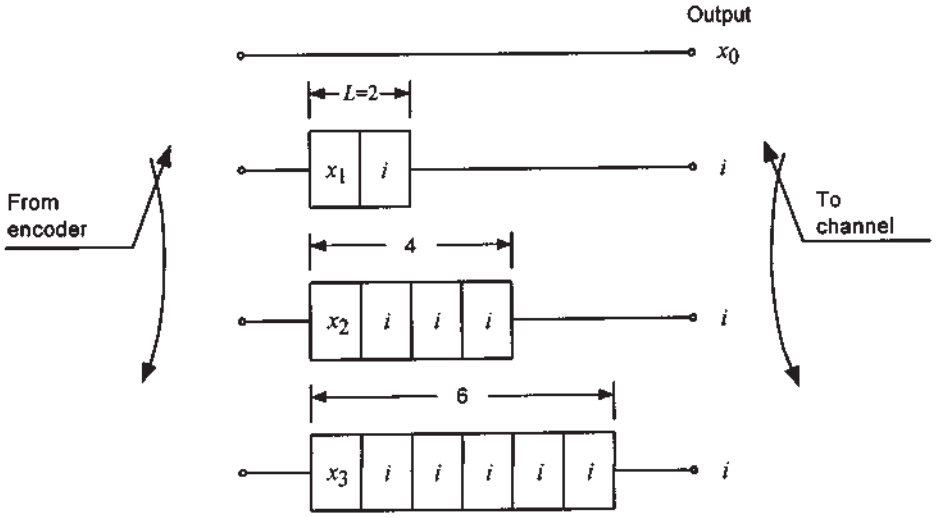

Figure 4A.4 Interleaver after first commutator period.

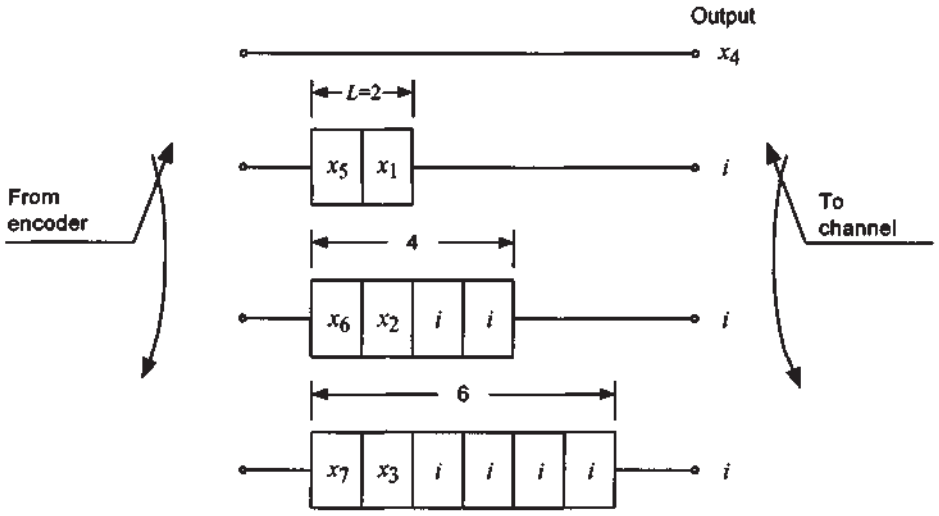

Figure 4A.5 Interleaver after second commutator period.

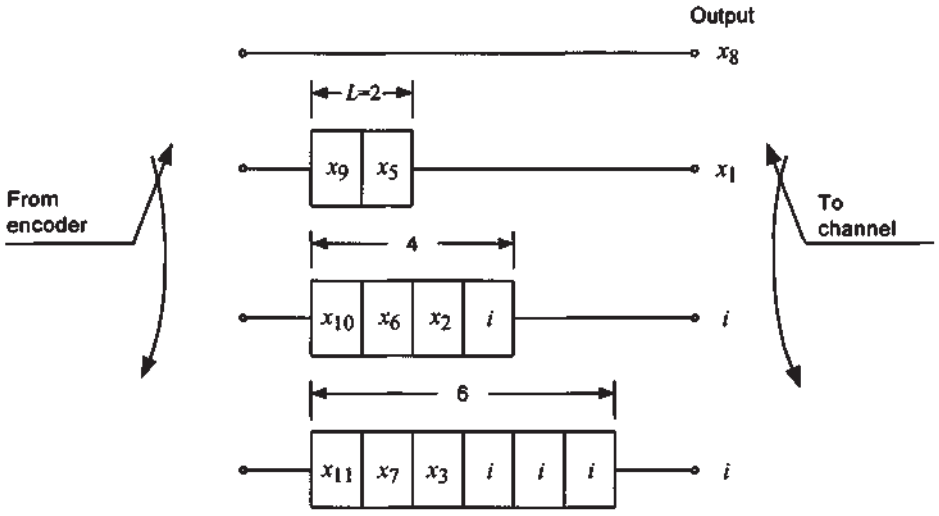

Figure 4A.6 Interleaver after third commutator period.

The interleaver input and output for the example are shown in Table 4A.1. The initial symbols are scattered throughout the desired data and are required to be gated or transmitted to the channel, which increases overhead,

Table 4A.1 Input and output of the interleaver

Period	Input	Output
1	x_0, x_1, x_2, x_3	x_0, i, i, i
2	x_4, x_5, x_6, x_7	x_4, i, i, i
3	x_8, x_9, x_{10}, x_{11}	x_8, x_1, i, i
4	$x_{12}, x_{13}, x_{14}, x_{15}$	x_{12}, x_5, i, i
5	$x_{16}, x_{17}, x_{18}, x_{19}$	x_{16}, x_9, x_2, i
6	$x_{20}, x_{21}, x_{22}, x_{23}$	x_{20}, x_{13}, x_6, i
7	$x_{24}, x_{25}, x_{26}, x_{27}$	$x_{24}, x_{17}, x_{10}, x_3$
8	$x_{28}, x_{29}, x_{30}, x_{31}$	$x_{28}, x_{21}, x_{14}, x_7$
9	$x_{32}, x_{33}, x_{34}, x_{35}$	$x_{32}, x_{25}, x_{18}, x_{11}$
10	$x_{36}, x_{37}, x_{38}, x_{39}$	$x_{36}, x_{29}, x_{22}, x_{15}$
11	$x_{40}, x_{41}, x_{42}, x_{43}$	$x_{40}, x_{33}, x_{26}, x_{19}$
12	$x_{44}, x_{45}, x_{46}, x_{47}$	$x_{44}, x_{37}, x_{30}, x_{23}$

but if continuous operation is employed, these initial symbols need only be sent once. Table 4A.2 contains the input and output of the deinterleaver corresponding to the interleaver. It is assumed that the deinterleaver is initially loaded with d symbols. Note that after the first 24 symbols, the symbol ordering is restored.

By observing the interleaver output, the minimum separation between any symbols of a burst of length B is found to be

Table 4A.2 Input and output of the deinterleaver

Period	Input	Output
1	x_0, i, i, i	d, d, d, i
2	x_4, i, i, i	d, d, d, i
3	x_8, x_1, i, i	d, d, i, i
4	x_{12}, x_5, i, i	d, d, i, i
5	x_{16}, x_9, x_2, i	d, i, i, i
6	x_{20}, x_{13}, x_6, i	d, i, i, i
7	$x_{24}, x_{17}, x_{10}, x_3$	x_0, x_1, x_2, x_3
8	$x_{28}, x_{21}, x_{14}, x_7$	x_4, x_5, x_6, x_7
9	$x_{32}, x_{25}, x_{18}, x_{11}$	x_8, x_9, x_{10}, x_{11}
10	$x_{36}, x_{29}, x_{22}, x_{15}$	$x_{12}, x_{13}, x_{14}, x_{15}$
11	$x_{40}, x_{33}, x_{26}, x_{19}$	$x_{16}, x_{17}, x_{18}, x_{19}$
12	$x_{44}, x_{37}, x_{30}, x_{23}$	$x_{20}, x_{21}, x_{22}, x_{23}$

$$S = \begin{cases} 7, & B \leq 4 \\ 4, & B = 5 \\ 3, & 6 \leq B \leq 9 \\ 1, & B \geq 10 \end{cases}$$

The number of memory elements can be determined by direct count to be

$$M = 0 + 2 + 4 + 6 = 12$$

The delay is equal to the number of memory elements at the transmitter and the number at the receiver, or

$$D = 2 \times 12 = 24$$

These observations can be extended to any (K, L) convolutional interleaver. The minimum-separation profile is given by

$$S = \begin{cases} KL - 1, & 2 \leq B \leq K \\ K, & K + 1 \leq B \leq K(L-1) + 1 \\ K - 1, & K(L-1) + 2 \leq B \leq KL + 1 \\ 1, & B \geq KL + 2 \end{cases} \quad \text{(4A.1)}$$

The number of storage elements is given by

$$M = L \sum_{i=0}^{K-1} i = \frac{LK(K-1)}{2} \quad \text{(4A.2)}$$

The delay is twice the number of storage elements, or

$$D = 2M = LK(K-1) \quad \text{(4A.3)}$$

4A.3 Comparison of Block and Convolutional Interleaving

The comparison is based mainly on the S/D and S/M ratios for the two interleavers. For the block interleaver, the ratios can be found by using equations (4.10), (4.11), and (4.12):

$$\frac{S}{M}(\text{block}) = \frac{J}{2IJ} = \frac{1}{2I} \quad \text{for } B \leq I \tag{4A.4}$$

$$\frac{S}{D}(\text{block}) = \frac{J}{2IJ} = \frac{1}{2I} \quad \text{for } B \leq I \tag{4A.5}$$

For the convolutional interleaver, the ratios can be found using equations (4A.1), (4A.2), and (4A.3):

$$\frac{S}{M}(\text{convolutional}) = \frac{KL-1}{KL(K-1)/2} \quad \text{for } B \leq K \tag{4A.6a}$$

$$\approx \frac{2KL}{KL(K-1)} = \frac{2}{K-1} \tag{4A.6b}$$

$$\frac{S}{D}(\text{convolutional}) = \frac{KL-1}{KL(K-1)} \quad \text{for } B \leq K \tag{4A.7a}$$

$$\approx \frac{1}{K-1} \tag{4A.7b}$$

The S/M ratio is approximately four times as large with convolutional interleaving as with block interleaving. The S/D ratio for convolutional interleaving is approximately twice that for block interleaving. Convolutional interleaving also has the advantage that for $B > K$, the minimum separation is greater than unity, which is not the case for block interleaving. As noted previously, the original contents of the convolutional registers must be transmitted over the channel, which can reduce overhead. Because of its simplicity and the fact that most data are grouped in blocks, however, block interleaving is more commonly employed.

4A.4 Interleaver Design

The main purpose of interleaving is to disperse bursts of errors over time so that an error control code can correct the errors. Therefore, the longest expected burst should be dispersed over a great enough time to allow correction. The memory span N of a code is defined as the number of code symbols required to achieve the full error-correcting capability t. For block error-correcting codes, the decoder span is the block length ($N = n$). For convolutional codes, the decoder span is more difficult to define. It is

generally accepted that two to five constraint lengths of channel symbols is sufficient ($N = 2nK'$ to $5nK'$, where n is the branch length and K' is the constraint length).

The following example illustrates the distribution of errors within a decoder span. Consider the (31, 16) BCH code that corrects $t = 3$ errors, and $N = n = 31$. The interleaver should ensure that no more than $t = 3$ errors occur within one memory span. To satisfy this requirement, the minimum separation for the interleaver must be greater than or equal to 11, as shown in Figure 4A.7. If the minimum separation is less than 11, then it is possible to have four errors within one memory span, as illustrated in Figure 4A.8.

The number of errors in any memory span should be less than the error-correcting capability of the code. The average number of errors in a decoder span is N/S. Because there must be t or fewer errors in a memory span:

$$t \geq \frac{N}{S} \tag{4A.8}$$

Solving for the minimum separation gives

$$S \geq \left\lceil \frac{N}{t} \right\rceil \tag{4A.9}$$

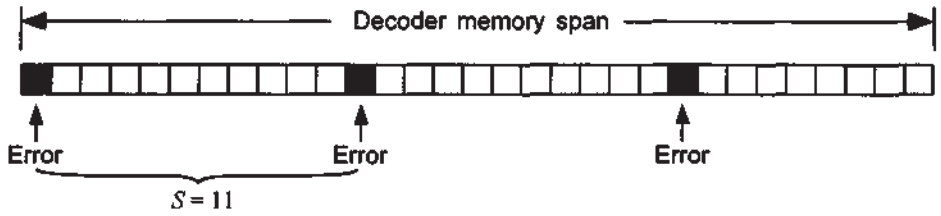

Figure 4A.7 Interleaving should ensure that at most t errors are within a memory span.

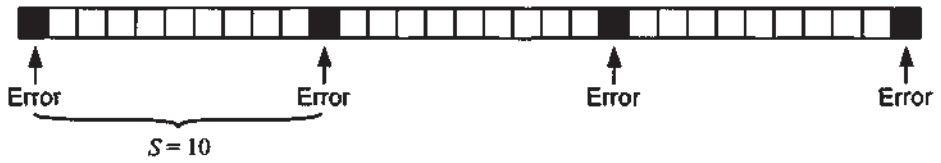

Figure 4A.8 If more than t errors occur, the code cannot correct them.

where $\lceil x \rceil$ denotes the smallest integer greater than of equal to x. For both convolutional and block interleaving, the largest minimum separation is achieved for $B \leq I$ or K. Thus, when determining interleaver structure, the longest burst expected should be less than I or K, and equation (4.31) should be satisfied.

Other practical factors affect interleaver structure. Data are usually arranged into blocks in order to be processed more manageably. Blocks can be determined by channel coding, voice coding, protocol requirements, and other framing requirements. Interleaving is usually performed within an integer number of frames. For example, in IS-95, interleaving is performed within a single frame. In IS-54 [2], interleaving is performed within two frames. Because delays of several hundred milliseconds are noticeable in speech, the total delay should be limited to this amount. Interleaver delay is a large part of the total delay, which also includes propagation, voice coding, and channel coding delays. When block codes or control messages are used, it is desirable to make the interleaver memory an integral number of code words or messages. If not, then the decoder must wait until the remainder of the code word or message is received before processing can begin.

Appendix 4B Hash Function Used in IS-95

In IS-95, the base or mobile is often presented with a number of resources and must choose which one to use. For example, if there are seven active paging channels, the base station must decide which of these seven channels to use when paging a particular mobile subscriber. The choice should be uniform and reproducible, in the sense that it should be

Uniform. All resources should be used uniformly to prevent collisions (contention for the use of the same resource by more than one user) or overloads (exceeding the capabilities of the resource). For example, page messages should be evenly distributed over all the paging channels and all of the slot resources within the paging channels to prevent overloading a single channel.

Reproducible. It is advantageous for both the base station and the mobile to be able to independently reproduce the choice of resources from information known to both. For example, from information known by both base station and mobile, the mobile can reproduce the base's choice of paging channel and monitor only that paging channel.

One method of making a uniform choice from among a number of resources is by using a "hash function." The hash function allows this uni-

form distribution through a method that is reproducible at both the mobile and the base station using as inputs (a) the number of resources and (b) a parameter (hash key) that is known by both terminals. We denote the hash key as K and the number of resources as N. With the input of a hash key K, the output of the hash function $h(K)$ will be an integer value between 0 and $N-1$, thus taking N values:

$$0 \leq h(K) \leq N-1 \tag{4B.1}$$

Because the keys in practice may differ only slightly, such as two telephone numbers differing only in the last digit, we must be careful to find a hash function that breaks up clusters of almost identical keys to reduce the number of collisions (the same hash function outputs).

A general form for a *normalized hash function* $h'(K)$, where $0 \leq h'(K) \leq 1$, is given by

$$h'(K) = (cK) \bmod 1, \quad 0 < c < 1 \tag{4B.2}$$

Taking a number modulo 1 is the same as discarding the integer part and keeping the mantissa (the part of the number to the right of the decimal point). Examples: $10.261 \bmod 1 = 0.261$, $11 \bmod 1 = 0$. The normalized hash function can be extended to generate an integer between 0 and $N-1$ by using the operation

$$h(K) = \lfloor N \times (cK) \bmod 1 \rfloor, \quad 0 < c < 1 \tag{4B.3}$$

where $\lfloor x \rfloor$ is the greatest integer less than x, and N is the number of resources.

One method for generating a fractional number c for use in hash functions is to take c as the ratio $c = A/w$, where $w = 2^B$, B is the word size of the processor, and $A < w$ is some positive integer that is relatively prime to w. Computers represent numbers by a certain number of binary digits; the number of digits that a processor uses is called the word size B. "Relatively prime" means that the numbers have no common divisors.

Example 4B.1 Suppose $A = 4$ and $w = 8$, where A and w are not relatively prime. Then, $c = A/w = 0.5$ and we have the values

K	1	2	3	4
$(cK) \bmod 1$	0.5	0	0.5	0

The values of $(cK) \bmod 1$ repeat for every second value of K, a highly undesirable characteristic. Now suppose that $A = 3$ and $w = 8$, where these two numbers are relatively prime. Then $c = A/w = 0.375$ and we have the values

K	1	2	3	4	5	6	7	8
$(cK) \bmod 1$	.375	.75	.125	.5	.875	.25	.625	0

When A is relatively prime to w, we have the *maximal period* of $w = 8$.

We have demonstrated that w is the maximal length of the period. Thus, we want the value of w to be large. It is also desirable to simplify the arithmetic involved in dividing A by w. Dividing a number by 2^i results in the number's being shifted i places to the right in binary notation. For example, 24 (binary 11000) divided by $4 = 2^2$ equals 6 (binary 110). Thus, we should make w the largest power of two that can be represented on the given processor, which for a B-bit processor is $w = 2^B$.

With w fixed, c is determined by the value of A, which should be chosen so that the numbers generated by the hash function have as uniform a distribution as possible. We will show that A should be chosen to be the integer relatively prime to w and closest to $0.618w$; that is, $A/w \approx 0.618 = \left(\sqrt{5} - 1\right)/2$, a fraction called the *golden ratio* in mathematics. To demonstrate that $A/w \approx 0.618$ provides a uniform distribution, a quick review of the golden ratio is covered before proceeding.

4B.1 Review of the Golden Ratio and Fibonacci Numbers

The golden ratio, denoted here by g, is defined as the ratio between the lengths of two portions of a line segment in which the ratio of the shorter portion to the longer portion equals the ratio of the longer portion to the total length:

$$g \triangleq \frac{d_2}{d_1} = \frac{d_1}{d_1 + d_2} = \frac{1}{1 + d_2/d_1} = \frac{1}{1 + g} \tag{4B.4}$$

Solving for g gives the quadratic equation $g^2 + g - 1 = 0$, for which the positive root is $g = \left(\sqrt{5} - 1\right)/2 = 0.618$.

Consider the equation $t^2 - t - 1 = 0$. The roots of this equation are

$$x = \frac{1 + \sqrt{5}}{2} = 1.618 \quad \text{and} \quad y = \frac{1 - \sqrt{5}}{2} = -0.618$$

Note that $x + y = 1$ and $xy = -1$. The *Fibonacci number* [4] F_n for integer $n = 0, 1, 2, \ldots$ is defined by

$$F_n \equiv \frac{x^n - y^n}{x - y} \quad \text{where } x \text{ and } y \text{ are the roots of } t^2 - t - 1 = 0 \tag{4B.5}$$

Note that $F_0 = \frac{x^0 - y^0}{x-y} = \frac{1-1}{x-y} = 0$ and $F_1 = \frac{x^1 - y^1}{x-y} = \frac{x-y}{x-y} = 1$. Because $x^2 = x + 1$ and $y^2 = y + 1$, it follows that

$$x^{n+1} = x^n + x^{n-1} \quad \text{and} \quad y^{n+1} = y^n + y^{n-1} \tag{4B.6}$$

giving the recursion for the Fibonacci numbers for $n > 1$:

$$F_{n+1} = \frac{x^{n+1} - y^{n+1}}{x - y} = \frac{x^n + x^{n-1} - y^n - y^{n-1}}{x - y} = F_n + F_{n-1} \tag{4B.7}$$

Therefore, the Fibonacci numbers are

$$F_0, F_1, F_2, \ldots = 0, 1, 1, 2, 3, 5, 8, 13, 21, 34, 55, 89, 144, \ldots$$

If we define $r_n \triangleq F_{n+1}/F_n$ as the ratio of successive Fibonacci numbers, we find that

$$r_n = \frac{F_{n+1}}{F_n} = \frac{F_n + F_{n-1}}{F_n} = 1 + \frac{1}{r_{n-1}} \tag{4B.8}$$

which leads to the continued fraction expression

$$r_n = 1 + \cfrac{1}{1 + \cfrac{1}{1 + \cdots \cfrac{1}{1 + \cfrac{1}{1 + \cfrac{1}{r_1}}}}} \tag{4B.9}$$

Because the roots x and y are such that $x > |y|$ and $\lim_{n \to \infty} (y/x)^n = 0$, the ratio r_n converges to a certain asymptotic value:

$$\lim_{n \to \infty} r_n = \lim_{n \to \infty} \frac{x^{n+1} - y^{n+1}}{x^n - y^n} = \lim_{n \to \infty} \frac{x - y(y/x)^n}{1 - (y/x)^n} = x \tag{4B.10}$$

Note that the ratio r_n converges to the inverse of the golden ratio:

$$\lim_{n \to \infty} r_n = x = \frac{\sqrt{5}+1}{2} = \frac{2}{\sqrt{5}-1} = \frac{1}{g} \tag{4B.11}$$

showing that the golden ratio and Fibonacci numbers are closely related. For that reason, hashing that uses the golden ratio has been termed Fibonacci hashing.

4B.2 Hash Function Example

The uniformity of the hash function $h(K) = \left\lfloor N \left[\left(\frac{A}{w} K \right) \bmod 1 \right] \right\rfloor$ is clearly due to its kernel, $\left(\frac{A}{w} K \right) \bmod 1$. If A/w is chosen to be the golden ratio $g = 0.618$, then the uniformity of this Fibonacci hashing can be found experimentally by plotting the various values of $(gK) \bmod 1$. These values for $K = 1, 2, \ldots, 14$ are shown in Table 4B.1. The values may be plotted as shown in Figure 4B.1, which reveals the high degree of uniformity achieved by employing the golden ratio in the hash function kernel.

Table 4B.1 Values of the hash function kernel

K	1	2	3	4	5	6	7
$(gK) \bmod 1$	0.6180	0.2360	0.8541	0.4721	0.0902	0.7082	0.3262
K	8	9	10	11	12	13	14
$(gK) \bmod 1$	0.9443	0.5623	0.1803	0.7984	0.4164	0.0344	0.6525

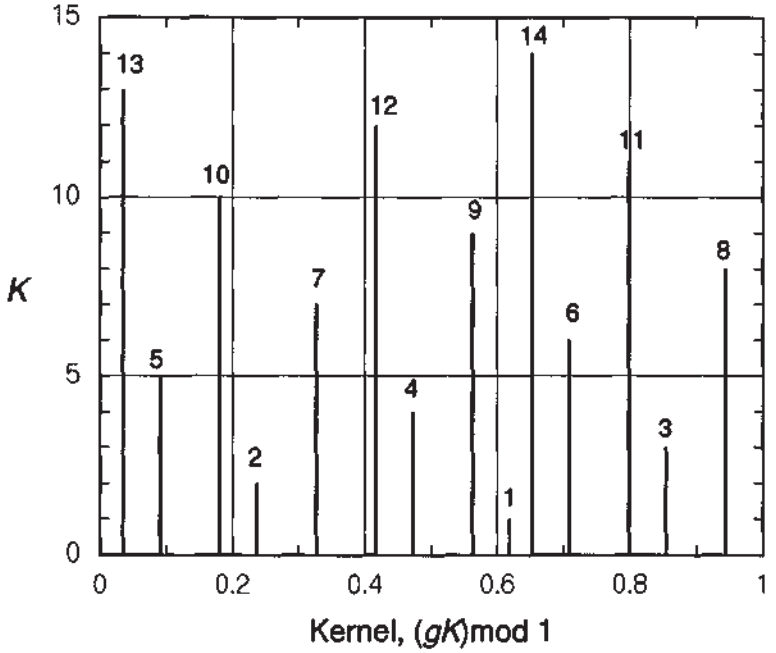

Figure 4B.1 Uniformity of the hash function kernel.

Figure 4B.1 demonstrates the truth of the following theorem, proved in [5]:

Theorem: Let θ be any irrational number. When the points $\theta \bmod 1$, $2\theta \bmod 1, \ldots, n\theta \bmod 1$ are placed in the unit interval, the next point placed, $[(n+1)\theta] \bmod 1$, falls in the largest existing segment.

In the example of Table 4B.1 and Figure 4B.1, the first point ($K = 1$) was placed in the unit interval at $g = 0.618$, creating two two segments:

$$d_1 = [0, g \bmod 1] \text{ with length } l_1 = 0.618$$

$$d_2 = [g \bmod 1, 1] \text{ with length } l_2 = 1 - 0.618 = 0.382$$

Obviously, $l_1 > l_2$, and in accordance with the theorem, the second point ($K = 2$) was placed at $2g \bmod 1 = 0.2360$ in the interval d_1, as illustrated in Figure 4B.2. After the placement of the second point, there are three segments:

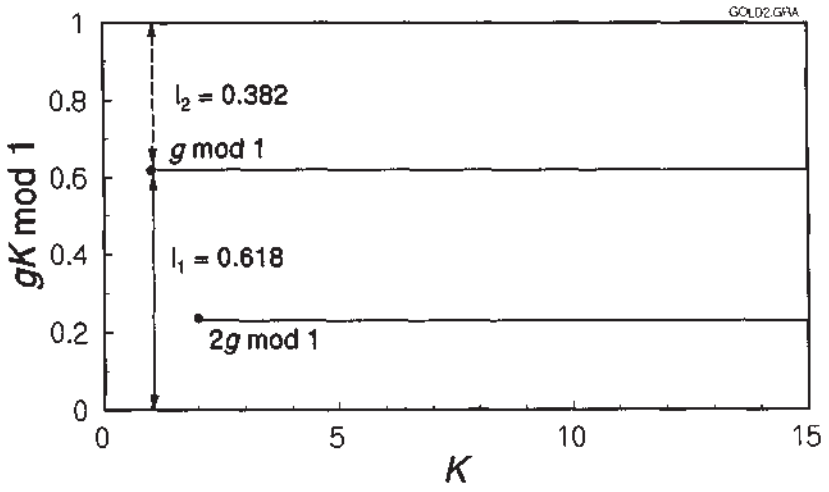

Figure 4B.2 Placement of second point.

$$d_1 = [0,\ 2g \bmod 1] \text{ with length } l_1 = 0.236$$

$$d_2 = [2g \bmod 1,\ g \bmod 1] \text{ with length } l_2 = 0.618 - 0.236 = 0.382$$

$$d_3 = [g \bmod 1,\ 1] \text{ with length } l_3 = 0.382$$

The largest of these three intervals is a tie between d_2 and d_3 because $l_2 = l_3$, and the third point ($K = 3$) is placed at $3g \bmod 1 = 0.8541$, which is in d_3, splitting this interval into two segments. Thus, d_2 becomes the longest segment and the next point ($K = 4$) should fall, according to the theorem, into d_2—it does, because $4g \bmod 1 = 0.4721$ is in d_2, as can be observed in Figure 4B.1.

The fact that there were two segments with the same length after the placement of the second point is not unusual. A corollary to the theorem stated above declares that [5] the lengths of the segments will have at most three different values. This behavior of the hash function kernel is clearly seen regarding the sixteen segments of the x-axis in Figure 4B.1. There is one interval length (= 0.0557) between the following seven pairs of points: (K_1, K_2) = (5, 13), (2, 10), (4, 12), (1, 9), (6, 14), (3, 11), and between 8 and the upper end of the (0, 1) interval. There is a second interval length (= 0.0344) between the following two pairs of points: (K_1, K_2) = (1, 14) and between 13 and the lower end of the (0, 1) interval. Finally, there is a

third interval length (= 0.0902) between the following six pairs of points: $(K_1, K_2) = (5, 10), (2, 7), (7, 12), (4, 9), (6, 11)$, and $(3, 8)$.

According to [5], extensive experiments indicate that the two numbers, $A/w = g$ and $A/w = 1 - g$ lead to the most uniformly distributed sequences of kernel values, among all numbers θ between 0 and 1.

4B.3 The IS-95 Hash Function

The multiplicative Fibonacci hash function discussed above can be rearranged as follows:

$$h(K) = \left\lfloor N\left[\left(\frac{A}{w}K\right) \bmod 1\right]\right\rfloor = \left\lfloor N\left(\frac{A}{w}K - \left\lfloor\frac{A}{w}K\right\rfloor\right)\right\rfloor \tag{4B.12a}$$

because $x \bmod 1 = x - \lfloor x \rfloor$. Further, because $x \bmod y = x - y\left\lfloor\frac{x}{y}\right\rfloor$:

$$h(K) = \left\lfloor N\frac{AK - w\left\lfloor\frac{A}{w}K\right\rfloor}{w}\right\rfloor = \left\lfloor N\frac{(AK) \bmod w}{w}\right\rfloor \tag{4B.12b}$$

In IS-95, a word size of 16 bits is assumed, giving $w = 2^{16} = 65{,}536$, and the ratio $A/w = g = \frac{\sqrt{5}-1}{2} = 0.618034$ is used, or

$$A = gw = 0.618034 \times 65{,}536 = 40{,}503.476 \tag{4B.13}$$

The integer closest is $A = 40{,}503$, which is also relatively prime to w. Therefore, IS-95 specifies the following hash function, denoted R:

$$R \equiv h(K) = \left\lfloor N \times \frac{(40{,}503 \times K) \bmod 2^{16}}{2^{16}}\right\rfloor \tag{4B.14}$$

where the value of N is the number of resources from which to choose, and K is the hash key.

The hash key is determined from the IS-95 parameter HASH_KEY, which is a binary number generated from either the 32-bit binary electronic serial number (ESN) or the least significant 32 bits of the binary encoded international mobile station identity (IMSI) of the mobile station; the binary coding of the IMSI is described below. These 32-bit binary numbers can be

written in the general form HASH_KEY $= L + 2^{16}H$; that is, L is the number formed by the 16 least significant bits of the number HASH_KEY, and H is the number formed by the 16 most significant bits of the number HASH_KEY. Using this notation, the IS-95 hash key is computed as

$$K = L \oplus H \oplus \text{DECORR} \tag{4B.15}$$

where DECORR is a modifier intended to decorrelate the different hash function selections made by the same mobile station. Let L' denote the twelve least significant bits of HASH_KEY; then Table 4B.2 shows the values of the parameters used in the IS-95 hash function.

The structures of the ESN and IMSI are shown in Figure 4B.3. Note that the ESN originates at the factory and is a fixed binary number, while the IMSI is a decimal number that is assigned to the mobile telephone unit when the country code and other information on the unit's specific use is known at the time of purchase.

As indicated in Figure 4B.3, the IMSI can be up to 15 decimal digits in length. For use in generating a hash key in IS-95, a number denoted IMSI_S is derived from the IMSI by taking its 10 least significant digits and converting it to a 34-bit binary number. If the IMSI has fewer than ten digits, zeros are appended on the most significant side of the number make it have 10 digits. For the purpose of this discussion, let us suppose that the 10-digit IMSI_S comprises a three-digit area code (d_1, d_2, d_3), a three-digit exchange number or prefix (d_4, d_5, d_6), and a four-digit local number (d_7, d_8, d_9, d_{10}). The mapping of the IMSI_S into a binary number is performed as follows:

(1) If any of the numbers d_i to d_{10} is a zero, change it to a ten; then subtract 1 from each of the numbers. This results in the 10 numbers $(d'_1, d'_2, \ldots, d'_{10})$ that are rotated in value as shown in Table 4B.3.

Table 4B.2 Parameters used in IS-95 hash function

Application	N	DECORR	Return value
CDMA channel # (center frequency)	No. channels (up to 10) in list sent to mobile	0	$R + 1$
Paging channel #	No. channels (up to 7) in list sent to mobile	$2 \times L'$	$R + 1$
Paging slot #	2,048	$6 \times L'$	R
Access channel randomization	2^M, where $M \leq 512$ is in broadcast message	$14 \times L'$	R

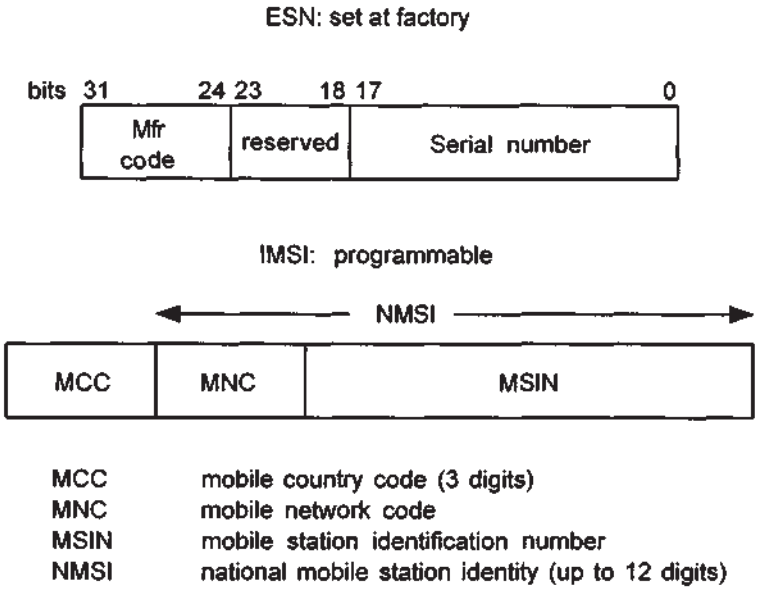

Figure 4B.3 ESN and IMSI structures.

Table 4B.3 Initial rotation of IMSI digit values

d_i	0	1	2	3	4	5	6	7	8	9
d_i'	9	0	1	2	3	4	5	6	7	8

This "rotation" procedure to determine IMSI_S digits (also used in IS-54 and AMPS to determine the mobile identification number, (MIN)) is a convention carried over from earlier cellular practice.

(2) The first three numbers (derived from the area code) are converted directly to a 10-bit binary number. For example, the area code 607 after rotation of the digits becomes 596, which in binary is $(596)_2 = 1001010100$.

(3) The next three digits (the exchange) is converted to a 10-bit binary number in the same way as the area code.

(4) The first of the last four (local number) digits is converted directly to a 4-bit binary number, except that if it is zero, it is treated as if signified the number ten and is converted to the $(10)_2 = 1010$.

(5) The last three digits are converted to a 10-bit binary number in the same way as the area code.

Example 4B.2 The 34-bit binary number corresponding to the IMSI_S given by 301-294-3463 is calculated as

$$301 \Rightarrow 290;\ (290)_2 = 0100100010$$
$$294 \Rightarrow 183;\ (183)_2 = 0010110111$$
$$(3)_2 = 0011$$
$$463 \Rightarrow 352;\ (352)_2 = 0101100000$$
$$\Rightarrow 0100100010001011011100110101100000$$

The hash key makes use of the 32 least significant bits of this number. In the notation introduced above:

$$H = 0010001000101101$$
$$L = 1100110101100000$$
$$L' = 110101100000$$

Then, the hash key to determine the paging channel number is calculated as

$$\begin{array}{ll} L & 1100110101100000 \\ \oplus H & 0010001000101101 \\ \oplus 2L' & \underline{0001101011000000} \\ & 1111010110001101 \Rightarrow K = 62{,}861 \end{array}$$

Assuming that there are $N = 7$ active paging channels, the hash function calculation (4B.14) gives

$$R = \left\lfloor 7 \times \frac{(40{,}503 \times 62{,}861) \bmod 2^{16}}{2^{16}} \right\rfloor$$
$$= \left\lfloor 7 \times \frac{2{,}546{,}059{,}083 \bmod 2^{16}}{2^{16}} \right\rfloor = \left\lfloor 7 \times \frac{51{,}019}{65{,}536} \right\rfloor$$
$$= \lfloor 5.4494 \rfloor = 5$$

The IS-95 paging channel assignment in this case is $R + 1 = 6$. The reader may verify that the IMSI_S differing in only one digit, 301-294-3464, results in $K = 62{,}862$ and the selection of paging channel 3 for the same assumptions.

4B.4 IS-95 Random Number Generator

In IS-95, the mobile is sometimes presented with a choice of resources from which to choose. For example, which of the 32 access channels associated with a particular paging channel (distinguished by long PN code offsets commanded by masks) should the mobile station use when attempting an access? This choice should be uniform and random to minimize collisions and overloads on particular channels. For the pseudorandom case, as opposed to the hashing case, the receiving link is not required to reproduce the choice of resources, and thus the choice will appear random to the receiver.

A good random number generator (RNG) satisfies three basic criteria:

- The generator should produce a "nearly infinite" sequence of numbers. This means that the generator should have a "nearly infinite" period.
- The generator should produce a random sequence of numbers. In other words, the sequence should have no obvious pattern.
- The generator should be easily implementable on whatever processor it is to be used on. In other words, the arithmetic involved should not cause overflow or erroneous results.

Most RNGs produce a *periodic* sequence of numbers, each of which is based on the previous number:

$$z_{n+1} = f(z_n) \quad n = 1, 2, \ldots \tag{4B.16}$$

and is initialized by choosing an initial seed z_1. For our purposes, the form of the RNG will be limited to the linear congruent generator form

$$z_{n+1} = (az_n) \bmod m \tag{4B.17}$$

where the modulus m is a large prime integer, and the multiplier a is any integer such that $1 < a < m$. If a or $z_n = 0$, then the sequence is all zeros. Thus, $z_1 \neq 0$.

For example, let an RNG be given by $z_{n+1} = 3z_n \bmod 7$; this recursive algorithm produces the following values:

z_n	z_{n+1}
1	$3(1) \bmod 7 = 3$
3	$3(3) \bmod 7 = 2$
2	$3(2) \bmod 7 = 6$
6	$3(6) \bmod 7 = 4$
4	$3(4) \bmod 7 = 5$
5	$3(5) \bmod 7 = 1$

The sequence 1, 3, 2, 6, 4, 5, 1,... is produced. We can make two observations about this generator. First, the numbers range from 1 to $m - 1 = 6$ (0 and m are excluded); 0 is excluded because only $m \bmod m = 0$ and $az_n \neq m$, because m is prime, and m is excluded because $x \bmod m < m$, by definition of the modular operation. Second, the maximal period P before any number is repeated is $m - 1 = 6$; because 0 and m are excluded, the generator can produce all numbers from 1 to $m - 1$, which is $m - 1 = P$.

It has been suggested [6] that an appropriate choice for a modulus is $m = 2^{31} - 1$. This modulus is prime and produces a maximal period sequence of $P = m - 1 = 2^{31} - 2$, which is "nearly infinite." Because a can be any integer such that $1 < a < m$, there are $m - 1 - 1 = 2^{31} - 3$ or about 2.1×10^9 possible choices for the multiplier a. These choices can be narrowed by applying the three criteria. After applying the three criteria, only a handful of choices for a good random number generator remain.

Because we have chosen $m = 2^{31} - 1$, we must use at least a 32-bit processor to process values of m because $2^{31} - 1$ is the largest integer that can be represented by 32 bits (including one sign bit). It is desirable to implement the entire generator on a 32-bit processor, so that the generator can be compatible with a large number of computers. Because az_n can be much greater than $2^{31} - 1$, it is useful to perform the calculation in the following manner to prevent overflow:

Let $m = aq + r$ where $q = \lfloor m/a \rfloor \ll m$ (so that $aq < m$) and let $r = m \bmod a$; from the definition of the modular calculation, the generator can be expressed as

$$f(z) = az \bmod m = az - m\left\lfloor \frac{az}{m} \right\rfloor$$

Adding and then subtracting $m \lfloor z/q \rfloor = (aq + r) \lfloor z/q \rfloor$ from the equation yields

$$f(z) = az - m\left\lfloor \frac{az}{m} \right\rfloor + m\left\lfloor \frac{z}{q} \right\rfloor - (aq + r)\left\lfloor \frac{z}{q} \right\rfloor$$

$$= a\underbrace{\left(z - q\left\lfloor\frac{z}{q}\right\rfloor\right)}_{z \bmod q < q} - r\left\lfloor\frac{z}{q}\right\rfloor + m\underbrace{\left(\left\lfloor\frac{z}{q}\right\rfloor - \left\lfloor\frac{az}{m}\right\rfloor\right)}_{f_2(z)}$$

$$= \underbrace{a(z \bmod q) - r\left\lfloor\frac{z}{q}\right\rfloor}_{f_1(z)} + mf_2(z)$$

$$= f_1(z) + mf_2(z) \tag{4B.18}$$

This ordering of the calculation prevents overflow, because

$$f_1(z) = a(z \bmod q) - r\left\lfloor\frac{z}{q}\right\rfloor < a(z \bmod q) < aq < m$$

and, using ϵ to denote a positive number less than 1:

$$f_2(z) = \left\lfloor\frac{z}{q}\right\rfloor - \left\lfloor\frac{az}{m}\right\rfloor = \left\lfloor\frac{z}{q}\right\rfloor - \left\lfloor\frac{z}{q+\epsilon}\right\rfloor$$

$$< \left\lfloor\frac{z}{q}\right\rfloor - \left\lfloor\frac{z}{q+1}\right\rfloor = \frac{z}{q(q+1)} + \epsilon_1 - \epsilon_2$$

$$< \frac{m}{q(q+1)} + 1 \Rightarrow mf_2(x) \lesssim \left(\frac{m}{q}\right)^2 < a^2$$

For the IS-95 RNG, $a^2 = (16{,}807)^2 = 2.8 \times 10^8 < m = 2.15 \times 10^9$.

Even though some generators do not rank the highest on the randomness test, they are used in modern systems because they have been used in the past with great success. An example of such a generator is the one used in IS-95, given by

$$z_{n+1} = 16{,}807z_n \bmod (2^{31} - 1)\,, \text{ where } 16{,}807 = 7^5 \tag{4B.19}$$

For this RNG, $m = 2^{31} - 1 = 2{,}147{,}483{,}647$ and z_0 = the generator seed. The generator seed is determined from information stored in the permanent memory of the mobile and information found on the sync channel.

During mobile initiation, the mobile receives the pilot channel to obtain synchronization with the base station and obtain the sync channel. On the sync channel is found the sync channel message, which contains a 36-bit parameter SYS_TIME corresponding to the system time. The 32 least

significant bits of SYS_TIME form a parameter RANDOM_TIME. The mobile computes the generator seed by using the 32-bit ESN stored in permanent memory and the 32-bit parameter RANDOM_TIME as follows:

$$z_0 = (\text{ESN} \oplus \text{RANDOM\_TIME}) \bmod m$$

If z_0 is computed to be 0, then it is replaced by $z_0 = 1$.

Example 4B.3 Find z_0, given that

ESN = 01001011101001010110100010101111

and

SYS_TIME = 10100011000101101111010011000101001O.

Solution: RANDOM_TIME is the 32 least significant bits of SYSTEM_TIME:

$$\text{SYS\_TIME} = 10100011000101101111010011000101001O$$
$$\underbrace{\qquad\qquad\qquad\qquad\qquad\qquad\qquad\qquad}_{\text{RANDOM\_TIME}}$$

$z_0 = (\text{ESN} \oplus \text{RANDOM\_TIME}) \bmod m$:

$$\begin{aligned} \text{ESN} &= 01001011101001010110100010101111 \\ \text{RANDOM\_TIME} &= \underline{00110001011011110100110001010010} \\ \text{ESN} \oplus \text{RANDOM\_TIME} &= 01111010110010100010010011111101 \\ &= 2060068093 \end{aligned}$$

$$\begin{aligned} z_0 &= (\text{ESN} \oplus \text{RANDOM\_TIME}) \bmod m \\ &= (2060068093) \bmod 2147483647 = 2060068093 \end{aligned}$$

For those applications that require a binary fraction u_n: $0 < u_n < 1$, IS-95 specifies that the mobile station shall use the following value: $u_n = z_n/m$. For those applications that require a small integer k_n: $0 \le k_n \le N - 1$, the mobile station shall use the following integer value: $k_n = \lfloor N \times (z_n/m) \rfloor$.

Example 4B.4 Suppose that a mobile is attempting access to the base station to register. The link is poor, and the mobile must transmit three accesses before the base station receives and correctly acknowledges the access. Find

the access channel number used for each of the accesses (IS-95 states that before each access, a new access channel number is randomly determined.)

Solution assumptions:

There are $N = 32$ access channels.

The mobile station ESN is 01001011101001010110100010101111.

The parameter SYSTEM_TIME is 10100100101110100101011010001010111l.

$$\text{SYSTEM\_TIME} = \underbrace{10100100101110100101011010001010111l}_{\text{RANDOM\_TIME}}$$

The seed is $z_0 = (\text{ESN} \oplus \text{RANDOM\_TIME}) \bmod m$:

$$\begin{aligned} \text{ESN} &= 01001011101001010110100010101111 \\ \text{RANDOM\_TIME} &= 01001011101001010110100010101111 \\ \text{ESN} \oplus \text{RANDOM\_TIME} &= 00000000000000000000000000000000 = 0 \end{aligned}$$

$$z_0 = (\text{ESN} \oplus \text{RANDOM\_TIME}) \bmod m = 0 \bmod 2{,}147{,}483{,}647 = 0$$

because z_0 was calculated to be 0, it is replaced by $z_0 = 1$. The random number for the first access attempt is determined using

$$z_1 = a \times z_0 \bmod m = 16807 \times 1 \bmod 2{,}147{,}483{,}647 = 16{,}807$$

The access channel number for the first attempt is given by

$$k_1 = \left\lfloor \frac{N \times z_1}{m} \right\rfloor = \left\lfloor \frac{32 \times 16{,}807}{2{,}147{,}483{,}647} \right\rfloor = \lfloor 0.00025 \rfloor = 0$$

The random number for the second access attempt is determined using

$$\begin{aligned} z_2 &= a \times z_1 \bmod m = (16807 \cdot 16807) \bmod 2{,}147{,}483{,}647 \\ &= 282{,}475{,}249 \end{aligned}$$

The access channel number for the second attempt is given by

$$k_2 = \left\lfloor \frac{N \times z_2}{m} \right\rfloor = \left\lfloor \frac{32 \times 282{,}475{,}249}{2{,}147{,}483{,}647} \right\rfloor = \lfloor 4.209 \rfloor = 4$$

The random number for the third access attempt is determined using

$$\begin{aligned} z_3 &= a \times z_2 \bmod m = 16{,}807 \times 282{,}475{,}249 \bmod 2{,}147{,}483{,}647 \\ &= 1{,}622{,}649{,}381 \end{aligned}$$

The access channel number for the third attempt is given by

$$k_3 = \left\lfloor \frac{N \times z_3}{m} \right\rfloor = \left\lfloor \frac{32 \times 1{,}622{,}649{,}381}{2{,}147{,}483{,}647} \right\rfloor = \lfloor 24.18 \rfloor = 24$$

the sum of the gains of all the simulated channels, or ± 2.2374; we see from Figure 11.26 that the total amplitude for the particular Walsh functions that are used in this example varies between −1.85 and +1.75, and the amplitude waveform, in addition to having a period of 64 chips, is quite "peaky."

After the waveform of Figure 11.26 is separately combined with I- and Q-channel PN codes, and then is filtered and used to modulate cosine and sine carriers, the resulting envelope is the waveform shown in Figure 11.27. Note that the envelope waveform is characterized by relatively large peaks that occur periodically if the channel input data are held constant, as in this simulation. There are two practical implications of this characteristic behavior of the IS-95 forward link waveform. First, the forward link transmitter's power amplifier must have very good linearity in order to deliver the Walsh-multiplexed waveform without significant distortion. Second, it is obvious that the testing of such amplifiers using a channel simulator cannot be performed using bandlimited noise, even though the signal spectrum resembles that of bandlimited noise, because the envelope of the actual IS-95 time waveform does not resemble that of a noise waveform but has distinctive pulse-like features with a significantly large dynamic range.

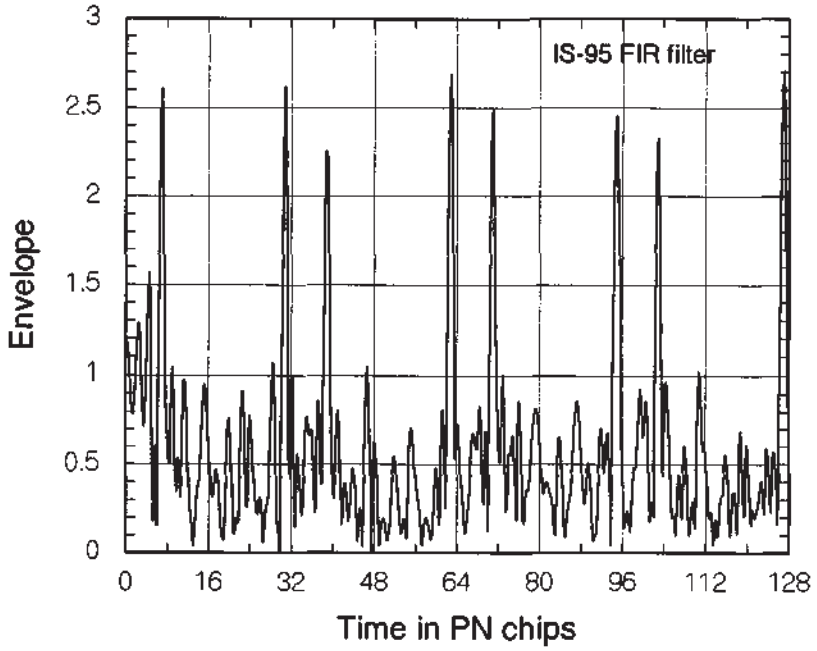

Figure 11.27 Envelope of simulated IS-95 signal.

Implementation of power allocation using measurements. The solution for forward link powers presented in Section 11.2 is based on modeling the total forward link power using the quantity K_{traf}, the forward link power control factor, to estimate the total traffic channel power in terms of the power needed to transmit to a mobile user at the edge of the cell. An alternative solution can be based on using a measurement of the actual total traffic power instead of that estimate. Under this approach, the equations to be solved, equations (11.18a) to (11.18e), are replaced by the following:

$$P_{total} = P_{pil} + P_{sync} + N_p P_{pag} + P_{tt} \leq P_{max} \tag{11.45a}$$

$$\left(\frac{E_c}{\mathcal{N}_{0,T}}\right)_{pilot} = \frac{(PG)_{pil} P_{pil}}{N_m L_T(R) + K_f P_{total}} \geq \rho_{pil} \tag{11.45b}$$

$$\left(\frac{E_b}{\mathcal{N}_{0,T}}\right)_{sync} = \frac{(PG)_{sync} P_{sync}}{N_m L_T(R) + K_f P_{total}} \geq \rho_{sync} \tag{11.45c}$$

$$\left(\frac{E_b}{\mathcal{N}_{0,T}}\right)_{pag} = \frac{(PG)_{pag} P_{pag}}{N_m L_T + K_f P_{total}} \geq \rho_{pag} \tag{11.45d}$$

where P_{tt} denotes the actual total traffic channel power on the forward link, assuming that this power is being controlled by the CDMA system on a per-user basis. Taking the case of equality for each of these equations, the corresponding joint solutions for the signaling (non-traffic) channels are

$$P_{pil} = \frac{\left(N_m L_T + K_f P_{tt}\right) \rho_{pil}/(PG)_{pil}}{1 - K_f\left(\rho_{pil} + \dfrac{\rho_{sync}}{(PG)_{sync}} + N_p \dfrac{\rho_{pag}}{(PG)_{pag}}\right)} \tag{11.46a}$$

$$P_{sync} = \frac{\left(N_m L_T + K_f P_{tt}\right) \rho_{sync}/(PG)_{sync}}{1 - K_f\left(\rho_{pil} + \dfrac{\rho_{sync}}{(PG)_{sync}} + N_p \dfrac{\rho_{pag}}{(PG)_{pag}}\right)} \tag{11.46b}$$

$$P_{pag} = \frac{\left(N_m L_T + K_f P_{tt}\right) \rho_{pag}/(PG)_{pag}}{1 - K_f\left(\rho_{pil} + \dfrac{\rho_{sync}}{(PG)_{sync}} + N_p \dfrac{\rho_{pag}}{(PG)_{pag}}\right)} \tag{11.46c}$$

In this solution, the SNR requirements with margin (ρ'_{pil}, ρ'_{sync}, and ρ'_{pag}) may be used in place of the requirements with zero-margin. Note that the formulation does not result in a solution for traffic channel power, since it is assumed that the forward link power control is operative. If desired, however, we can calculate a value of traffic channel power for initializing the forward traffic power control loop by replacing ρ_{pag} and $(PG)_{pag}$ in the numerator of (11.46c) with ρ_{traf} and $(PG)_{traf}$, respectively.

Also, instead of estimating other-cell interference as K_{other} times the received forward link power at the cell edge, we can find the signaling channel powers using measurements or some other estimate of the term I_{other}, resulting in the pilot channel power solution (for example) given by

$$P_{pil} = \frac{\left[(N_m + I_{other})L_T + K_{same}P_{tt}\right]\rho_{pil}}{1 - K_{same}\left(\rho_{pil} + \dfrac{\rho_{sync}}{(PG)_{sync}} + N_p\dfrac{\rho_{pag}}{(PG)_{pag}}\right)} \tag{11.47}$$

Note that, with or without these measurements, the solution for pilot power results in a value of the pilot power fraction ζ_{pil} that is not a fixed value but adapts to the amount of traffic and interference.

References

[1] "Mobile Station-Base Station Compatibility Standard for Dual-Mode Wideband Spread Spectrum Cellular System," TIA/EIA Interim Standard 95 (IS-95), Washington, DC: Telecommunications Industry Association, July 1993 (amended as IS-95-A in May 1995).

[2] Singer, A., "Improving System Performance," *Wireless Review*, pp. 74–76, Feb. 1, 1998.

[3] Owens, D., "The Big Picture," *CDMA Spectrum*, pp. 36–39, Dec. 1997.

[4] Qualcomm, Inc., *CDMA System Engineering Training Handbook*, draft version X1, 1993.

[5] Lee, J. S., and L. E. Miller, "Dynamic Allocation of CDMA Forward Link Power for PCS and Cellular Systems" (invited paper), *Proc. 2nd CDMA Internat'l Conf.*, pp. 95–99, Oct. 21–24, 1997, Seoul, Korea.

About the Authors

Jhong Sam Lee received his B.S.E.E. from The University of Oklahoma in 1959, his M.S.E. from The George Washington University in 1961, and his D.Sc. from The George Washington University in 1967, all in electrical engineering. He is founder and President of J. S. Lee Associates, Inc. (JSLAI), and has been responsible for all program initiations and management in the areas of special communications, electronic warfare (EW) systems, anti-submarine warfare (ASW) signal processing, and spread-spectrum systems. Dr. Lee is a Fellow of the IEEE.

He was an Assistant Professor at The George Washington University (1965 to 1968) and an Associate Professor at The Catholic University of America (1969 to 1973), teaching digital communications and detection and coding theories. Dr. Lee has authored or co-authored more than 70 papers in IEEE publications.

From 1973 to 1976, Dr. Lee was Associate Director at Magnavox Advanced Systems Analysis Office. From 1968 to 1969, he was Advisory Engineer at IBM. He was a consultant with the U.S. Naval Research Laboratory (1965 to 1973) and with COMSAT Laboratories (1965, 1971).

Leonard E. Miller received his B.E.E. from Rensselaer Polytechnic Institute in 1964, his M.S.E.E. from Purdue University in 1966, and his Ph.D. in electrical engineering from The Catholic University of America in 1973.

Dr. Miller is Vice President for Research with JSLAI. Since joining JSLAI in 1978, he has performed detailed analysis of the design and performance of military tactical communications and EW systems, as well as commercial communications systems. He developed analytical models for independent evaluation of the survivability of tactical communications networks, including MSE, JTIDS, and EPLRS.

From 1964 to 1978, Dr. Miller was an electrical engineer at the Naval Surface Weapons Center in Maryland, where he developed and evaluated underwater detection and tracking algorithms and designed instrumentation for submarines and underwater weapons.

In addition to many technical reports and memoranda, Dr. Miller has more than 40 papers in IEEE publications. He serves as a reviewer for several IEEE transactions and for *Electronic Letters*. He is a Senior Member of the IEEE.